Escola de Camins
Escola Tècnica Superior d'Enginyeria de Camins, Canals i Ports
UPC BARCELONATECH

TREBALL FINAL DE MÀSTER

Numerical Modelling of Out-of-Plane Behaviour of Structural Members using Mixed Finite Elements

Treball realitzat per:
Miguel Angel Hidalgo Calvo

Dirigit per:
Miguel Cervera Ruiz
Michele Chiumenti

Màster en:
Enginyeria de Camins, Canals i Ports

Barcelona, 20 de Juny de 2016

Departament de Ingenieria Civil i Ambiental

Abstract

This thesis presents an exhaustive comparison between a stabilized mixed strain/displacement finite element formulation and the classical irreducible formulation for linear and non-linear problems. A total of six straight and curved, 2D and 3D, structural elements under out-of-plane bending are analysed to contrast both FEM effectiveness and precision. The results are assessed by means of accuracy, displacement/stress convergence rate, mesh sensitivity, integration points through thickness, failure mode, model size, computational time, damage pattern, intensity and extension amidst several other. Numerical examples show improved results for the stabilized mixed formulation over the irreducible formulation.

Keywords: Mixed finite element; Non-linear solid mechanics; Out-of-plane loading; Convergence study; Tensile damage.

Resumen

Se presenta una comparación exhaustiva entre un elemento finito desplazamiento/deformación mixto estabilizado y la clásica formulación irreducible, para problemas lineales y no lineales. Un total de seis, en 2D y 3D, elementos estructurales bajo flexión fuera de plano son analizados para contrastar la eficacia y precisión de ambos elementos finitos. Los resultados son comparados por medio de precisión, velocidad de convergencia en los campos de desplazamiento y deformación, sensibilidad de la malla, puntos de integración en el espesor, modo de fallo, tamaño del modelo, coste computacional, patrón, intensidad y extensión del daño entre otras. Los ejemplos numéricos muestran un comportamiento mejorado de la formulación desplazamiento/deformación mixta estabilizada con respecto a la formulación irreducible.

Palabras clave: Elemento finito mixto; Mecánica de sólidos no lineal; Carga fuera de plano; Estudio de la convergencia; Daño por tracción.

Resum

Es presenta una comparació exhaustiva entre un element finit desplaçament/deformació mixt estabilitzat i la clàssica formulació irreductible, per a problemes lineals i no linealsUn total de sis, en 2D i 3D, elements estructurals sota flexió fora de plànol són analitzats per contrastar l'eficàcia i precisió de tots dos elements finits. Els resultats són comparats per mitjà de precisió, velocitat de convergència en els camps de desplaçament i deformació, sensibilitat de la malla, punts d'integració en l'espessor, manera de fallada, grandària del model, cost computacional, patró, intensitat i extensió del dany entre unes altres. Els exemples numèrics mostren un comportament millorat de la formulació desplaçament/deformació mixta estabilitzada respecte a la formulació irreductible.

Paraules clau: Element finit mixt; Mecànica de sòlids no lineal; Càrrega fora de plànol; Estudi de la convergència; Dany per tracció.

摘要

本文系统比较了线性及非线性问题下的一种稳定化应变/位移混合有限元公式及经典不可约公式。为了比较两种方法的效率及精度，本文对比分析了直线、曲线、二维、三维、及平面外弯曲等六种结构单元。并根据计算的准确性，位移/应力收敛速度，网格敏感性，失效模式、厚度方向上的集成点，破坏模式，模型的大小，计算时间，损伤模式，破坏方向、破环强度等方面对其进行评估。算例表明，相比经典不可约公式，稳定化应变/位移混合有限元公式有更好的计算结果。

关键词：混合有限元;非线性固体力学;平面外加载;收敛性研究;拉伸破坏。

ACKNOWLEDGEMENT

I would first like to thank my thesis advisors Miguel Cervera Ruiz and Michele Chiumenti for their continuous support, motivation and continuous feedback during my Master's thesis research.

Besides my advisors, I would like to express my gratitude towards Mr Savvas Saloustros and Dr. Narges Dialami for their help during the modelling process.

Special thanks to Xu Hongsheng and Xu Zhenzhen for their encouragement and motivation, without them I would not be the individual I am.

Last but not least, I would like to thank my parents, José and Soledad, and brother, José María, for their counsel and giving me strength to reach my dreams, inspiring and supporting me throughout my life.

Table of contents

List of figures

List of tables

List of equations

1. Introduction

1.1 General overview

In structural engineering the applicability of a finite element method formulation is highly related to computational time, stability and accuracy. Nowadays, the mixed finite element method successfully provides stable and accurate solutions in the displacement and stress/strain fields, within a reasonable processing time.

The concept of mixed fined element was firstly used in the mid-1960s, referring to the finite element formulations in which displacement and stress are approximated as main variables. Originally the mixed forms aim to solve problems in incompressible situations, as well commonly applied in fourth-order and bending problems.

This thesis focuses on the numerical modelling of out-of-plane behaviour comparison between the mixed finite element formulation and the irreducible methods, in the linear and non-linear ranges, of brittle or quasi-brittle isotropic homogeneous materials.

A total of six examples are studied throughout this thesis, modelled using mixed and classical finite element forms:

- Validity check examples: 2D straight and curved cases; the solution of this two examples provides a start point comparison among the theoretical elastic solution and the two finite element formulations.
    - Example 1: Wall supported on two sides.
    - Example 2: Clamped arch.

- Structural examples (I): 3D straight cases.
    - Example 3: Wall supported on three sides.
    - Example 4: Wall supported on four sides.

- Structural examples (II): 3D straight and curved cases; the results are focused on the non-linear analysis.
    - Example 5: Ribbed arch vault.
    - Example 6: Masonry four-wall box-structure.

A displacement and principal stress convergence evaluation is used as comparison factor in the elastic range. The non-linear results are compared by means of interpolation points or Gauss points, maximum load, post-peak/softening behaviour and failure mode. Moreover, computational time for all models is compared.

1.2 Motivation

This thesis is based in the previous works of M. Cervera and M. Chiumenti [1-3], which propose a stabilized strain/displacement mixed element approach using equal order linear interpolation. The stabilization method uses the projection of the displacement symmetric gradient to circumvent the strictness of compatibility requirements.

The strain/displacement mixed formulation in the set of the three papers [1-3] effectively proves:

- Well posed and stable discrete FE model.
- Accurate and robust scheme.
- Improved accuracy in stress and strain fields evaluation with respect the irreducible methods.
- Advantage of the mixed formulation to forecast the failure mechanism with respect the irreducible methods.
- Able to solve compressible and incompressible inelastic behaviour, avoiding volumetric locking and pressure oscillations.
- Able to represent directional inelastic behaviour.
- The results converge and not spuriously dependent of the mesh used.
- Suitable for application in 2D and 3D engineering problems

Furthermore, the investigation carried out by Z. Salat [4] in 2015 with shell elements has a strong influence in this thesis. Zsofia's research successfully shows the advanced approximation of shell finite element over plane stress and 3D elements. As a result, and for focused on a future research between stabilized strain/displacement mixed and shell element formulation, this thesis will use models with a single element through the thickness.

This technical background does prove, in general terms, the enhanced performance of the MFEM in numerous facets. Nonetheless, several questions about the comparison of these two FEM can be asked: Does the mixed formulation provide better solutions for displacement field? Do both method show akin behaviour in the non-linear range? Is computational time similar for two mixed and irreducible solutions, linear and non-linear, with alike results?

1.3 Objective

This thesis goal is to validate and further investigate Cervera et al. [1-3] performance-improved mixed formulation over the irreducible one under out-of-plane bending in the linear and non-linear ranges.

A selection of two test and four experimental testing examples, are selected to carry out a detailed study of the known and unexplored advantaged as well as the possible handicaps of the MFEM. Moreover a computational running time analysis for similar accuracy models, aiming to shed light to the goodness of both finite element method.

2. Related literature and theoretical focus

In continuum mechanics there are several problems presented as a set of partial differential equations, involving several physical variables needed to be approximated at the same time. Particularly, in structural analysis and material resistance stress, strain, displacement and pressure approximation are parameters of great importance. These problem solving approaches are known as mixed finite element methods (MFEM).

In the engineering field, the mixed methods make available solutions to incompressible problems, such as the classical Stoke problem, where the classical irreducible methods shows a terrible performance.

Parallel to mixed finite element investigation, several other researchers focused on a multi-field finite element by using Lagrange multipliers to enhance the constrain conditions along the internal element boundaries. In the finite element method discipline, this methodologies are commonly recognised as hybrid finite element method (HFEM). However this schemes are not discussed in the thesis.

2.1 Mixed finite element method brief history

In 1965, *Stress analysis* presented ten papers related with finite difference, finite element method and the boundary integral procedures. Chapter 9 introduced the concept of a multiple approximation variables in finite element method by B. Fraeijs de Veubeke [5], up today it is considered to be the first publication discussing MFEM. The publication also introduces a so called limitation principle for mixed formulation, which was obviated by other authors during the 1960s and 1970s but recovered into some texts by the end of 1980s. The aim of this limitation principle is to ensure the improved behaviour results of MFEM with respect the irreducible method, if not satisfied the results aroused are identical with the direct displacement form, or instability is present.

Other early publications by Herrmann [6] and Hellan [7] in 1967 analysed structural plates under bending conditions using mixed formulations. It is important to highlight that some of the applications of these method failed due to the lack of successfully satisfy the limitation principle condition stated by Veubeke et al. [5].

MFEM evolution at that point concentrated on decreasing or avoiding the volumetric locking and pressure oscillations of a pure incompressible problem, reducing the vast computational expense by using a reducing or selecting integration techniques [8-9].

In the late 1980s appeared the assumed enhanced strain method (AESM), which used the discretisation of strain in terms of nodal values proposed in the Hu-Washizu principle [10]. The mathematical basis of the AES is based on Simo et al. [11-12], the papers suggested an extension to the three-field Hu-Washizu principle accompanied by the addition of a local multiplicative decomposition.

With the new millennium emerged the average nodal pressure and strain methods [13-15]. As the AES methods, they are based on the Garlekin approach, which derives in volumetric locking. This technique alleviates integration errors by averaging the pressure and strain.

Thomas Hughes [16] proposed a Variational Multi Scale approach targeting to avoid the difficulties of the inf-sup condition. VMS uses variational projections instead of the traditional filtered equations, moreover focuses the modelling on a fine-scale rather than on a coarse-scale equations.

In the recent past, Codina [17] introduced a displacement/pressure formulation with Orthogonal Sub Scale (OSS) stabilization system, and applied by Cervera and Chiumenti [18] to incompressible elasticity. Following the excellent performance, the same authors extended the approach into non-linear problems [19-21] and further to strain localization analysis using J2 plasticity and J2 damage constitutive models [22-24], in to linear/linear simplicial elements in 2D and 3D, finally studying tensile and mixed-mode cracking using a strain/displacement mixed formulation [25]. Results provide robustness and effectiveness, besides achieve a fully stable and mesh independent discrete problem, without volumetric locking or pressure oscillations.

Recently, in 2010, Cervera, Chiumenti and Codina proposed a mixed form by means of stress/displacement formulation which uses linear/linear interpolation for both variables [1-2]. In this case, inf-sup condition imposes severe restrictions on the compatibility of the interpolations, which are successfully bypassed using VMS approach stated before.

The stabilized mixed strain/displacement formulation show excellent results not only in incompressible conditions, but approximating strains and stresses at singular points. For instance, **Figure 1** considers a 2x2 metres square provided with a 0.02 maximum width and 1 meter long V-shaped notch subjected to a tension force. As it is shown at P1 coarse and P1 fine, the irreducible method results in a rough approximations with greater principal stresses not even present at the tip of the notch. On the other hand, stabilized mixed formulation offers consistency between both, fine and coarse meshes, while locating the maximum principal stress at the tip of the notch; moreover strain directions are notably improved.

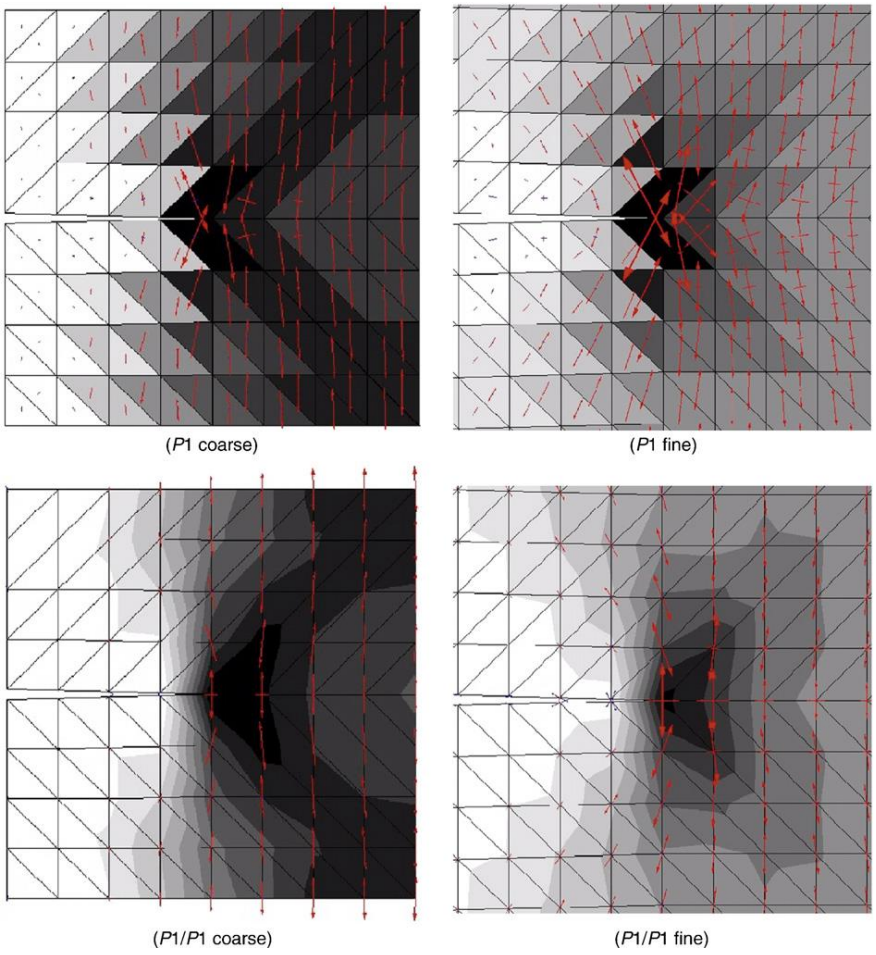

Figure 1. Principal stresses for V-notched specimen under tension [1]

In 2015, Cervera investigated and developed a further application of stabilized mixed strain/displacement formulation in non-linear solid mechanics problems, concerning compressible and incompressible plasticity [3].

It is shown that the mixed stress/displacement finite element methods have upgraded stress/strain accuracy in linear and non-linear analysis, additionally capability to successfully capture stress and strain concentration, for example the one shown in **Figure 1**.

The state-of-the-art introduces a third master field to the MEFM, a mixed three-field formulation based on displacement/stress/pressure variables using linear interpolation for all [26]. Once again, the formulation applies VMS approach method to overcome the inf-sup condition.

Cook's membrane problem classical linear elastic test example is used to compare the displacement/pressure against the displacement/pressure/strain mixed formulation. The problem consist of a tapered panel fixed on one end and subjected to shear loading at the free end. **Figure 2** show the heightened performance, in terms of stress and pressure, for the displacement/pressure/strain formulation, whereas both MFEM provide similar approximations in the displacement master field.

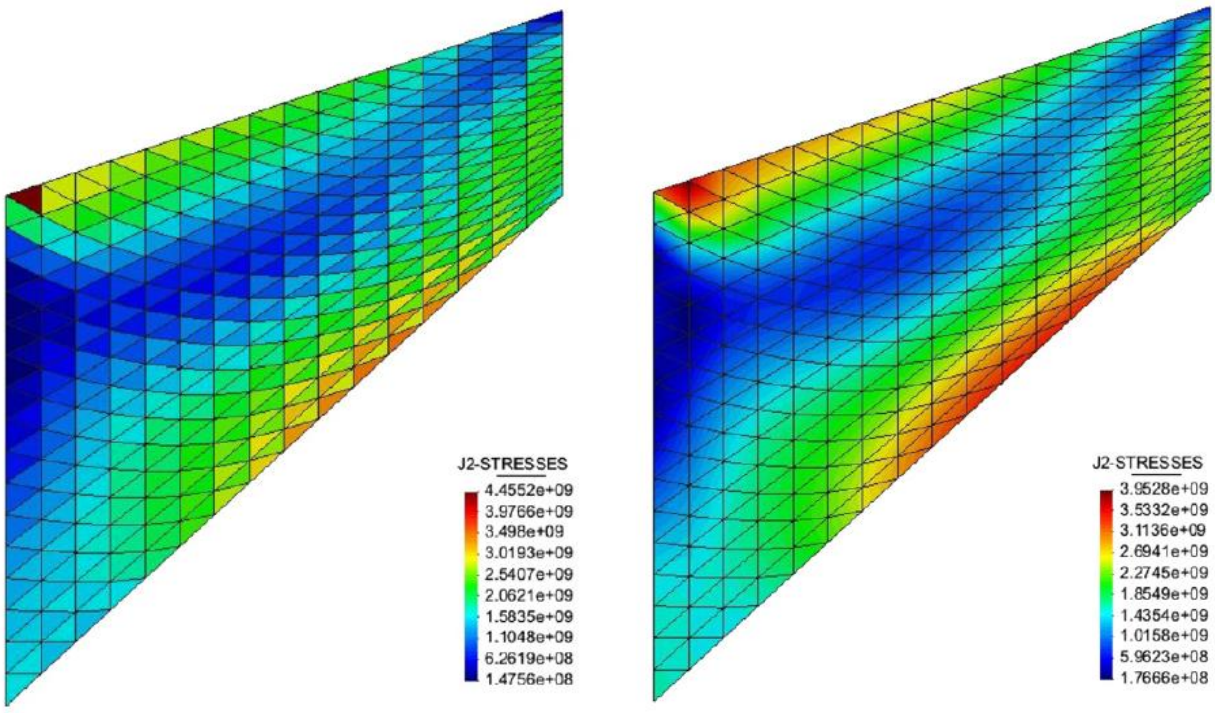

(a) u/p formulation *(b) u/s/p formulation*

Figure 2. Cook's membrane problem: J2 deviatoric stress value. [3]

MFEM is currently being applied to multiple fields, such as structures, thermal diffusion, impact analysis among others [27]. However, the future of the mixed formulation lays on the applicability in several other non-material related disciplines, with special attention to the biomedical [28-29]. A further study using mixed finite element formulations to the alternative

application to historical masonry constructions is provided by Roca et al. [30], in which FEM macro- and micro-modelling and DEM are considered, is a future investigation path.

2.2 Shell finite element influence

In previous sections it was stated the influence of shell finite elements to this research, according to what the meshing process is restricted to one element in the minor dimension of the structural element. For a better understanding a simple introduction of shell elements is presented.

Shell finite elements join the degrees of freedom of a plate element, two rotations and one out-of-plane displacement, and the plane stress element, two in-plane displacement, to a single element with a total five degrees of freedom per node, three displacement and two rotations.

The limiting one element through thickness requirement to the scope of this thesis is based on two factors: as in mixed and hybrid finite element method, shell element is capable of bypassing volumetric locking and pressure oscillations; the second factor states for the SFE successfully simplifies structural elements in which two dimensions are greater than the third one, by using only a single layer of shells. Accordingly, for the porpoise of a future comparison between shell elements and stabilized mixed element formulation under the same conditions, one layer of shell element is translated to one element through thickness in the meshing of both FEM models.

2.3 Scope

The scope of the stabilized mixed and irreducible finite element formulation is limited to:

- 2D and 3D, straight and curved elements.
- Out-of-plane bending.
- Linear elastic range.
- Inelastic range with regularised softening behaviour.
- Isotropic Rankine damage model.
- Tensile damage.
- Meshes with one element through thickness in the minor dimension.

3. The finite element model

In the recent years, the Polytechnic University of Barcelona (UPC) with the additional support of the Generalitat de Catalunya and the cooperation of UNESCO created a research organisation, CIMNE, aiming to develop the numerical methods and computational techniques in engineering and applied sciences.

In 1998, CIMNE developed and marketed a numerical simulation pre and post processing software (GiD), able to successfully represent geometrical modelling, effective definition of analysis data, meshing, data transfer to analysis software, as well as the visualization of numerical results.

Further research on thermomechanical problems in solid and structural mechanics, culminated in a finite element code for non-linear analysis capable of working together with GiD [31], known as COMET (Coupled Mechanical and Thermal Analysis) [32]. Since M. Cervera and M. Chiumenti research on 2010, this stabilized mixed formulation was uploaded to COMET. As a result, this thesis will be based on the context of GiD and COMET commercial/research software.

3.1 The material model

In COMET several materials are available based on the range of study being elastic, plastic (isotropic hardening, kinematic hardening and viscosity) or isotropic damage, the three possible options. Examples one to four are calculated using elastic material for the linear elastic stress/displacement convergence study, in addition all six cases non-elastic study selected isotropic damage as its material model.

Elastic material model: a linear problem with unique solution is solved. The slope of the elastic branch is defined by Young's Modulus (E). Additionally, the relation between stress/strain is achieved by means of the elasticity tensor (C), thus, Poisson's ratio is the second constant parameter necessary to achieve a solution for the elastic problem.

Isotropic damage material model: the problem is divided into a linear elastic region that once overpassed the plastic limit, non-linarites appear. Isotropic damage models are commonly used to represent the non-linear behaviour of brittle or quasi-brittle materials with softening, such as concrete or masonry. Since an initial elastic problem with identical characteristic as the stated before is solved, Young Modulus and Poisson's ratio are required. Regarding the non-elastic material's behaviour, only three factors are needed: uniaxial strength, which states the maximum possible tension, type of hardening law and the fracture energy.

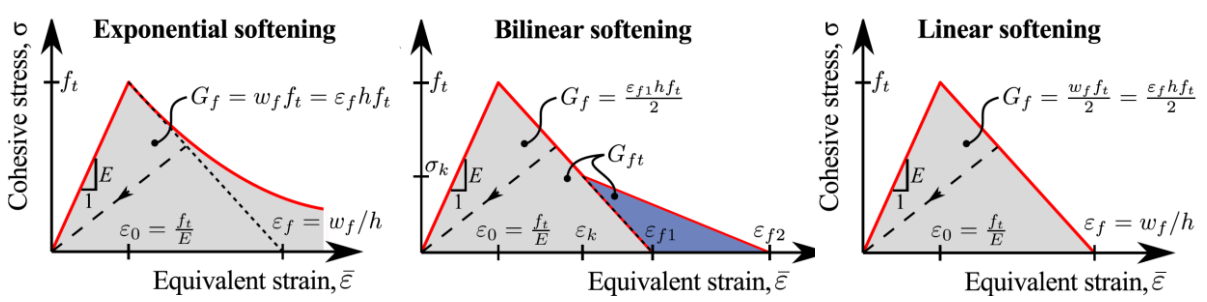

Figure 3. Typical fracture energies for exponential, bilinear and linear softening. [33]

3.2 The finite elements

3.2.1 Mixed element particularities

The stabilized strain/displacement mixed formulation is characterised by the use of not only the displacement as unknown in the nodes but also the strain, resulting in stresses by simply multiplying by the elastic tensor. It is thus obvious that the main field approximation are doubled.

The stabilized MFEM formulations are:

Equation 1. Stress/displacement formulation.

$$\boldsymbol{\sigma}_h = P_{C^{-1}}(\boldsymbol{C}{:}\nabla \boldsymbol{u}_h) \quad \varepsilon_h = \boldsymbol{C}^{-1}{:}P_{C^{-1}}(\boldsymbol{C}{:}\nabla \boldsymbol{u}_h)$$

$$\tau_u \left(\nabla \cdot \boldsymbol{\tau}_h, \tilde{P}_u(\boldsymbol{f})\right)(\nabla^s \boldsymbol{v}_h, \boldsymbol{\sigma}_h) + \tau_\sigma \left(\nabla^s \boldsymbol{v}_h, \tilde{P}_u(\boldsymbol{C}{:}\nabla \boldsymbol{u}_h - \boldsymbol{\sigma}_h)\right) = F(\boldsymbol{v}_h)$$

Equation 2. Strain/displacement formulation.

$$\boldsymbol{\sigma}_h = \boldsymbol{C}{:}P_C(\nabla \boldsymbol{u}_h) \quad \varepsilon_h = P_C(\nabla \boldsymbol{u}_h)$$

$$\tau_u \left(\nabla \cdot (\boldsymbol{C}{:}\gamma_h), \tilde{P}_u(\boldsymbol{f})\right)(\nabla^s \boldsymbol{v}_h, \boldsymbol{C}{:}\varepsilon_h) + \tau_\varepsilon \left(\nabla^s \boldsymbol{v}_h, \boldsymbol{C}{:}\tilde{P}_\varepsilon(\nabla \boldsymbol{u}_h - \boldsymbol{\epsilon}_h)\right) = F(\boldsymbol{v}_h)$$

In addition to the nodal strain values in the formulation, two stabilizing parameters appear: τ_u and τ_ε. The key ideal of these coefficients is to add or subtract a term that is reduced in every iteration and at the exact solution shall be zero.

On one hand, the porpoise of τ_u parameter is to avoid the classical incompressible problems, volumetric locking and pressure oscillations; therefore, in this thesis it is not used.

The second parameter, τ_ε, is purely used to stabilize the mixed finite element method and its value is ranged between zero and one. Take for instance the fourth example in linear elastic range, it is shown in **Figure 4** the deflection of wall along its major dimension and at the centre of the minor. The effect of the stabilizing coefficient is clear, the more the coefficient is increased, the lower the oscillations in displacement and stress/strain field are observed. In this thesis a τ_ε stabilizing coefficient of 0.1 is used in all the examples.

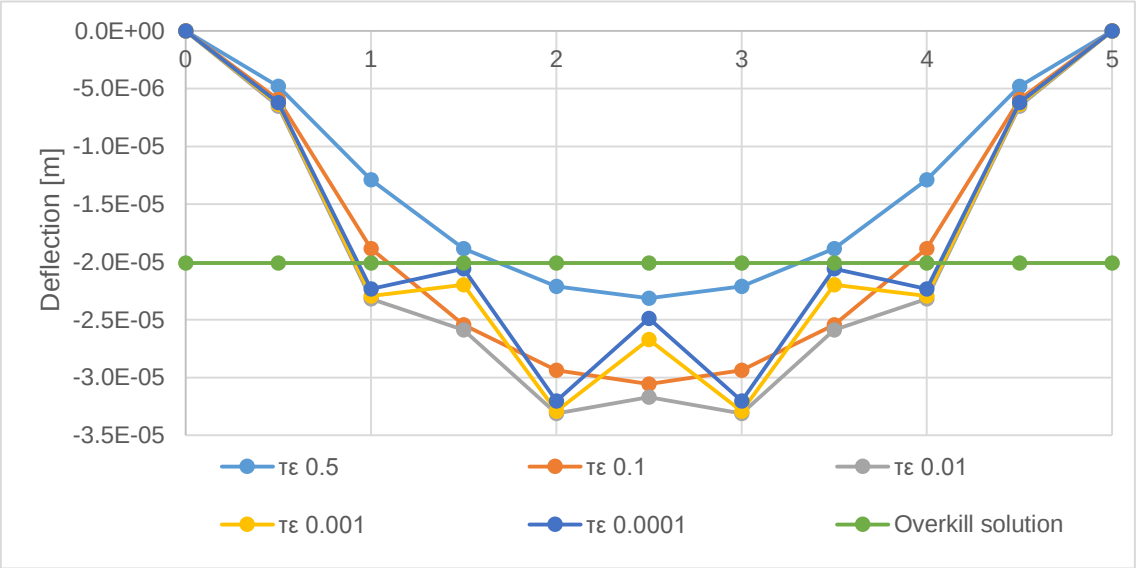

Figure 4. Instabilities solved by τ_ε coefficient.

3.2.2 Mixed and standard elements

In general terms stabilized mixed and irreducible models have akin features: plane strain elements are used for the first and second examples; 3D solid elements are used for the third to the sixth examples; identical boundary conditions, loading conditions and regular rectangular/hexahedra meshes are applied in both models.

Shell elements influence limits the number of elements in this thesis to one, nonetheless increasing the number of integration points and the integration rule from opened to closed, we can achieve improved solutions for the same model mesh.

Linear-elastic range is limited to opened or closed integration rule with the minimum integration points, 4 for 2D problems and 8 for 3D problems.

Regarding the non-linear range, for the 2D models, opened and closed integration rule is studied, moreover a set of 4, 9, 16 and even 25 Gauss points or interpolation points in the model are used. As for the 3D models, opened and closed integration rule is studied, additionally a set of 8, 27, 64 and 125 Gauss points in each model are studied.

3.3 The mesh

The meshing process is restricted to one element through thickness in the minor direction, at the same time structured rectangular and hexahedra meshes are generated for 2D and 3D models respectively.

At stress and displacement convergence study, meshes are refined, increasing the number of elements in every step, however respecting the meshing conditions stated before. Regarding the non-linear analysis, a set of one to three meshes granting stability are used for both formulations.

3.4 Solution methods and analysis parameters

All the examples but the second one use the following analysis parameters and solution methods:

- Loading and unloading control: spherical arc-length control limited by the node presenting the maximum displacement.
- Numerical solution method: Newton-Raphson's method, approaching the stiffness with the standard tangent stiffness matrix and limiting the iterations to 50 or 100.
- Convergence: 1% displacement and 1% force within 30 iterations.

For the second example similar numerical solution method and tolerance was chosen, however the loading and unloading control adopted is displacement control under the point load.

4. Methodology of the results interpretation and comparison

The six structural examples are modelled with the same mesh, loading and boundary, solution method and analysis parameters. The methodology the results interpretation is summarised in the following points:

Linear elastic analysis:

- Convergence of principal stress upon mesh refinement.
- Idem for displacement convergence.
- Principal stress convergence rate upon mesh refinement.
- Idem for displacement convergence rate.

Non-linear analysis:

- Comparison between irreducible and stabilized mixed methods and previously published experimental results.
- Load-displacement or load factor-displacement curves effect upon mesh refinement, integration rule and integration points through thickness.
- Comparison between stabilized mixed and irreducible finite element models in terms of failure mechanism, damage pattern, extension and intensity, stability and consistency.
- Finite element efficiency compares model sizes, accuracy and computational time.

5. Example 1 – Wall supported on two sides

5.1 Description of the model

The first example is a wall embedded in the bottom end and pinned in the top end, under a uniform load over one of its faces is applied. For simplification no gravity load are considered in the modelling process.

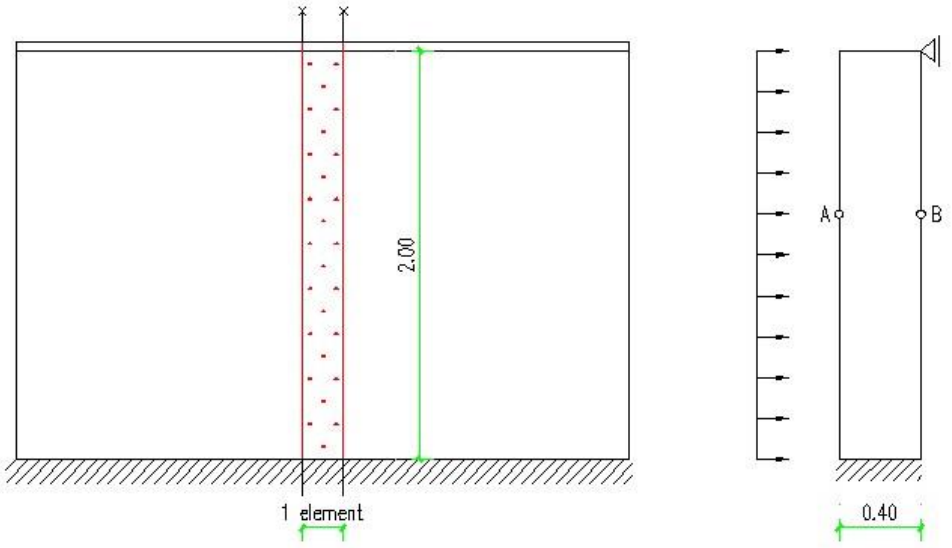

Figure 5. Wall geometry and load pattern

Due to the geometry and the loading the wall only experiences bending in one direction, as a result the wall is simplified to one element thickness through the length of the wall, achieving a 2D straight structural member analysis. In **Figure 5** it is shown in red the modelled part.

5.1.1 Mesh characteristics

A total of four different models were created, using 10, 20, 40 and 80 elements along the major length of the wall and only 1 element through the thickness. Moreover an overkill model, 50 element through the thickness and 500 along the length, for both mixed and standard elements was analysed.

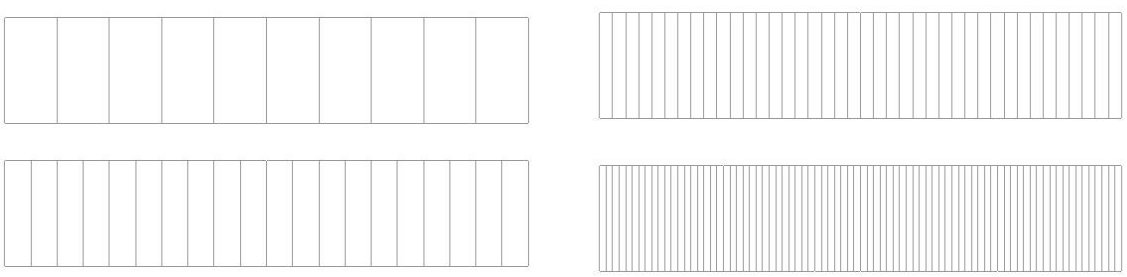

Figure 6. 10, 20, 40 and 80 elements mesh

Figure 7 shows the boundary conditions on the bottom edge (right) where both vertical and horizontal nodal translations are fixed, and on the top end (left) only horizontal translation are restrained.

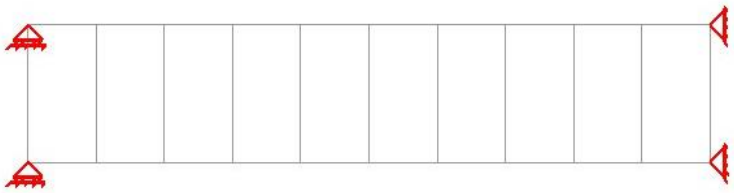

Figure 7. Boundary conditions

5.1.2 Material parameters

A typical Young's modulus and Poisson's ratio for concrete blocks masonry was used. In order to provide a stable non-linear analysis a notoriously high fracture energy was selected for the modelling.

Table 1 summarises the material parameters used in the analysis.

Table 1. Example 1 material parameters

Young's modulus	5.0 GPa
Poisson's ratio	0
Density	1800 kg/m^3
Tensile strength	0.18 MPa
Fracture energy	1.0*10^8 Nm/mm^2

5.2 Linear analysis results

A uniform 3000 N/m out-of-plane surface load was imposed in the left side of the wall. Lateral displacement at the maximum deflection point (point A at **Figure 5** and around 3/5 of the span) and the main stress in the longitudinal direction of the wall (point A and B at **Figure 5**), were compared for both standard and mixed elements. Furthermore a Timoshenko beam solution was calculated and compared to the finite element modelling results.

Figure 8 shows a faster convergence rate for the standard finite elements than for the mixed finite element. The coarsest mesh has a 14.1% difference between the Timoshenko's beam solution and the standard element's; moreover the mixed element results have a greater divergence, 39.3%. In the 40 elements model there is a 3.7% variation in the standard element against a 7.6% in the mixed element. As we refine the mesh it is clear that the irreducible method has a better displacement approach with faster convergence rate.

What is more, the convergence behaviour in the standard and the mixed elements has a clear distinction, the mixed element tends to the Timoshenko solution from the upper part whilst the standard element has an opposite comportment. This variation is due to the disparities in the numerical problem faced in the irreducible and stabilized mixed formulations.

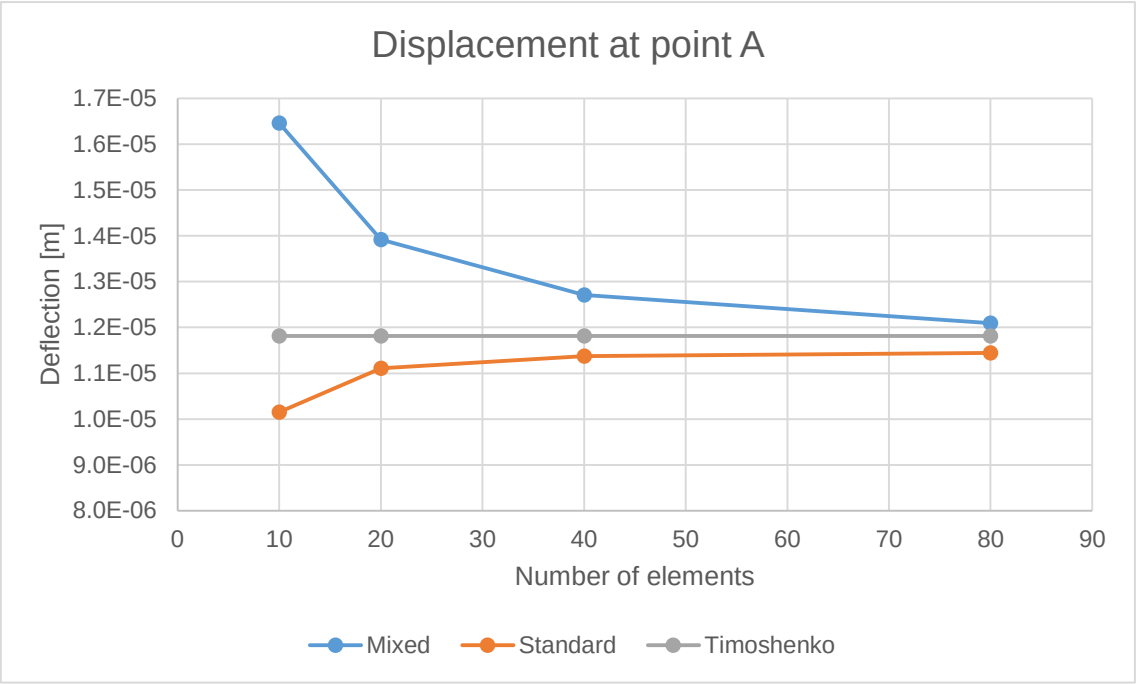

Figure 8. Convergence of the lateral displacement with mesh refinement

The mixed element strong point is the stress and strain calculations, a clear example of that is the results shown in **Figure 9**. Taking into account the coarsest mesh of 10 elements, the difference between Timoshenko's and the mixed element solution is only of 2.3%, on the other hand the standard element has a 15.4% discrepancy. Additionally, the finest mesh against the coarsest mesh results in the mixed element is 3.9%, at the same time in the standard element is 186.6%

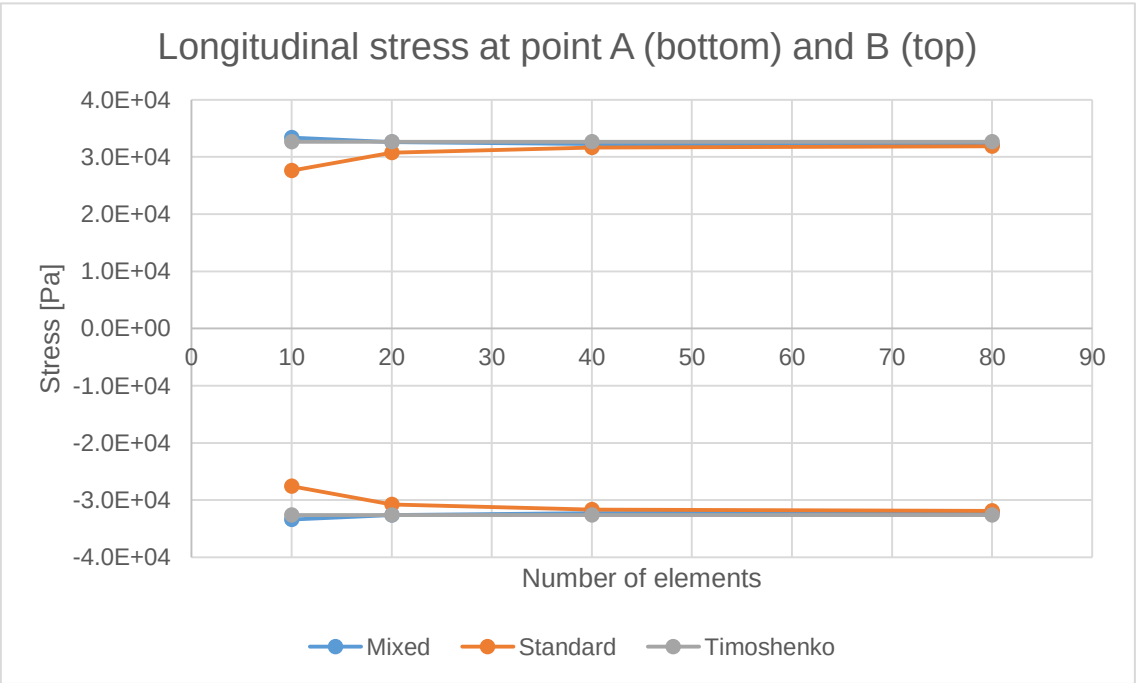

Figure 9. Convergence of the longitudinal stress with mesh refinement

In the stress convergence curve appears the same phenomena of two difference paths confluence, in both point A and point B standard and mixed have opposite convergence trends.

The longitudinal stresses along the wall and the lateral displacements for the finest mixed finite element mesh (80 elements) are shown in **Figure 10**.

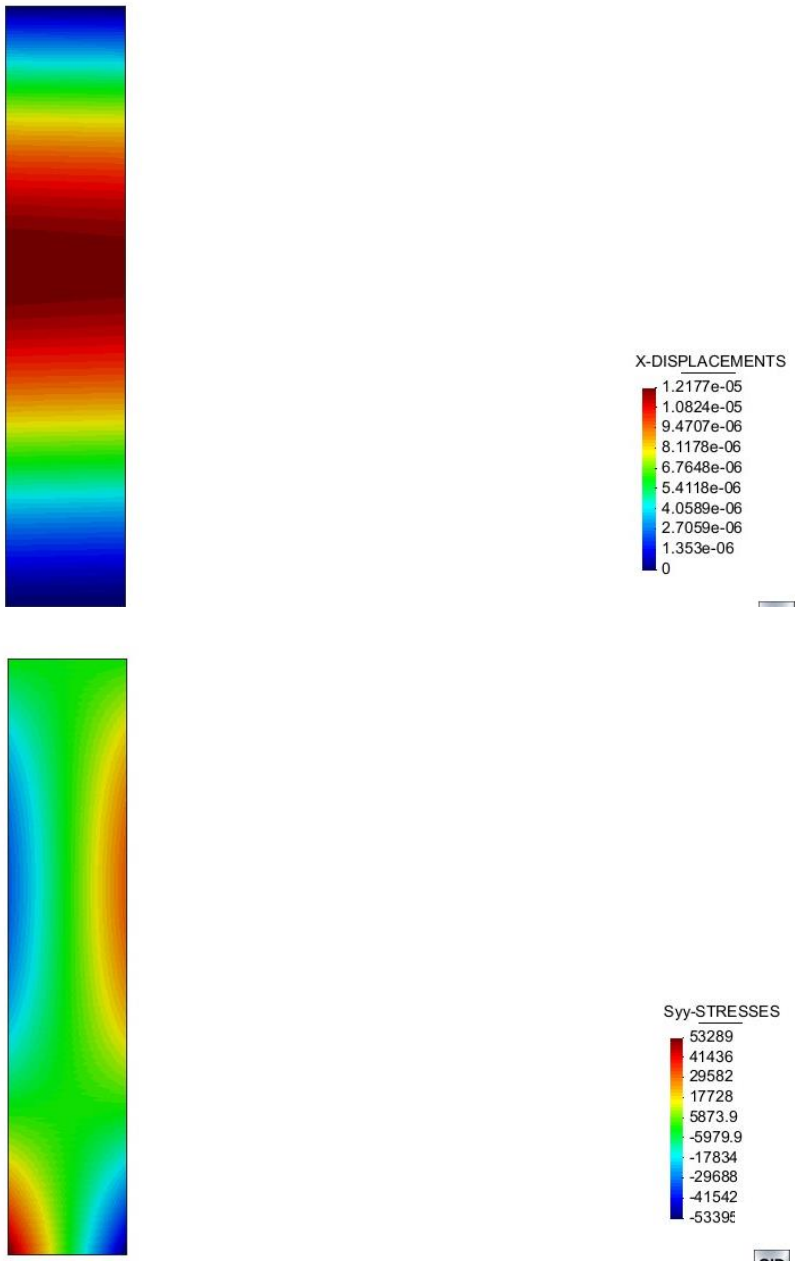

Figure 10. Wall supported on two sides displacement/stress results

Previously it was shown that the displacement convergence rate of the stabilized mixed element technique is considerably slower than the irreducible formulation's. One of the possible answer to this phenomena is the slenderness of the wall, with a 2 meter long and 0.4 meters thick, the slenderness of the wall is 1/5, in structural terms it does not behave like a common beam element, therefore the beam formulation does not successfully apply to this members.

Subsequently, a new numerical analysis is carried out for a beam of 0.1 thickness and 1/20 length to thickness ratio.

The ratio length to thickness reduction has a striking positive outcome on the displacement convergence of the mixed finite element, as it is shown in **Figure 11**, in which an enhanced behaviour of the mixed element with respect the irreducible method is shown. The difference between the coarsest mesh and the finest one in the mixed element is 7.4% whilst in the standard element is 65.8%.

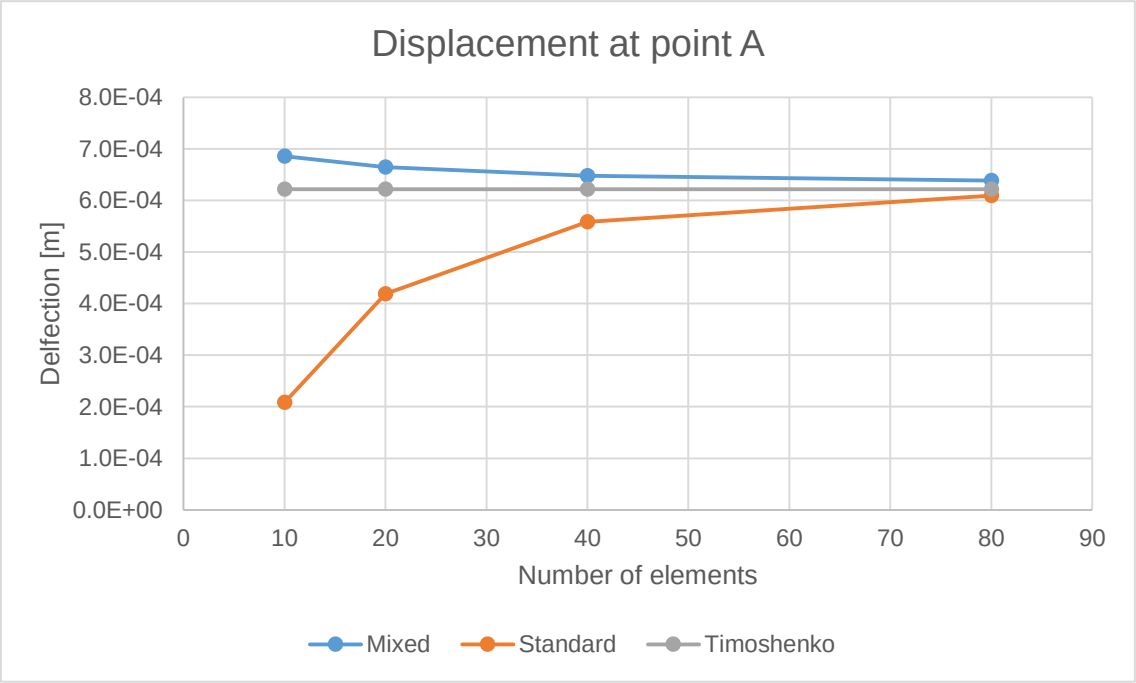

Figure 11. Convergence of the lateral displacement with mesh refinement

In terms of stress the mixed element still has a much better comportment. Besides, the 10 elements mesh along the length results are 1.1% apart from the Timoshenko's solution, even better than the 1/5 slenderness wall.

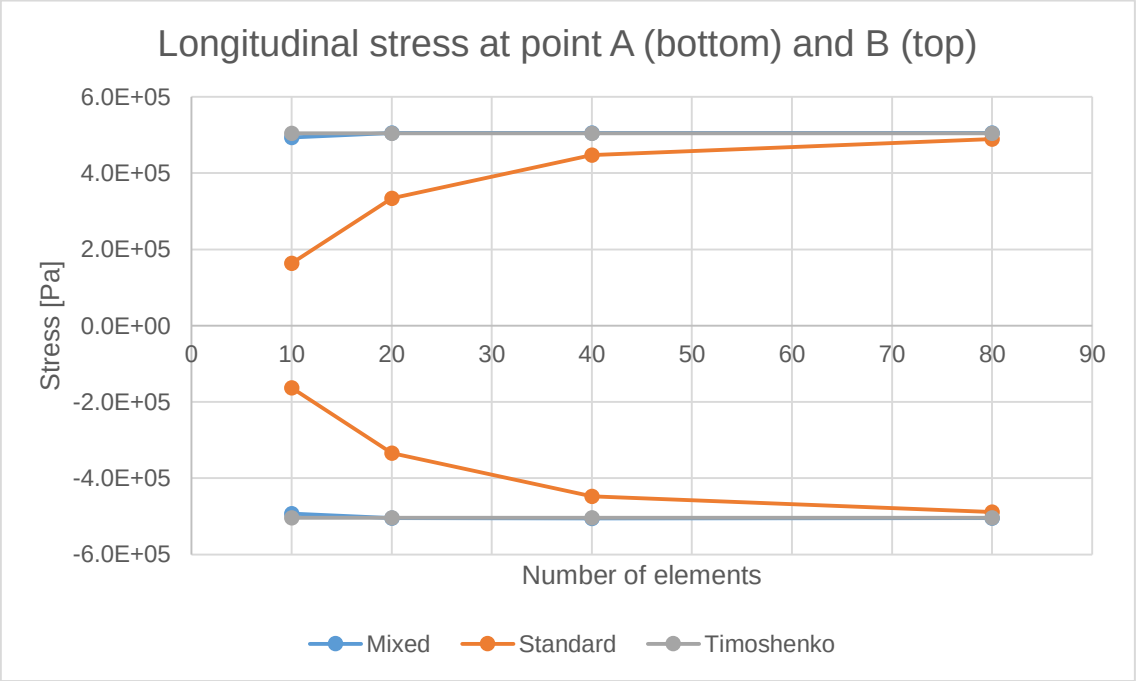

Figure 12. Convergence of the longitudinal stress with mesh refinement

5.3 Non-linear analysis results

A displacement control and force control non-linear analysis was studied. The results for the force control perfectly superpose the displacement's results in the elastic range, but do not match after the elastic limit. As a result only the displacement control result will be displayed, which uses a constant value times the actual loading to control the deflections, called load factor. This methodology is similar for the following examples and can be seen in the load factor against displacement graphs, instead of force against displacement.

The abruptness of the results is caused by the lack of more than one element through the thickness and it can be improved increasing the integration points.

5.3.1 Mesh sensitivity

Three meshes were used in the non-linear analysis, 10, 20 and 40 element meshes. **Figure 13** shows the non-linear analysis results for the irreducible formulation, the results are consistent for all of the three models. Moreover the refinement of the mesh has a reduction of the dissipated energy and the peak load. After the peak load in the 20 and 40 element model we have an accentuated softening behaviour of the wall, while the 10 element model displays a yielding plateau before the softening appears.

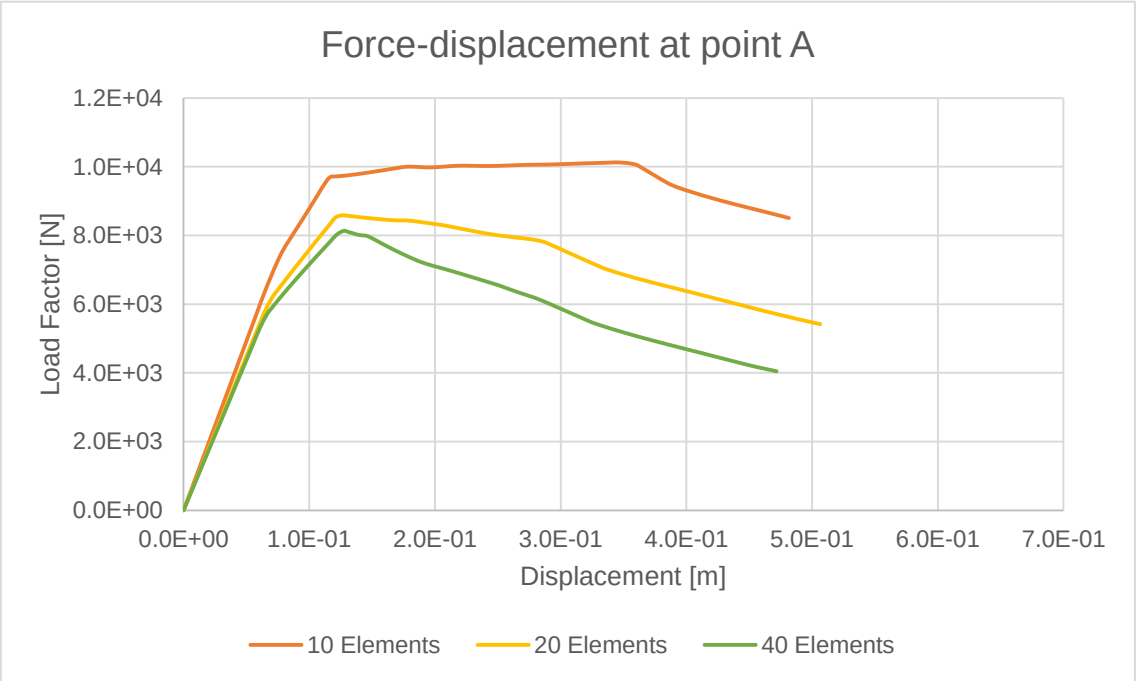

Figure 13. Standard finite element non-linear mesh sensitivity analysis results

The mixed finite element results show excellent consistency, also in this case all of the models do converge up to the final step. Besides, the more we refine the mesh the lower the peak load and the lower the dissipated energy are, but with almost a perfect match in all curves. **Figure 14** shows a softening behaviour but not as clearly marked as in the standard element non-linear analysis results.

Both of the elements have a similar overall behaviour. However, the greatest difference appears in the peak load, in which the mixed element shows compactness, 8.93E+03, 8.32E+03 and 8.07E+03 for the 10, 20 and 40 elements mesh respectively, while the standard experience a clear reduction from its coarsest mesh, 1.01E+04, to the finest, 8.13E+03, resembling the mixed element results at the finest mesh.

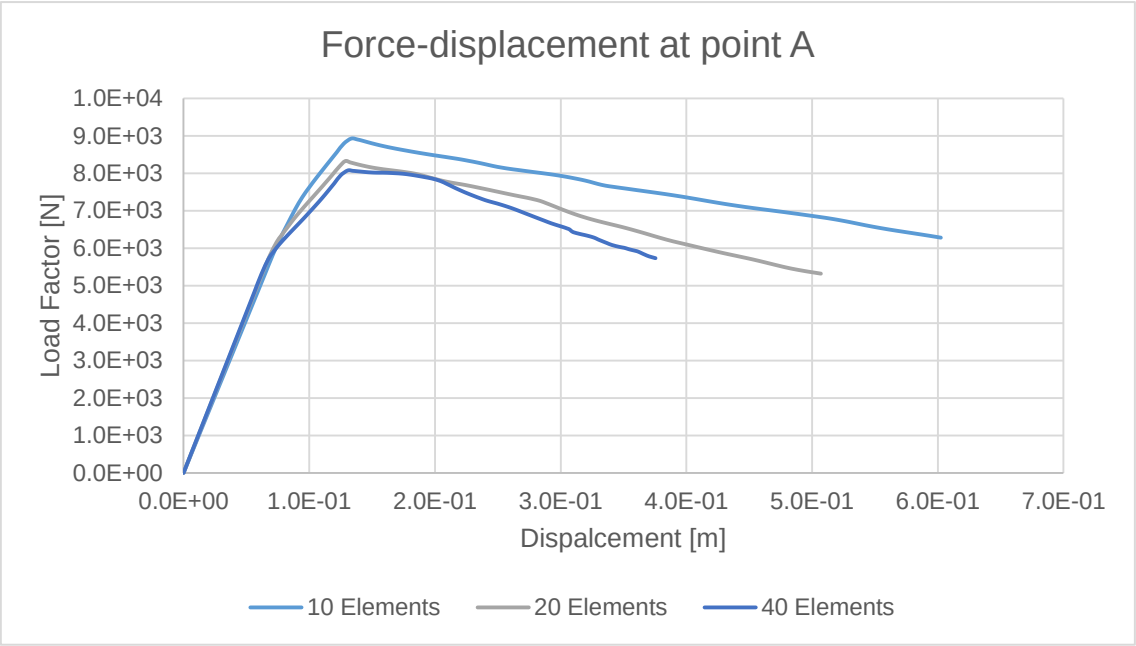

Figure 14. Mixed finite element non-linear mesh sensitivity analysis results

5.3.2 Integration through thickness

A study of the integration points through the element thickness was carried out, in which 9, 16 and 25 Gauss points were considered. For convenience only the 16 and 25 Gauss points' results will be shown.

5.3.2.1 Sixteen Gauss points

Figure 15 shows the results for the irreducible method, similar consistency but with smoother curves than the common 4 Gauss point results. Moreover at the inelastic range, it is observed the disappearance of the softening shown in the last section (**Figure 13**).

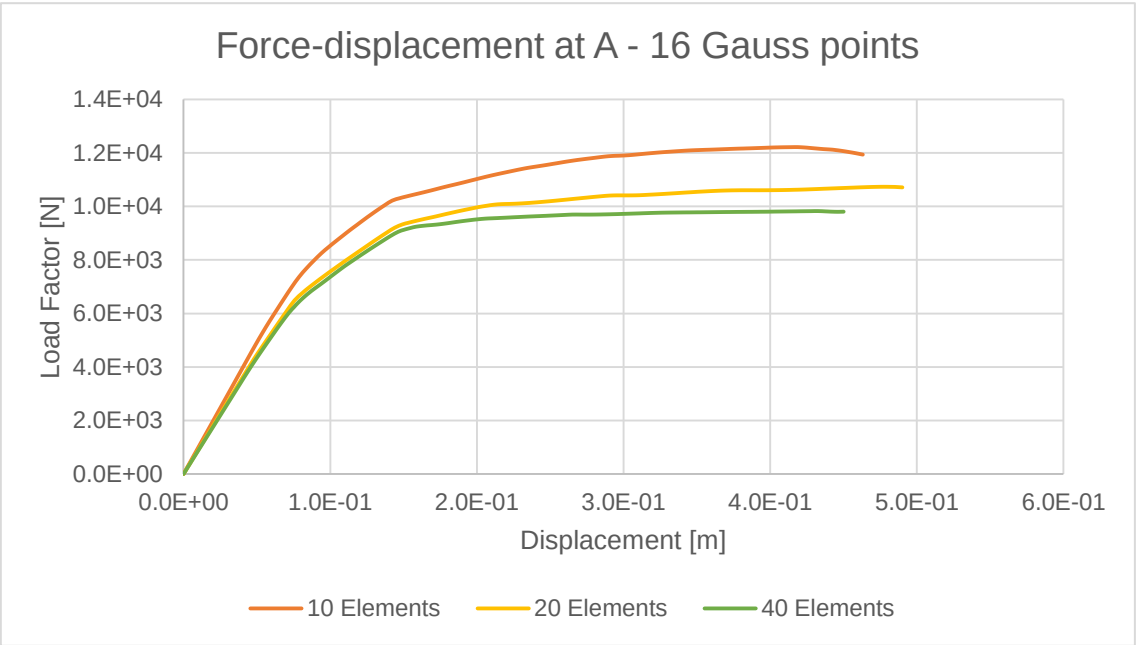

Figure 15. Standard finite element non-linear 16 Gauss points' analysis results

The stabilized mixed finite element results show excellent consistency for the 10, 20 and 40 elements models, smoother curves than in the previous 4 Gauss points results are obtained. Furthermore, there is softening behaviour present at the mixed elements that does not appear in the classical element, this is because in the MFEM models a mechanism is fully achieved, at the same time in the standard element model is not.

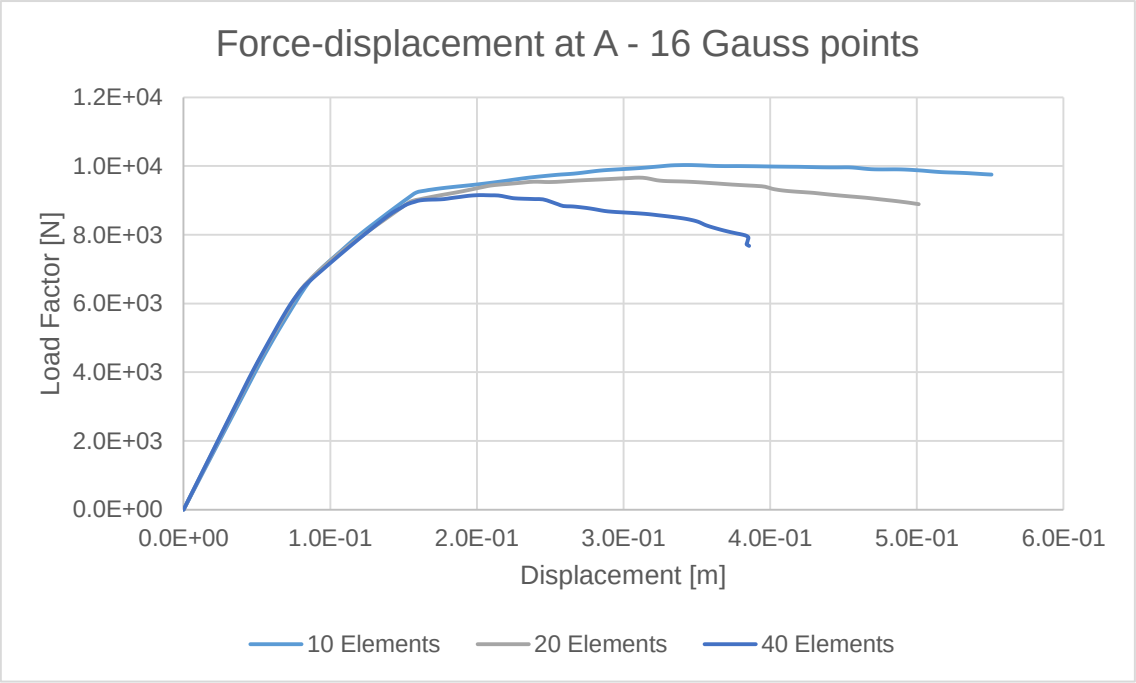

Figure 16. Mixed finite element non-linear 16 Gauss points' analysis results

5.3.2.2 Twenty-five Gauss points

The results for 25 Gauss points in both finite elements have accentuated mild curves, again the mixed element softening part is present.

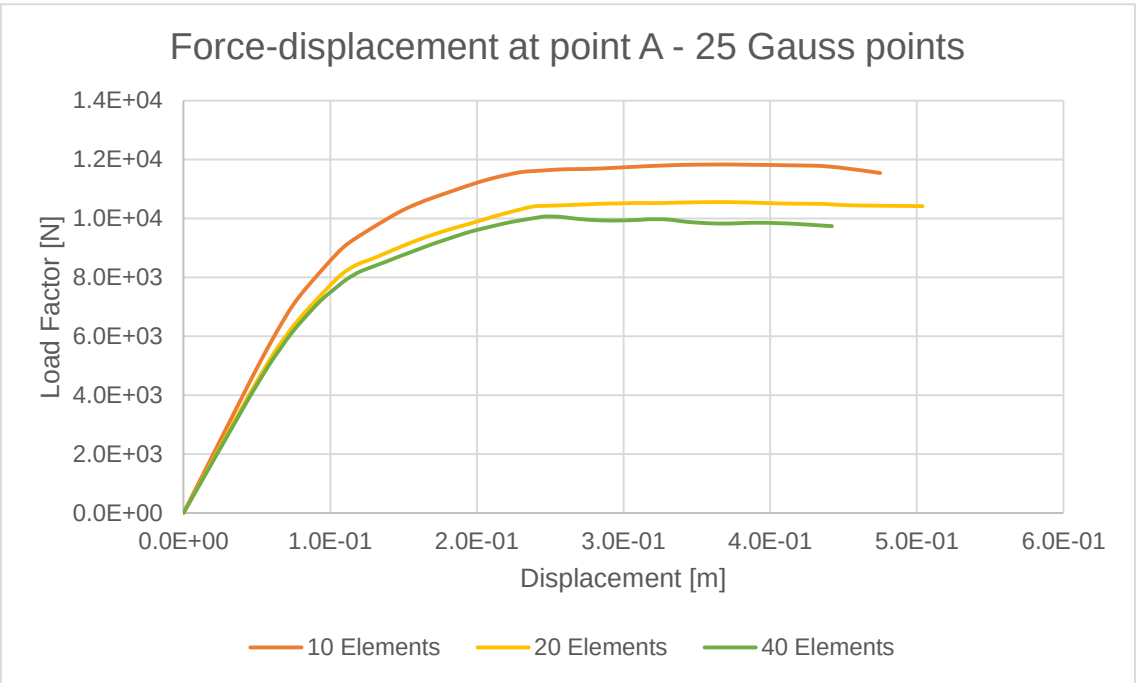

Figure 17. Standard finite element non-linear 25 Gauss points' analysis results

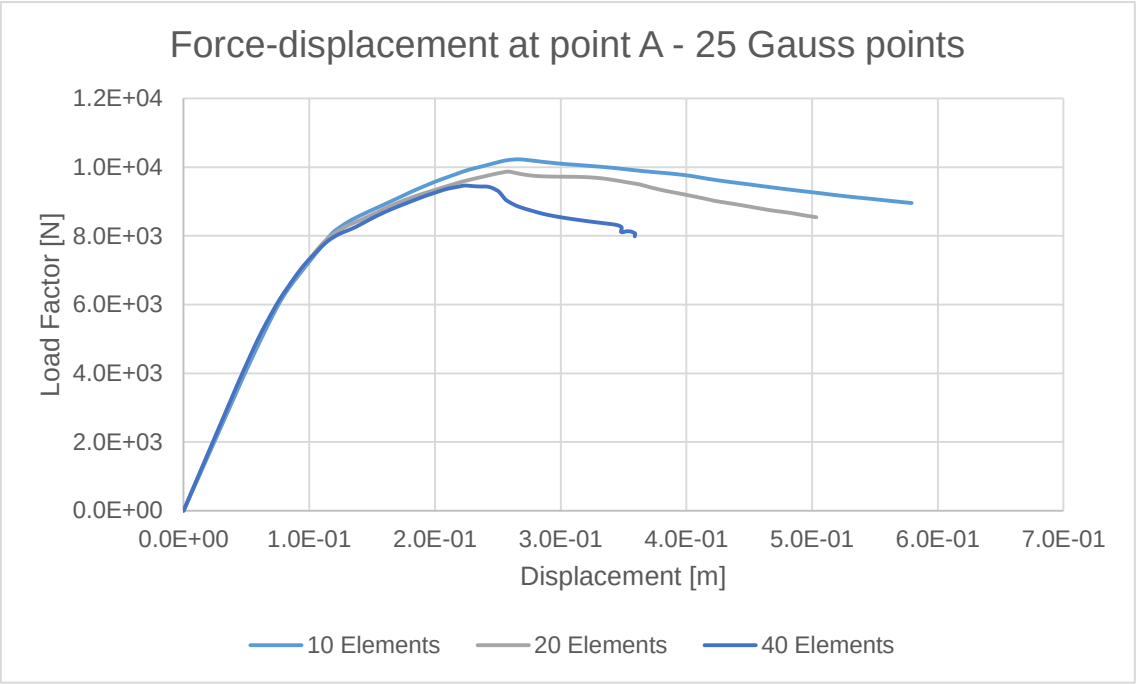

Figure 18. Mixed finite element non-linear 25 Gauss points' analysis results

With the increase of integration points and refinement of the mesh the classical element force-displacement curves severely reduce the peak load and the softening behaviour shown in the previous graphs is not present. Regarding the mixed element load-displacement results, the peak load is persistent, anyhow the softening is also reduced.

As **Figure 19** shows, standard's results tend to mixed element results as the mesh is refined. Moreover, in this case, the integration points do not play an important role, similar charts can be obtained for 4, 9 and 16 Gauss points with akin results.

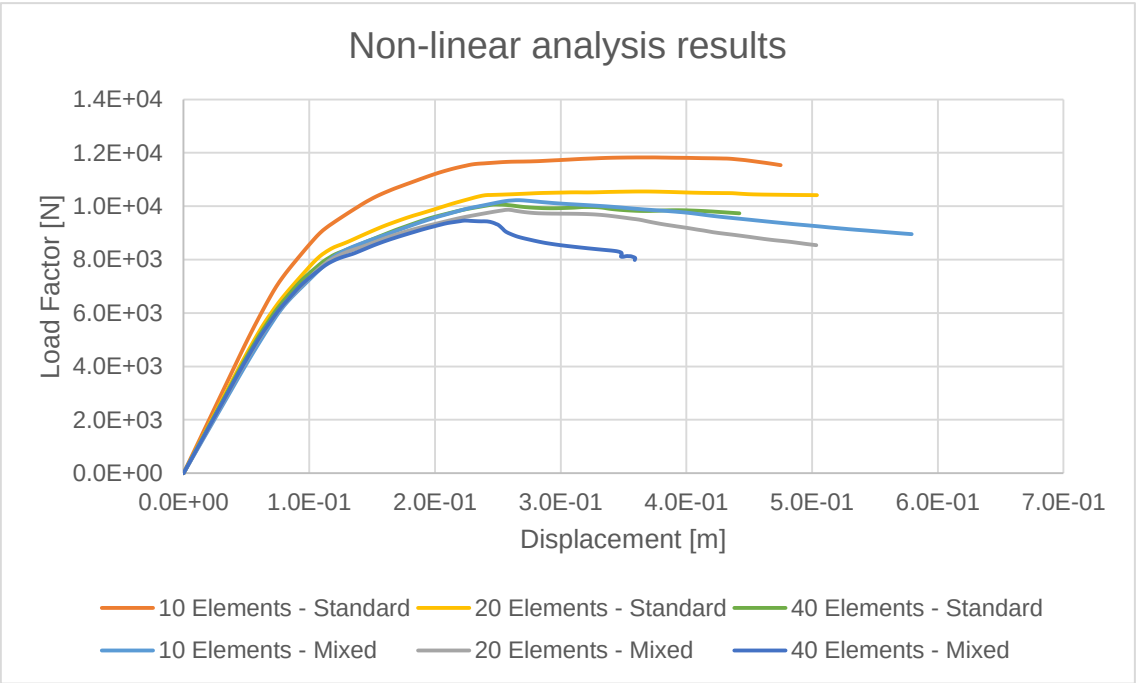

Figure 19. Non-linear analysis results comparison. 25 Gauss points

5.3.3 Non-linear results comparison

The comparison between both methods was carried out analysing the 20 elements models and 25 Gauss points.

Even though analogous results in terms of elastic behaviour and peak load can be observed, where the standard elements has 9.46E+03 versus the mixed 1.01E+04, a difference of 5.9%, the inelastic part has a clear disparity in softening.

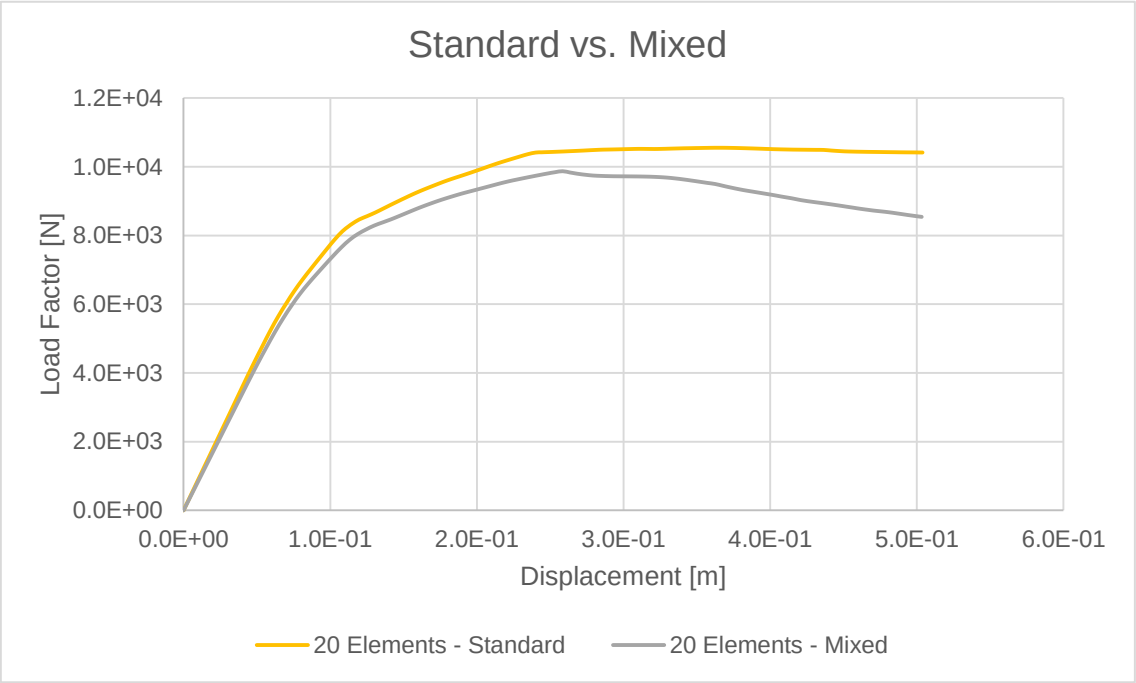

Figure 20. Non-linear analysis comparison. 20 Elements and 25 Gauss points

This outcome can be explained by the number of elements through the thickness used in the models, the ability of element to create a mechanism and the high fracture energy used.

The tensile damage at the peak load and at the last step are shown in **Figure 21** and **Figure 22**.

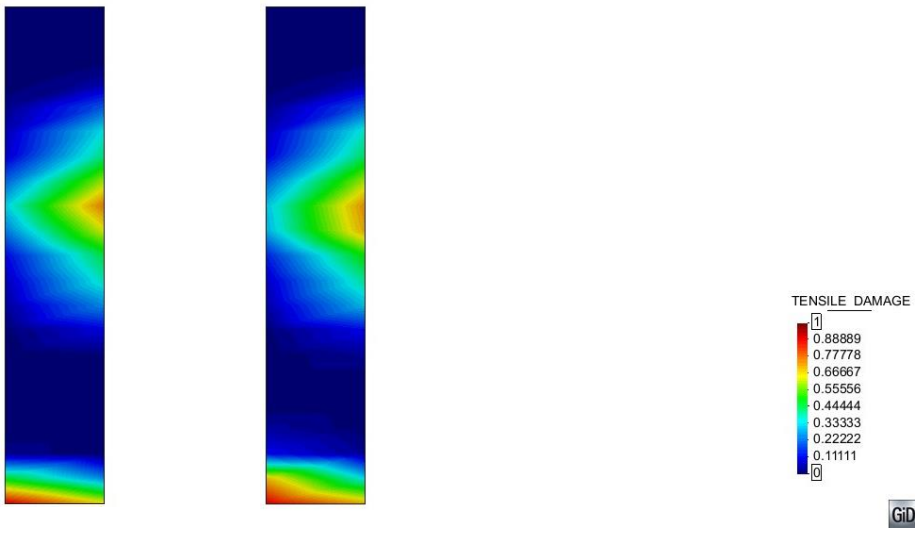

Figure 21. Tensile damage at peak load. Standard (left). Mixed (right)

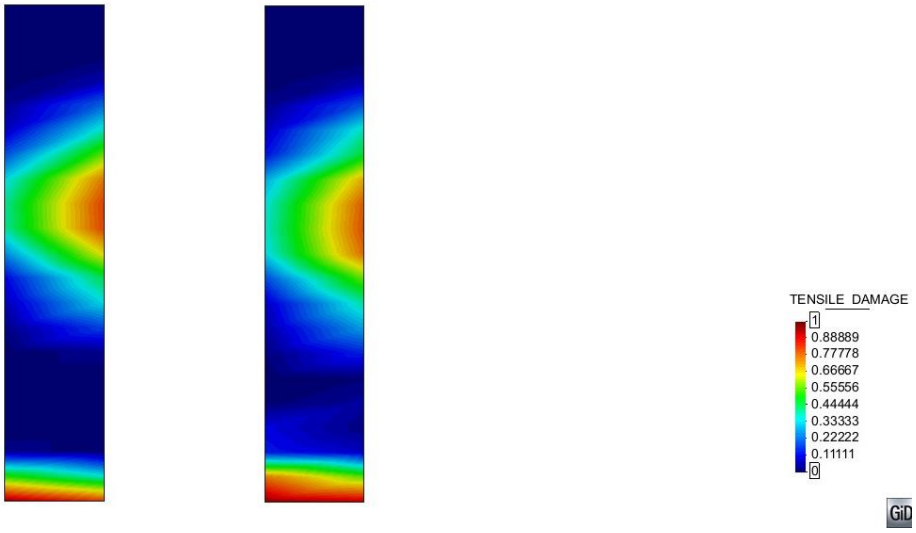

Figure 22. Tensile damage at last step. Standard (left). Mixed (right)

Both models display identical failure modes, at the first range cracks appear at the bottom of the wall generating a plastic hinge. Afterwards, due to the greater bending moments on the right side of the wall, cracks are generated at around 3/5 of the spam (point B at **Figure 5**).

At **Figure 21** and especially at **Figure 22**, a greater tensile damage appears at the mixed element, generating the softening behaviour shown in the graphs shown above.

5.4 Finite element efficiency

5.4.1 Linear-elastic analysis

A comparison of the eight different models with mixed and standard element was studied in terms of the size of the model, error and computational time.

The error in displacement and tension are calculated using **Equation 3**

Equation 3. Displacement/tension error

$$Error = \left| \frac{x_{FEM} - x_{overkill}}{x_{overkill}} \right| * 100$$

Comparison results for the example 1 are shown in **Table 2**.

Table 2. Example 1 linear-elastic analysis efficiency for wall thickness 0.4m.

Element Type	**Number of elements**	**Number of nodes**	**Number of DOF**	**Displacement Error (%)**	**Stress Error (%)**	**Time (s)**
Mixed	10	22	44	39.3	2.3	≤0.016
	20	42	84	17.8	0.1	
	40	82	164	7.6	1.1	
	80	162	324	2.4	1.6	
Standard	10	22	44	14.1	15.4	
	20	42	84	6.0	5.7	
	40	82	164	3.7	3.0	
	80	162	324	3.1	2.3	

An additional assessment for the thinner wall is shown in **Table 3**.

Table 3. Example 1 linear-elastic analysis efficiency for wall thickness 0.1m.

Element Type	**Number of elements**	**Number of nodes**	**Number of DOF**	**Displacement Error (%)**	**Stress Error (%)**	**Time (s)**
Mixed	10	22	44	8.9	1.1	≤0.016
	20	42	84	5.5	1.3	
	40	82	164	2.9	1.4	
	80	162	324	1.4	1.3	
Standard	10	22	44	66.9	67.2	
	20	42	84	33.6	33.0	
	40	82	164	11.3	10.2	
	80	162	324	3.2	1.9	

Our goal is to provide accurate solutions within a certain security margin, usually a 5%. Consequently, and supported by **Table 2** and **Table 3** results, mixed finite element has consistently improved results in stress calculation, what is more, even with the coarsest mesh we achieve first-rate solutions (2.3% and 1.1% eror for 0.4m and 0.1m walls respectively). On the other hand, the standard element does need finer meshes to obtain results within the 5% error, 40 element and 80 element meshes respectively.

In terms of displacement, it is clear that slenderness is a crucial parameter. The 0.1 metres thick wall provides good results for the standard element and passable for the mixed one. However, **Table 3** proves that with lower thickness to length ratios the mixed element enhanced performance.

5.3.2 Non-linear analysis

A comparison between the 20 element models and 25 Gauss points is provided at **Table 4**. In this case, similar number of elements, nodes and DOF are used, moreover equal Gauss points are studied in both models. As for the computational time, the mixed element is 1.376 times superior to the classical element elapsed time.

Table 4. Example 1 non-linear analysis efficiency.

Element Type	**Number of elements**	**Number of nodes**	**Number of DOF**	**Gauss Points**	**Time (s)**
Mixed	20	42	84	25	0.516
Standard					0.375

5.5 Conclusions of the example

The conclusions for the wall supported on two sides' example are:

- Displacement convergence is slenderness dependent, for typical beam slenderness (greater than L/8) the mixed element convergence rate is faster, nevertheless for thicker elements the classical element does.
- Stabilized mixed formulation shows faster convergence rate and accuracy in terms of stress and strain without any slenderness depended phenomena.
- Computational time for the elastic range proves the enhanced precision-to-time performance of stabilized mixed formulation.
- Results are consistent in the plastic range using all elements.
- Peak load and dissipated energy are reduced over mesh refinement and increase of Gauss points.
- Mixed and standard element have similar results up to the peak load, then standard element mechanism is not as pronounced.
- Mixed elements show accentuated softening and failure mechanisms.
- A minimum of 9 integration points through the thickness for the mixed element and 16 for the standard element are necessary for achieving accurate results.
- Inelastic range results for irreducible method provide faster solutions (27.3%) with similar accuracy and damage pattern, nonetheless damage intensity and extension are not as heightened as MFEM outcome.

6. Example 2 – Clamped arch

6.1 Description of the model

The second example is based on the numerical analysis studied by Cervera et al. [1], in which an arch, radius 10m and thickness 1m, fixed on both ends is subjected to a vertical point load applied at the key of the structural element.

In the original paper a comparison between linear displacement, linear strain/displacement, bilinear displacement, bilinear displacement/strain and bilinear displacement with enhanced strains was carried out, with an outstanding results in the last of them. Nevertheless, Cervera's research implemented the use of more than one element through the thickness of the arch, on the contrary this thesis is aiming to achieve a successful comparison between stabilized mixed and irreducible formulation with only one element through thickness.

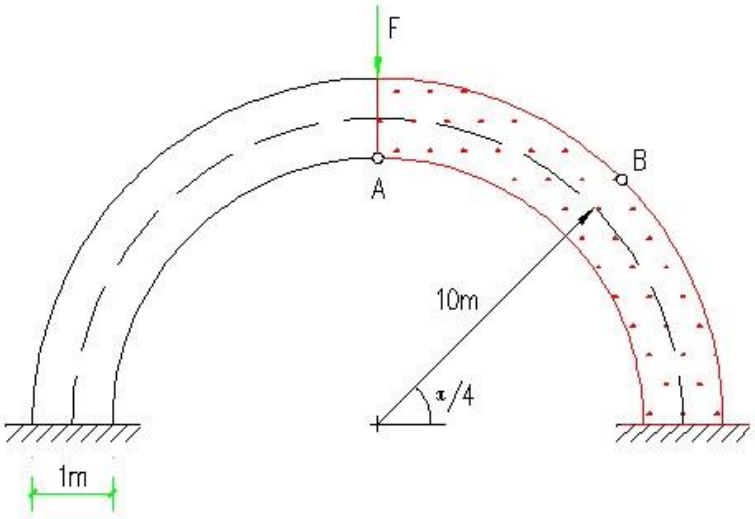

Figure 23. Clamped arch geometry

6.1.1 Mesh characteristics

Since the geometry and the load characteristics are symmetrical, only half of the clamped arch was considered (shown in red at **Figure 23**).

On the free end of the arch the horizontal translations are fixed and at the end of the arch all translation and rotations are fixed, shown in **Figure 24**.

A total of eight different meshes were applied, using 10, 20, 40, 80, 160, 320, 640, 1280 and 2560 elements, both mixed and standard finite element meshing characteristics are identical. Moreover and overkill solution with several elements through the thickness of the clamped arch is provided.

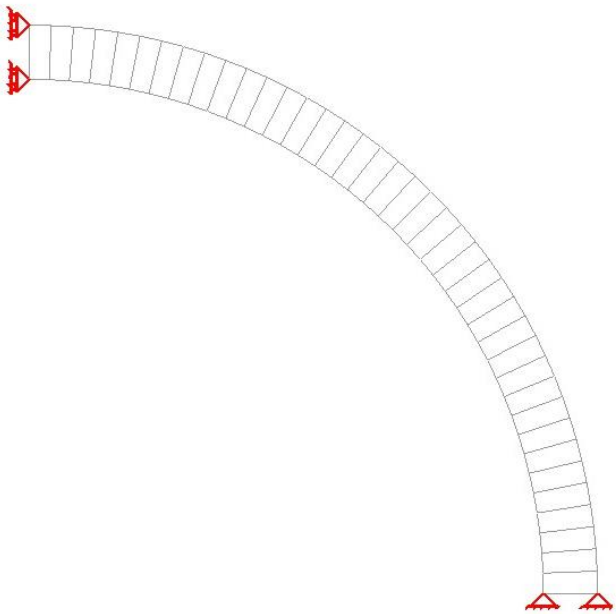

Figure 24. Clamped arch constraints (40 elements mesh).

6.1.2 Material parameters

A typical Young's modulus and Poisson's ratio of the steel are used in the numerical modelling. Additionally a high fracture energy and tensile strength were used to ensure a stable nonlinear analysis.

Table 5 summarises the material parameters used in the analysis.

Table 5. Example 2 material parameters

Young's modulus	200 GPa
Poisson's ratio	0.3
Tensile strength	3.0 MPa
Fracture energy	$1.0*10^5$ Nm/mm2

6.2 Linear analysis results

A point load of 1N is applied at the key of the arch. Vertical displacement under the load at the top of the arch's internal face (point A at **Figure 23**) and the principal stress at outer face of the arch at 45° with respect the horizontal axis (point B at **Figure 23**) are compared for all models. The displacement are plotted in function of the total number of elements. An overkill solution with 100 elements through the thickness of the arch was calculated.

Figure 25 shows similar results for the mixed finite element and the standard finite element in terms of displacement. On one hand the mixed finite element shows a difference between the finest mesh (2560 elements) and the coarsest mesh (10 elements) of 37.7%, on the same basis, the standard element shows a 38.1% difference. However, the convergence provided by the standard element is the fastest, if we repeat the mesh comparison with a mesh of only 320 elements we achieve a difference of 0.06%. In the same scenario the mixed element is still 8% away from the finest mesh solution.

In addition, there is a significant difference between the overkill solution and the converged solution for both of the elements. This is due to the modelling procedure used in this example, in which only one element through the thickness is considered cannot effectively approximate the curved structural beam stress distribution along a cross-section, as a result this phenomena is observed

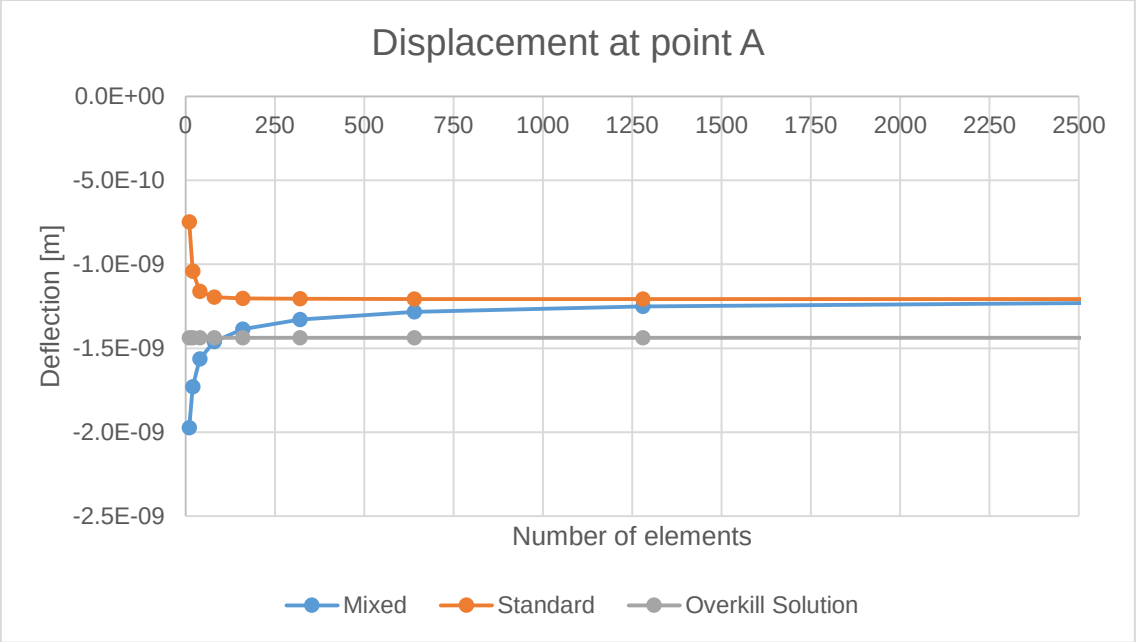

Figure 25. Convergence of the vertical displacement with mesh refinement.

Figure 26 shows the principal stress at point B. The mixed element provides excellent results even with the coarsest mesh, with a difference between the 10 element mesh and the 160 element mesh of only 5%. Using the same comparison but for the standard element, the difference is 127.3%. Thus, the mixed finite element has a clear improved behaviour in terms of principal stress approximation.

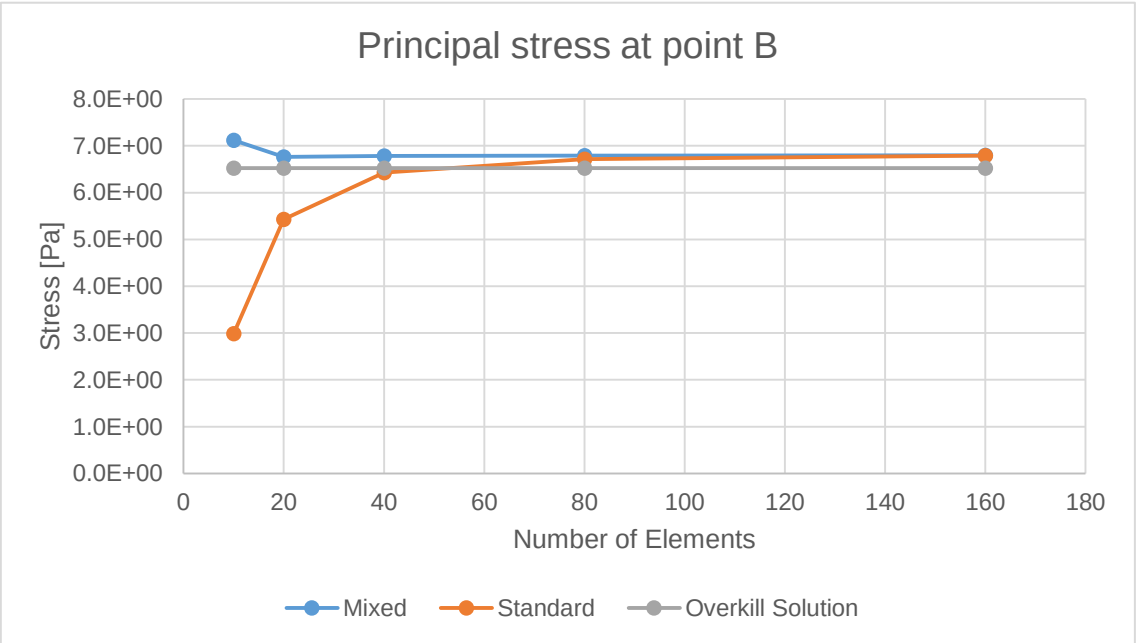

Figure 26. Convergence of the principal stress with mesh refinement

I have to highlight the fact that the deflection outcome from the converged standard and mixed elements clearly does differ from the overkill solution. However, in this case there is another reason apart from the elements through thickness. The difference is given that the stress distribution along the cross-section of a curved element is not constant, as in the standard element, or linear, as in the mixed element, but has a component depending on the radius of curvature.

Equation 4. Curved member stress distribution along the cross-section.

$$\sigma = \frac{My}{Ae(r_n - y)}$$

$$\sigma: stress$$

$$M: bending\ moment$$

$$y: distance\ from\ neutral\ axis\ to\ point\ of\ interest$$

$$A = cross - section\ area$$

$$e: distance\ from\ centroidal\ axis\ to\ neutral\ axis$$

$$r_n: radius\ of\ neutral\ axis$$

The maximum principal stress and vertical displacements for the finest mixed finite element mesh (2560 elements) are shown in **Figure 27**.

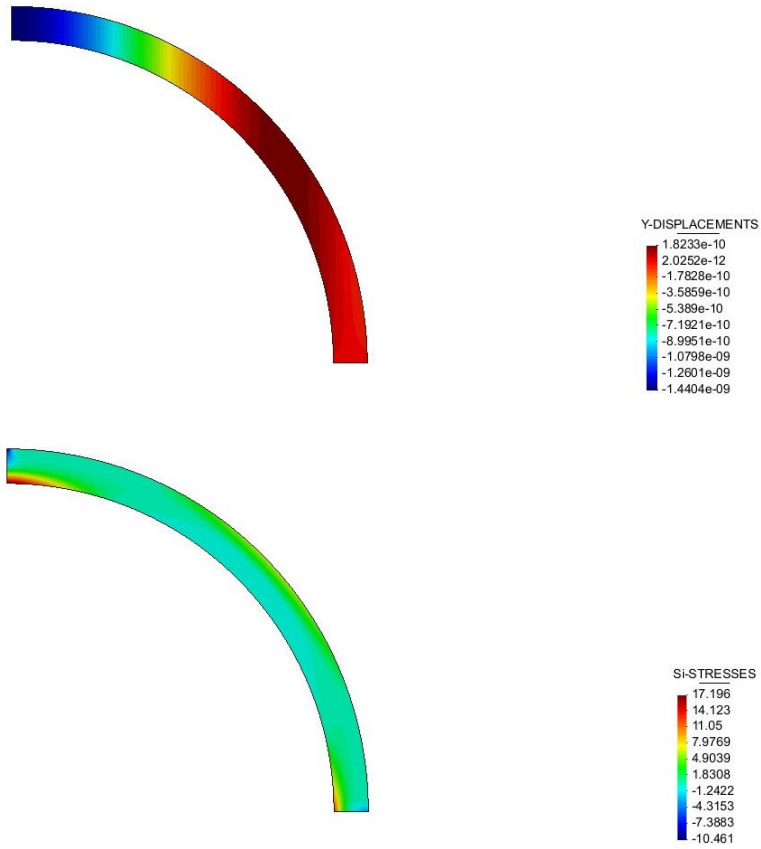

Figure 27. Clamped arch displacement/stress results

Since the number of elements through thickness is restricted to one, the results achieved in the displacement field for the mixed element are not as good as expected. As a result, a further study for the slenderness of the arch is provided. Cervera et al. [1] original model has a slenderness of 1/10 and in the second analysis an arch of 1/50 is used to compare irreducible and stabilized mixed formulations.

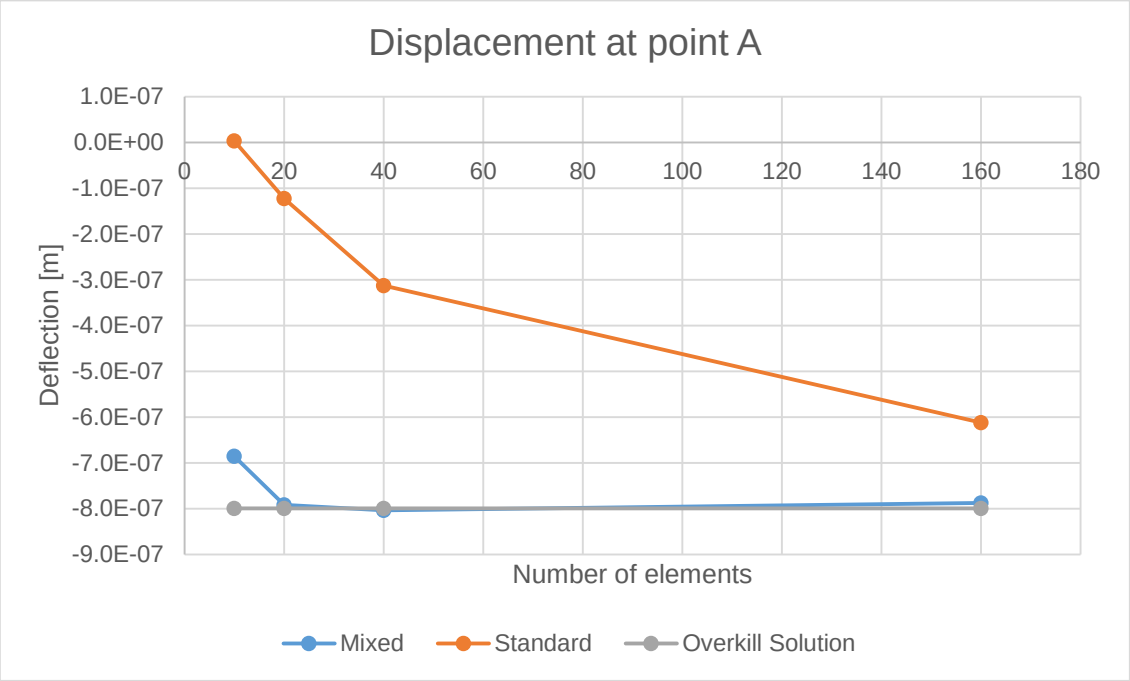

Figure 28. Convergence of vertical displacement with mesh refinement

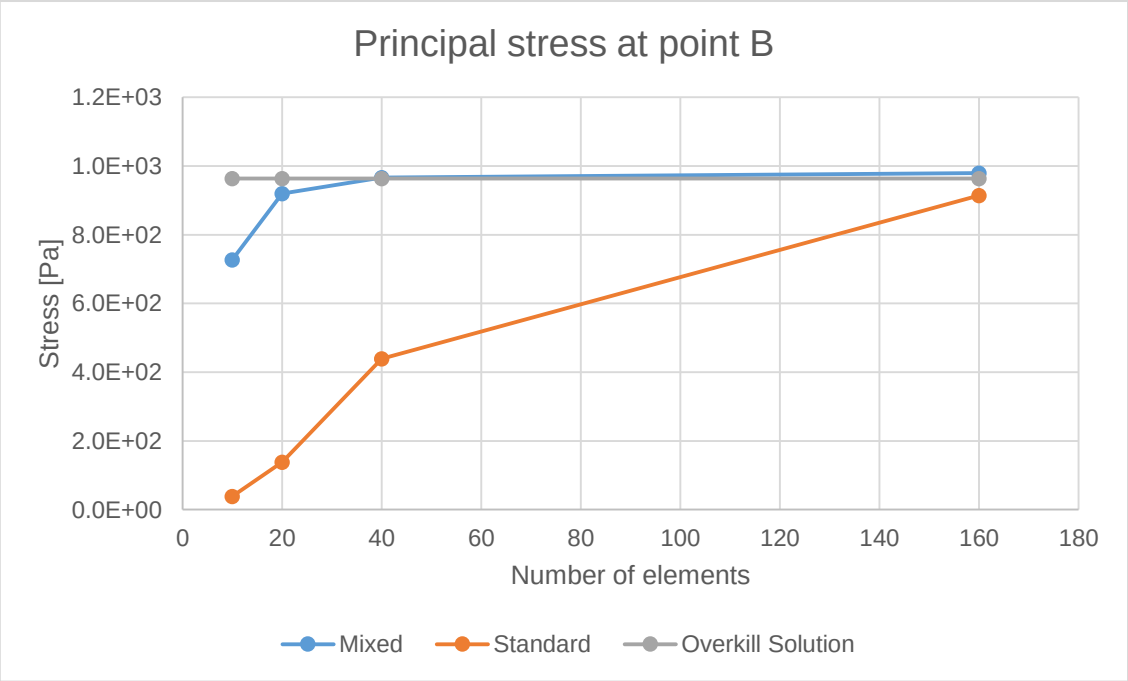

Figure 29. Convergence of principal stress with mesh refinement

The reduction of thickness in the arch has a clear positive effect in the convergence rate and accuracy of the mixed element, besides it counteracts the lack of elements through the thickness.

6.3 Non-linear analysis results

Three models were used in the non-linear analysis of the clamped arch, 20, 40 and 80 elements. For all results a force-displacement curve at point A is plotted, an amplitude of 10^6 is used for the load.

6.3.1 Mesh sensitivity

The results from both models are similar to the previous example, the two of them display a decrease of the peak load and the dissipated energy as the mesh is refined.

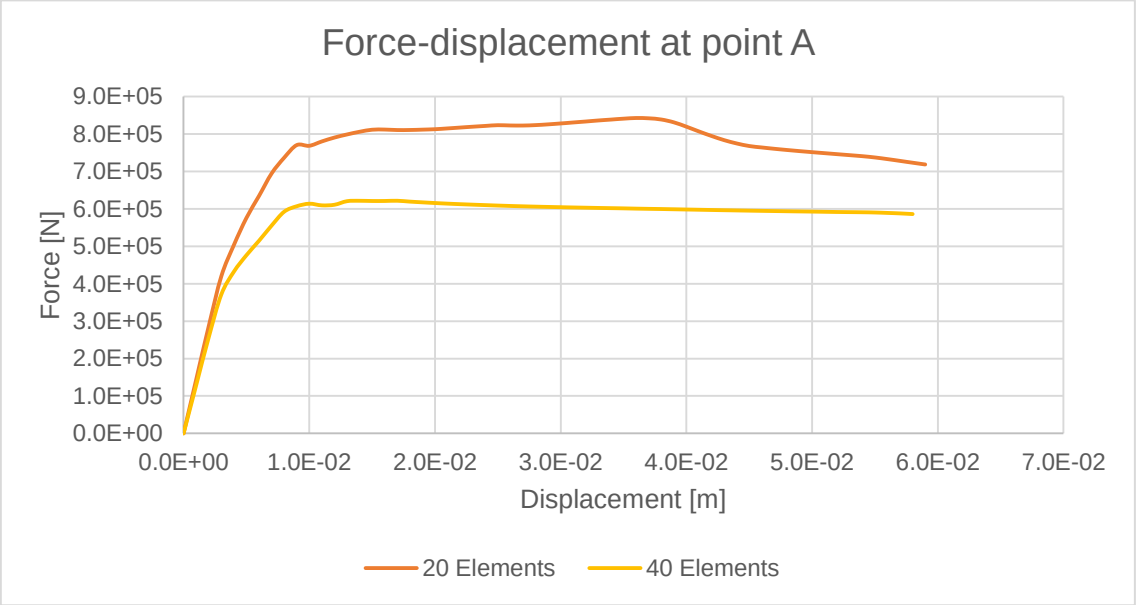

Figure 30. Standard finite element non-linear mesh sensitivity analysis results

Mixed element force-displacement curves have a lower peak force and with a clear softening behaviour, which is not present at the standard element.

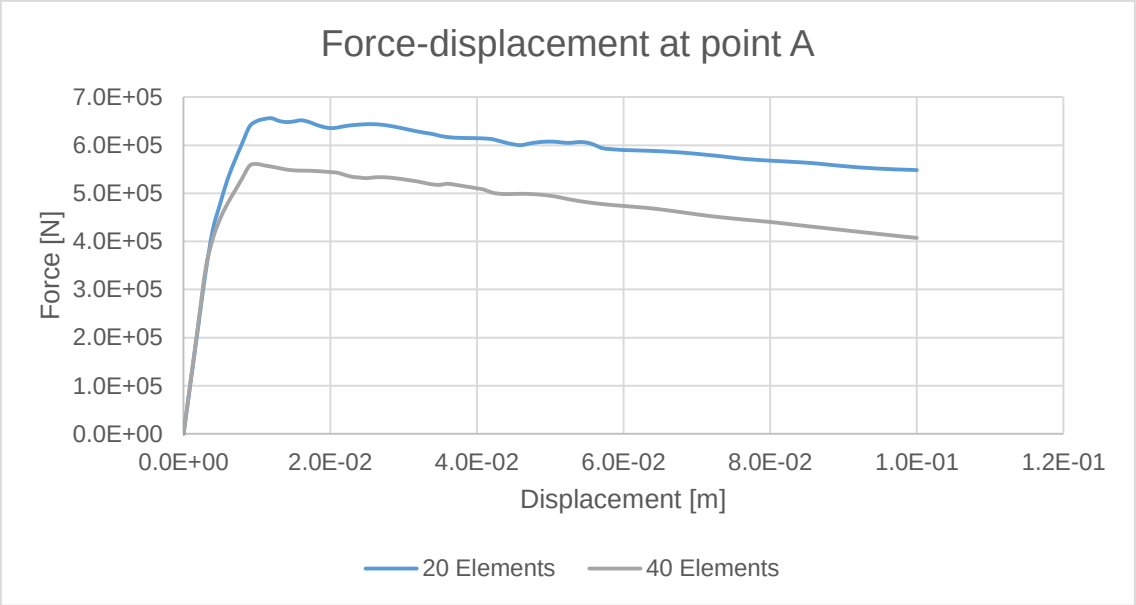

Figure 31. Mixed finite element non-linear mesh sensitivity analysis results

6.3.2 Integration through thickness

An investigation of the integration point through the element thickness using 9, 16 and 25 Gauss points is provided. For convenience, 9 and 25 Gauss points graphs are shown.

Standard element force-displacement curve using 9, 16 and 25 integration points and the 40 and 80 elements mesh have convergence problems. In the total of six cases, five of them do not converge after the elastic range and only in the most refined mesh with 25 Gauss points we can observe a fully non-linear force-displacement response.

Regarding the mixed finite element, convergence problem appears at the finest mesh, 80 elements, with 9 and 16 integration points.

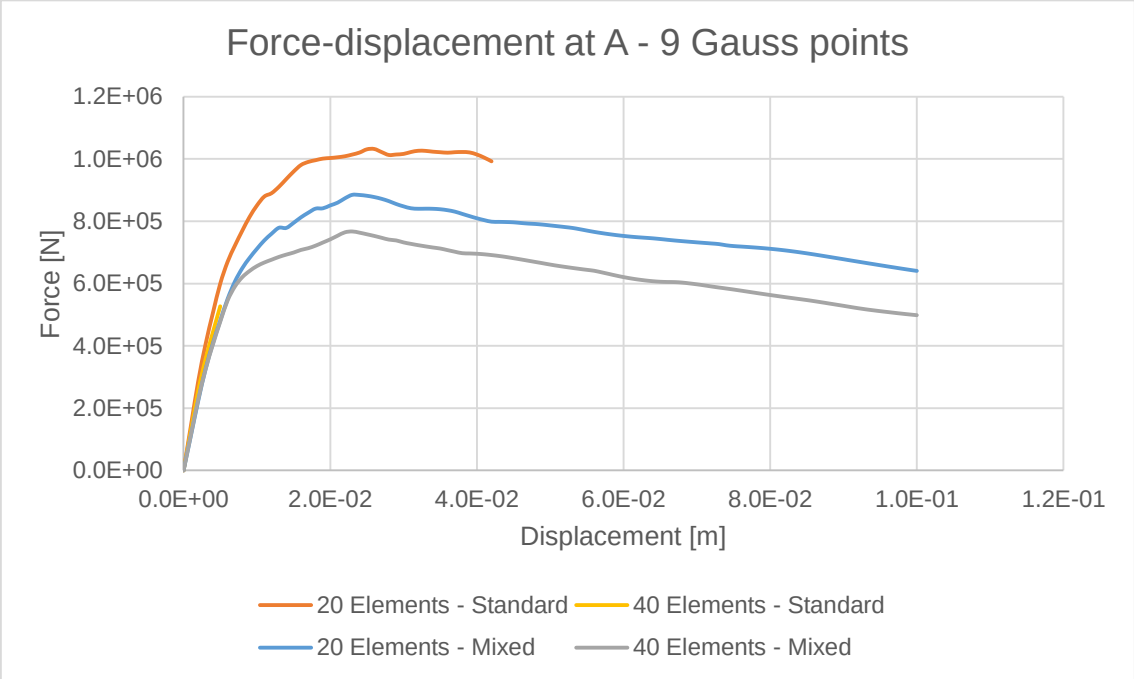

Figure 32. Non-linear analysis results comparison. 9 Gauss points

Figure 33 and **Figure 34** draw the results from 25 Gauss for irreducible and stabilized mixed formulations, good consistency is present, especially for the mixed element. Some irregularities are present in the coarsest mesh of 20 elements and are refined as the mesh scales down.

Results are in the line with the first example, where a softening behaviour can be clearly seen in the mixed element, at the same time the standard element has a higher peak-load that is slowly attenuated.

The consistency in the mixed element peak load results is outstanding, being 8.92E+05 and 7.98E+05 the coarsest and finest mesh results, where in the standard element is 1.14E+05 and 8.82E+05. As in the previous example, the refinement of the mesh and the increment of integration points tends the irreducible method solution to the stabilized mixed element force-displacement curve.

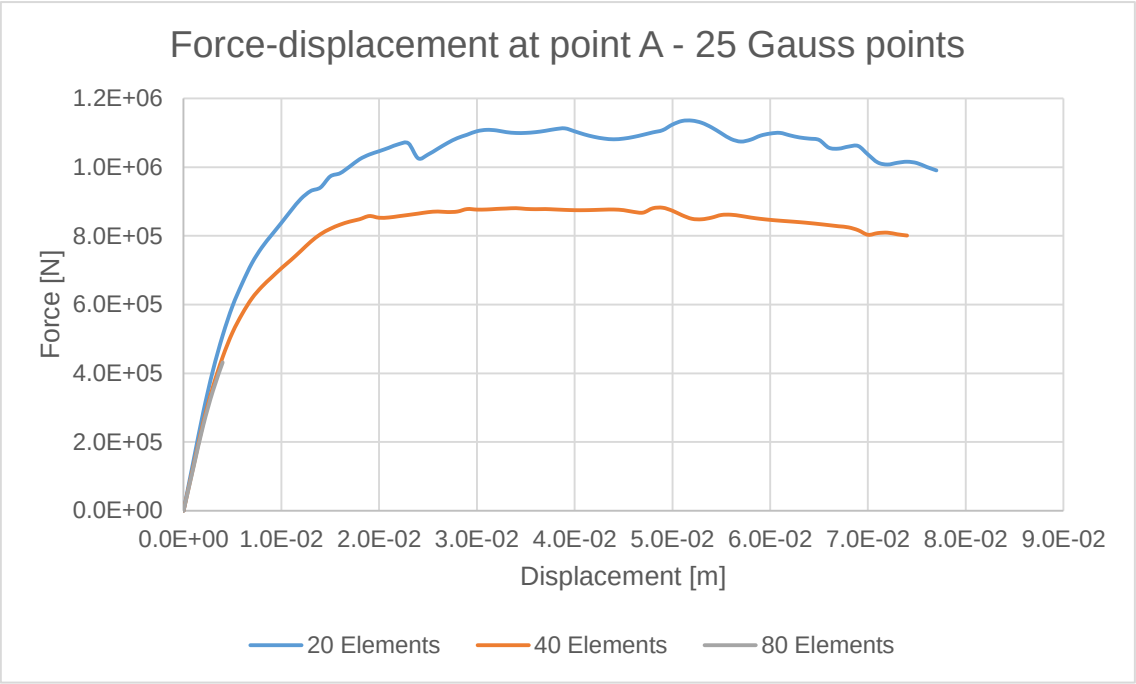

Figure 33. Standard finite element non-linear 25 Gauss points analysis results

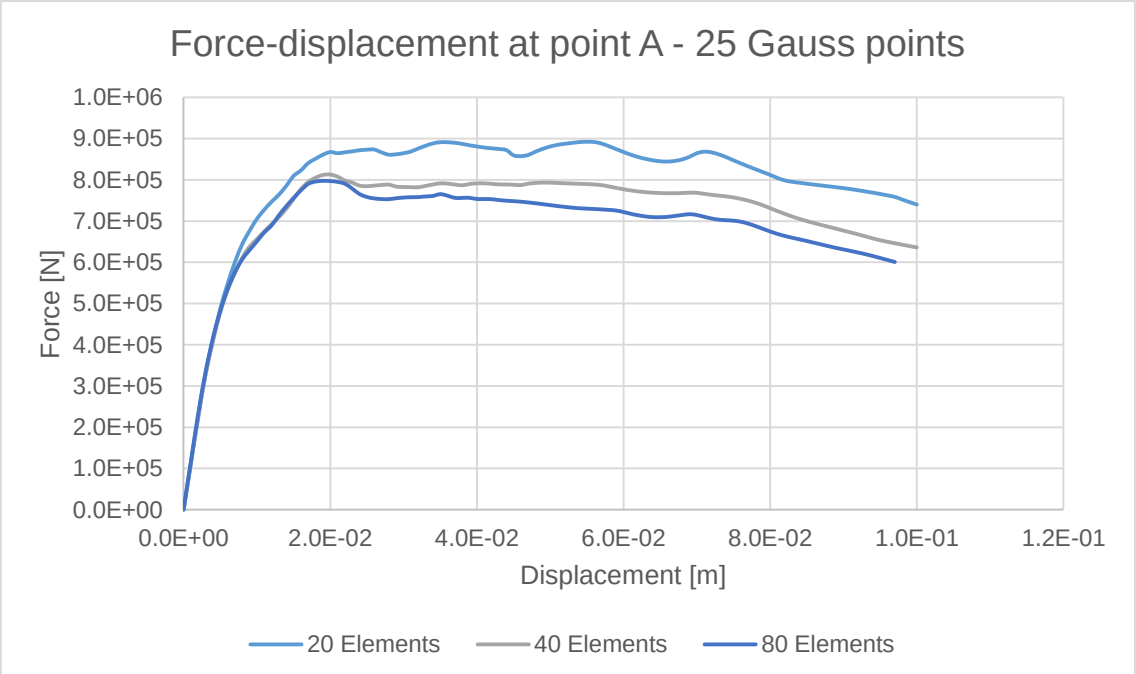

Figure 34. Mixed finite element non-linear 25 Gauss points analysis results

6.3.3 Non-linear results comparison

The comparison between both methods uses the 40 elements mesh with 25 Gauss points as reference.

Excellent match in the elastic behaviour is shown but with slightly different peak load and softening, additionally the standard element does not converge up to the final step, therefore the last step comparison will be determined by the standard element.

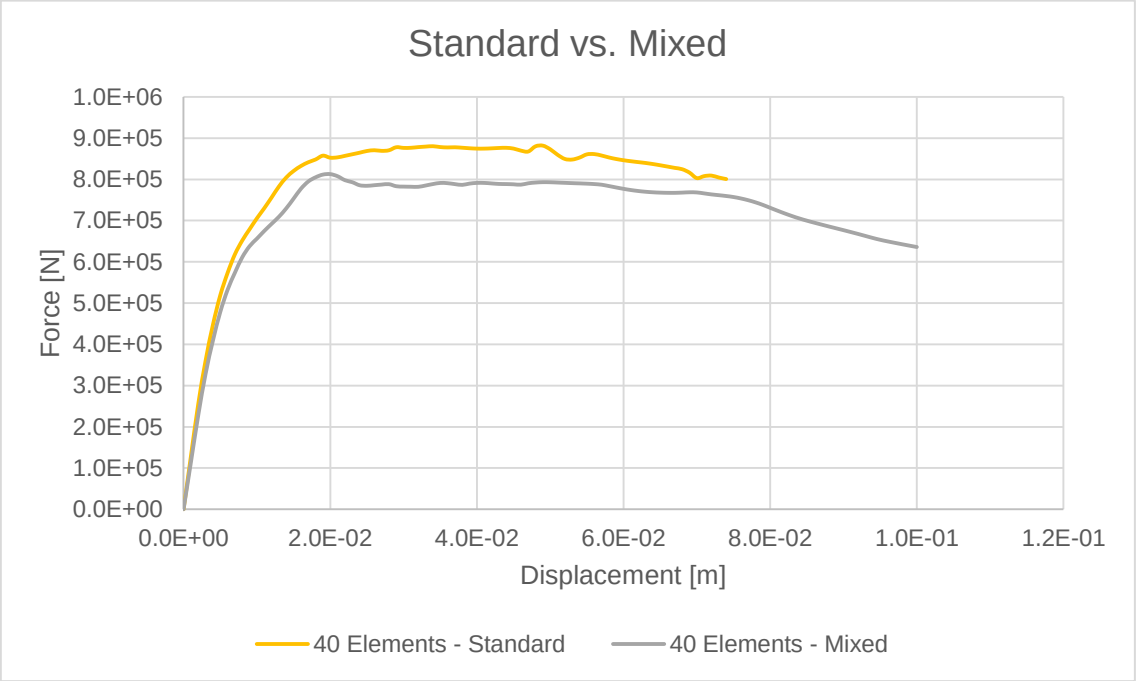

Figure 35. Non-linear analysis comparison. 40 Elements and 25 Gauss points

The tensile damage at the peak load and the last time step are shown in **Figure 36** and **Figure 37**.

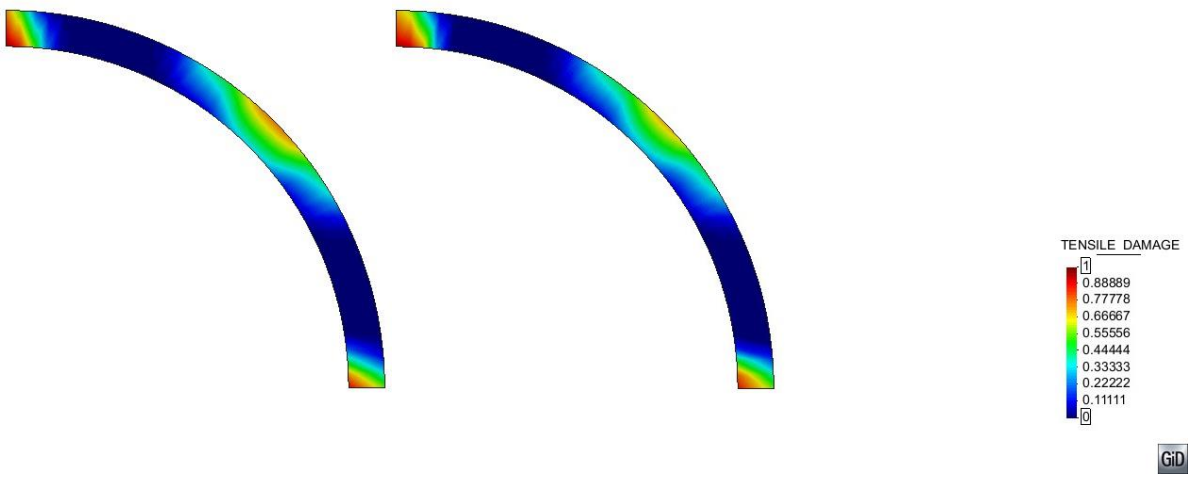

Figure 36. Tensile damage at peak load. Standard (left). Mixed (right)

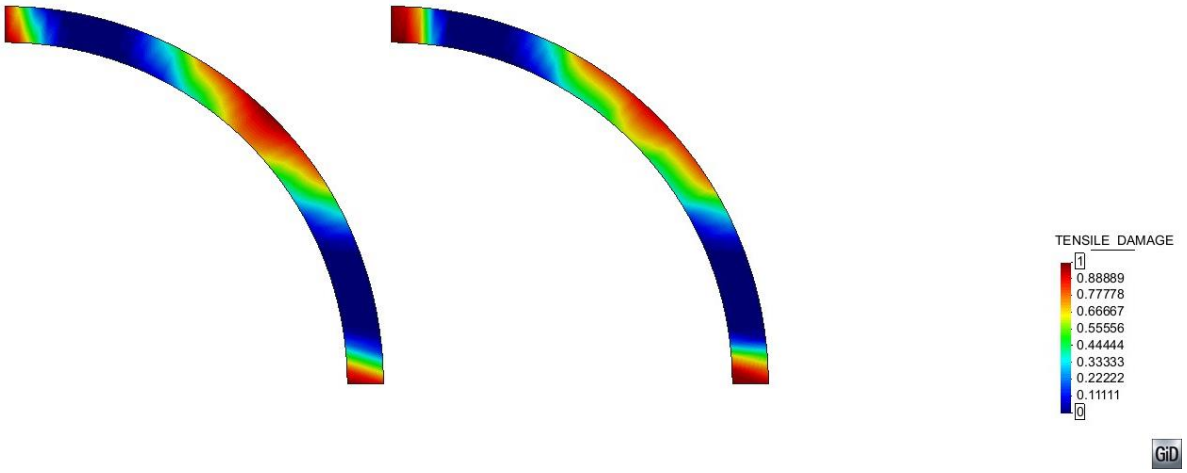

Figure 37. Tensile damage at last step. Standard (left). Mixed (right)

Standard and mixed element show the same failure mode. First plastic cracks appear at the arch´s supports and key, as the load increases, a third plastic hinge appears at 45° with respect the horizontal axis and the mechanisms is formed.

As **Figure 37** shows, the standard element tensile damage results are slightly different to the mixed ones. The classical element model has greater damage at point B while the mixed element model has a maximum tensile damage present at the key of the arch and the supports. The latter is the responsible for the emphasised softening behaviour of the mixed element with respect the standard element.

6.4 Finite element efficiency

6.4.1 Linear-elastic analysis

A comparison of the nine model for each FEM was made in terms of the size of the model, error and computational time is carried out.

Table 6. Example 2 linear-elastic analysis efficiency for arch slenderness 1/10.

Element Type	**Number of elements**	**Number of nodes**	**Number of DOF**	**Displacement Error (%)**	**Stress Error (%)**	**Time (s)**
Mixed	10	22	44	37.4	9.1	0.031
	20	42	84	20.3	3.6	0.031
	40	82	164	8.8	3.9	0.047
	80	162	324	1.6	4.0	0.078
	160	322	644	3.5	4.1	0.094
	320	642	1284	7.5	4.2	0.188
	640	1282	2564	10.7	4.3	0.297
	1280	2562	5124	13.0	4.4	0.531
	2560	5122	10244	14.4	4.4	1.016
Standard	10	22	44	48.0	54.2	0.016
	20	42	84	27.5	16.9	0.031
	40	82	164	19.3	1.6	0.047
	80	162	324	16.9	2.9	0.062
	160	322	644	16.3	4.0	0.047
	320	642	1284	16.1	4.3	0.078
	640	1282	2564	16.1	4.4	0.172
	1280	2562	5124	16.1	4.4	0.266
	2560	5122	10244	16.1	4.4	0.500

Computational comparison for the 1/10 slenderness arch is shown in **Table 6**, however the second example displacement and stress error is severely affected by the non-linear strain/stress distribution along the cross-section of a curved beam element.

As a result, the 1/50 slenderness arch will be used for the FEM comparison. Regarding the stress convergence, stabilized mixed formulation models achieve a satisfactory equilibrium differing 1.7% from the overkill solution elapsing only 0.188 seconds, on the other hand the irreducible model outcome obtains an identical precision by means of the finest mesh, elapsing 0.438 seconds.

Displacement error is not satisfactorily achieved by either of the FEM, not even with a slenderness of 1/50. Nonetheless, standard element shows consistency, for the 1/10 slenderness arch a difference of 16.1% is achieved in 0.078 seconds, while in the 1/50 arch a disparity of 18.3 elapsing 0.250 seconds. On the contrary, the mixed element provide a more accurate solution but without a clear convergence tendency.

Concluding, irreducible formulation has an improved behaviour in displacement convergence whereas mixed formulation imposes in stress/strain approximation and time consumption.

Table 7 Example 2 linear-elastic analysis efficiency for arch slenderness 1/50.

Element Type	**Number of elements**	**Number of nodes**	**Number of DOF**	**Displacement Error (%)**	**Stress Error (%)**	**Time (s)**
Mixed	10	22	44	14.2	24.6	0.031
	20	42	84	1.0	4.6	0.047
	40	82	164	0.5	0.3	0.078
	80	162	324	1.0	0.9	0.081
	160	322	644	1.5	1.6	0.094
	320	642	1284	3.3	1.7	0.188
	640	1282	2564	5.8	1.7	0.344
	1280	2562	5124	8.8	1.7	0.516
	2560	5122	10244	11.9	1.7	1.109
Standard	10	22	44	100.4	96.0	0.016
	20	42	84	84.6	85.6	0.031
	40	82	164	60.9	54.5	0.047
	80	162	324	42.2	11.5	0.062
	160	322	644	23.5	5.2	0.094
	320	642	1284	19.6	0.1	0.141
	640	1282	2564	18.6	1.3	0.234
	1280	2562	5124	18.3	1.6	0.250
	2560	5122	10244	18.2	1.7	0.438

6.4.2 Non-linear analysis

A computational cost comparison between the 40 element models and 25 Gauss points is provided in **Table 8**.

Table 8. Example 2 non-linear analysis efficiency.

Element Type	**Number of elements**	**Number of nodes**	**Number of DOF**	**Gauss Points**	**Time (s)**
Mixed	40	42	84	25	5.516
Standard					5.125

Akin model size is compared, above and beyond time consumed in the numerical computational solving is for the MFEM is only 7.6% higher than the irreducible formulation.

6.5 Conclusions of the example

The conclusions for the clamped arch example are:

- Displacement is a slenderness dependent parameter in the MFEM 2D curved structural elements; lower length to thickness ratios provide better solutions, however greater than L/10 results are similar to irreducible method.
- One element through thickness and curved structural element stress/strain cross-section distribution produce a constant error, proportional to r/10, in principal stress approximations.
- Stabilized mixed method show faster convergence rate without any slenderness dependency.
- Computational analysis in the linear-elastic range show more accurate solutions in a shorter computational time for the MFEM.
- Irreducible formulation show convergence problems in inelastic range using few Gauss points and/or thinner meshes.
- Stabilized mixed formulation show excellent consistency in inelastic range, except for thinner mesh models using 4 and 9 interpolation points.
- Peak load and dissipated energy are reduced over mesh refinement and increase of Gauss points for both FEM.
- Integration through thickness analysis show that mixed elements results with 9 integration points are sufficient, however, standard element requires a minimum of 25 integration points.
- Similar peak-load, mechanisms and softening approximations is obtained.
- Tensile damage location is akin for both formulations, however the intensity present at point B is greater for the classical element models, while the damage intensity at the fix end and under the point load is greater in the mixed element models.
- Computational for inelastic range applying irreducible formulation show a slightly faster solutions (7.0%). On the contrary MFEM stress/strain approximation and interpolation are more precise, providing marked failure mechanisms.

7. Example 3 – Wall supported on three sides

7.1 Description of the model

The next two examples are a couple of three dimensional wall structures subjected to out-of-plane load, extracted from Gazzola et al.[34] and numerically analysed by Lourenço et al [35].

So as to study the displacement/stress convergence and non-linear behaviour for strainght structural members, two different examples are analysed, example 3 and 4.

In this example a wall is simply supported on three sides and a free edge on the fourth side, shown in **Figure 38**. Due to the mesh coarseness through the thickness the whole wall was modelled to ensure perfect symmetry in the elastic analysis, as for reducing computational time in the inelastic analysis only the right half of the plate was modelled.

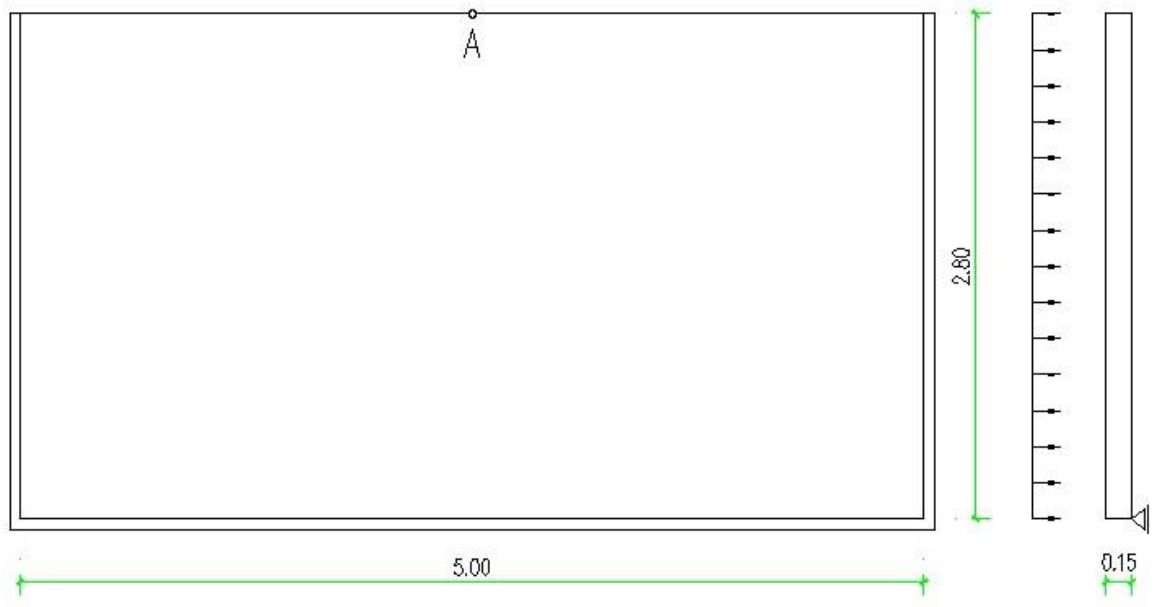

Figure 38. Wall supported on three sides' geometry

7.1.1 Mesh characteristics

On the three supported sides all out-of-plane and respectively horizontal or vertical in-plane translation and rotations are fixed, besides on the free end no restriction is applied (**Figure 39**). In the case of half wall modelling, an additional fixed in-plane translation is imposed at the wall's symmetry axis.

The meshing process uses only one element in the z-direction, through the thickness of the wall, additionally the x and y directions have the same number of divisions.

A total of eight different meshes are used, 100 (10x10), 400 (20x20), 1600 (40x40), 6400 (80x80), 10000 (100x100) and 14400 (120x120) elements respectively. Both irreducible and stabilized mixed formulation use the same meshes for the analysis.

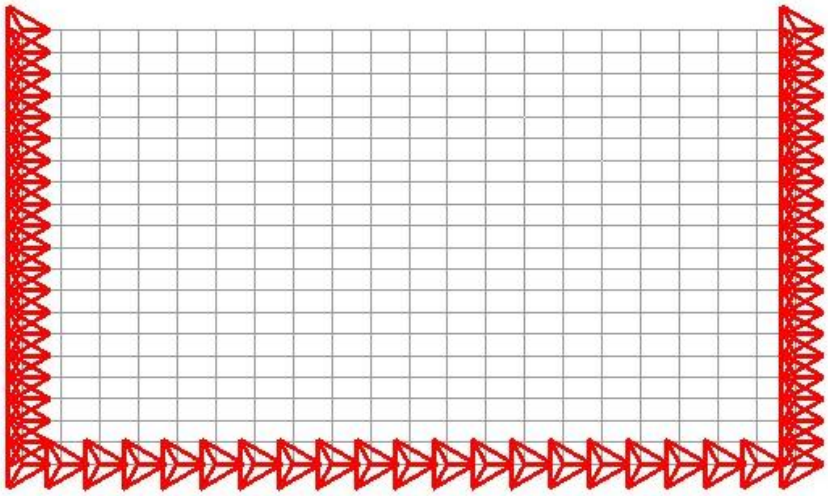

Figure 39. Wall supported on three sides' constrains and 400 elements mesh

7.1.2 Material parameters

The material parameters used by Lourenço et al. [35] are orthotropic, as a result the chosen value are extracted from the anisotropic analysis.

Table 9 summarises the material parameters used in the model.

Table 9. Example 3 material parameters

Young's modulus	5.00 GPa
Poisson's ratio	0.3
Tensile strength	2.5 MPa
Fracture energy	500 Nm/mm2

7.2 Linear analysis results

A 3000 N/M out-of-plane uniform load is applied on the wall. Out-of-plane displacement and the principal stress at the mid-point of the free edge are compared for all models (point A at **Figure 38**). Displacement and stress are plotted against the total number of elements. Finally, an overkill solution with 4 elements through thickness was calculated.

Figure 40 shows that mixed element convergence rate is clearly faster than the standard element. Take for instance the difference between the coarsest mesh, 100 elements, and the finest mesh, 14400 elements, under such criteria the classical element shows a 75.8% difference, while the mixed element only a 0.5%. Furthermore, the divergence between the overkill solution and the coarsest mesh for the mixed element is only 0.7%, at the same time the standard element has a 76%.

This results match perfectly with the conclusions extracted from example 1 and 2, which affirm that the MFEM convergence is tightly related with the slenderness of the element, being the wall slenderness approximately 1/18. Hence, we can foresee that for the 2D straight walls structural elements may occur the same phenomena.

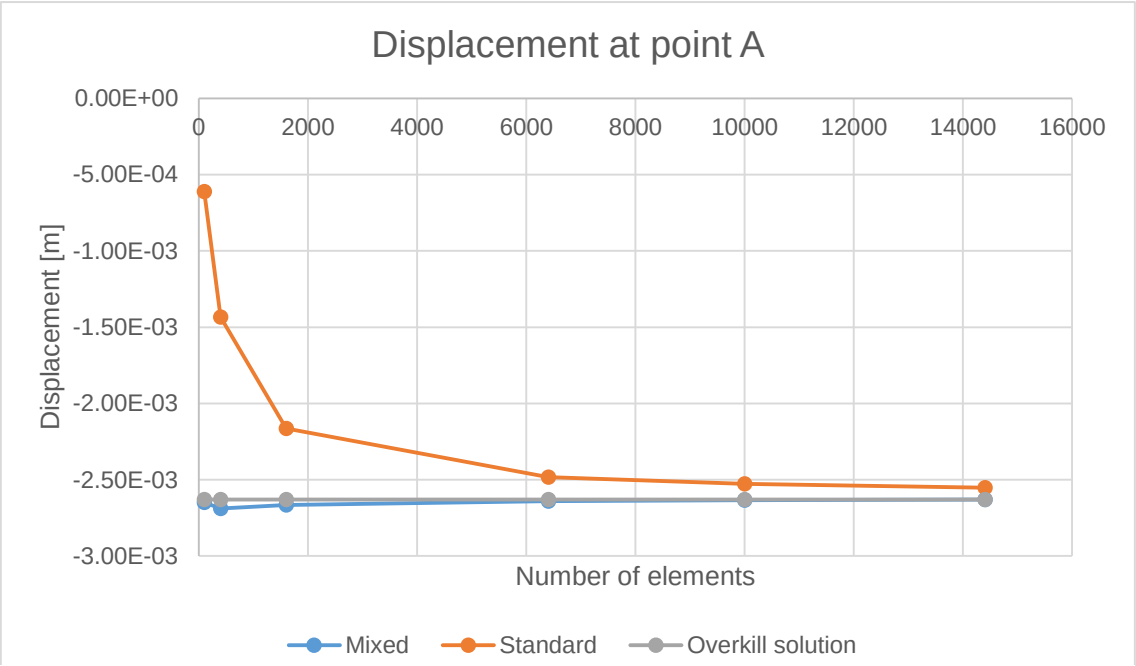

Figure 40. Convergence of the out-of-plane displacement with mesh refinement

As for the stress convergence, **Figure 41** displays again a faster approach of the stabilized mixed formulation with respect the irreducible one. If we repeat the comparison between the finest and coarsest mesh, the standard element shows a 74.3% different during the time the mixed element shows only a 7.7% disparity.

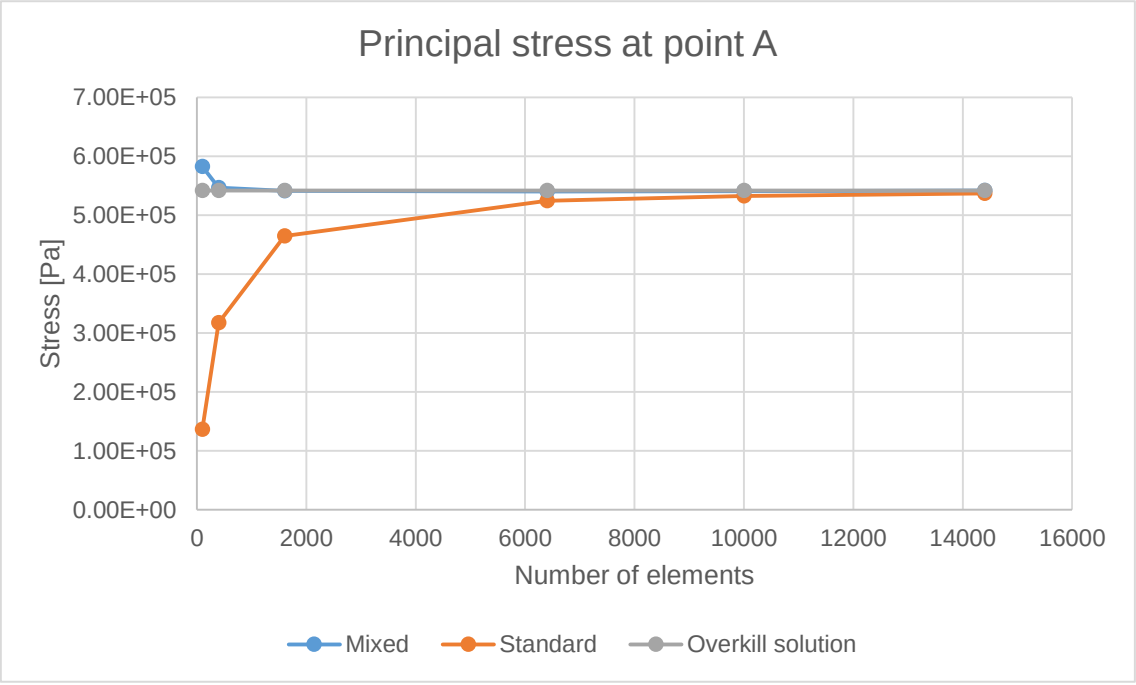

Figure 41. Convergence of the principal stress with mesh refinement

Regarding the convergence rate, **Figure 40** and **Figure 41** undoubtedly prove an enhanced performance from Cervera et al. [1-3] stabilized mixed formulation.

The out-of-plane displacement and the principal stress, loaded face on top, for the finest mixed finite element mesh (120x120 elements) are shown in **Figure 42.**

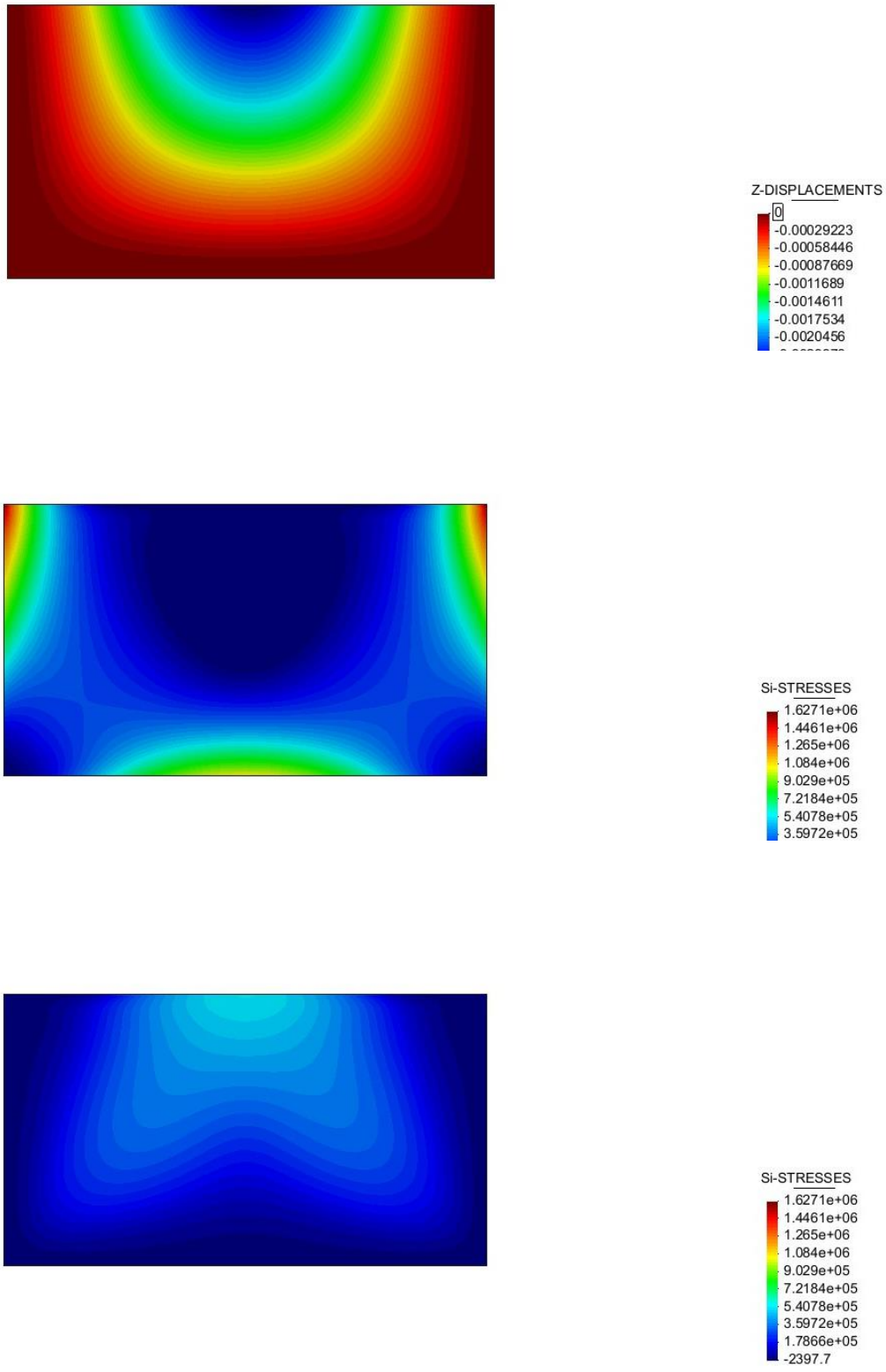

Figure 42. Wall supported on three sides displacement, loaded face stress and opposite face stress results

7.3 Non-linear analysis results

Two models were used in the non-linear analysis of the wall, 100 and 400 elements. All results show the force-displacement (load factor-displacement) curve at the middle of the free edge.

7.3.1 Mesh sensitivity

The non-linear analysis for the irreducible form is displayed in **Figure 43**. Mesh refinement decreases the peak load and dissipated energy, good consistency is observed.

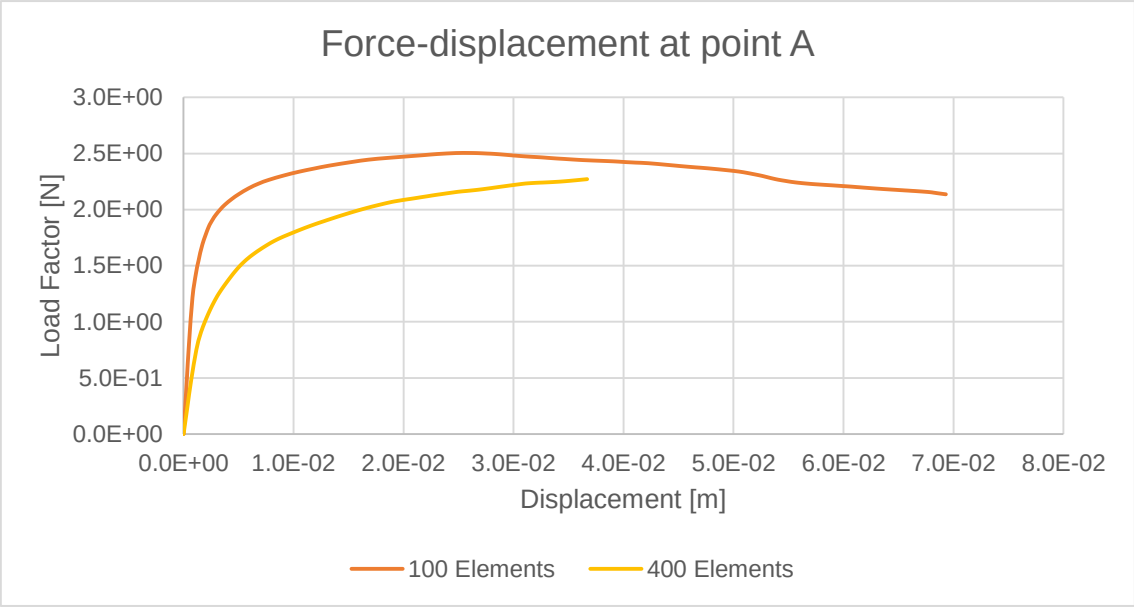

Figure 43. Standard finite element non-linear mesh sensitivity analysis results

MFEM results are shown in **Figure 44**. Similar outcome in terms of dissipated energy and peak load can be extracted. Additionally, the peak load achieved at the MFEM are consistently lower than the classical element results.

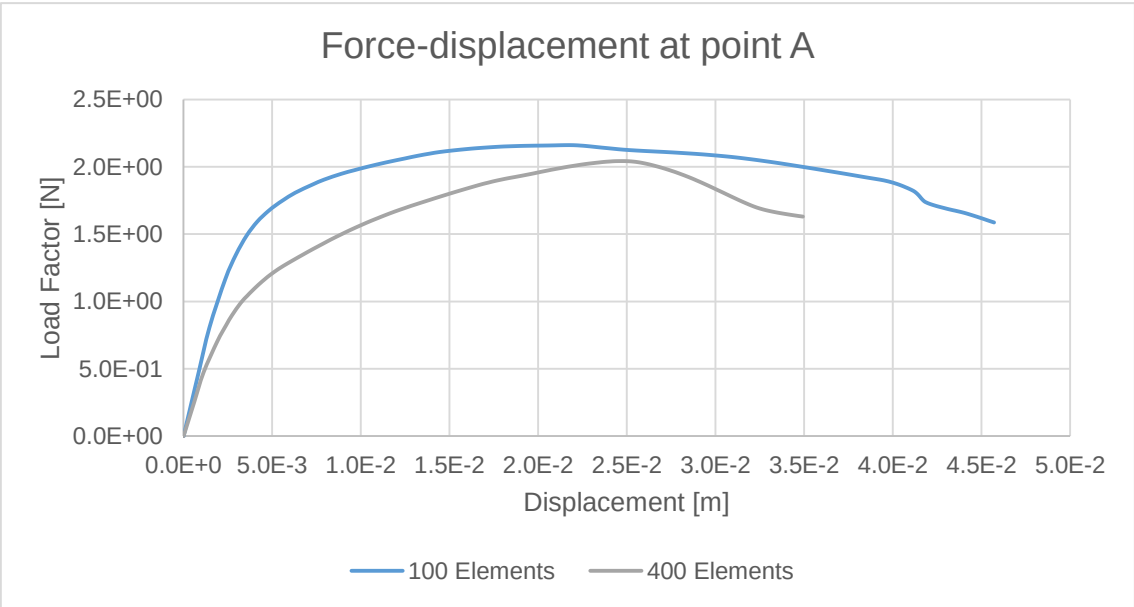

Figure 44. Mixed finite element non-linear mesh sensitivity analysis results

7.3.2 Integration through thickness

In this example only 27 Gauss points models are used, due to instabilities in the irreducible method for further integration points (64 and 125), the force-displacement graphs are not valid for a comparison.

Figure 45 shows a comparison between mixed and standard finite element models. The graph show an enhanced consistency of the mixed element; the mesh refinement approaches the standard element peak load results to the mixed element ones.

Moreover, if we increase the elements through thickness, using two or four, it is clear that the mixed element has a better behaviour in terms of peak load and softening.

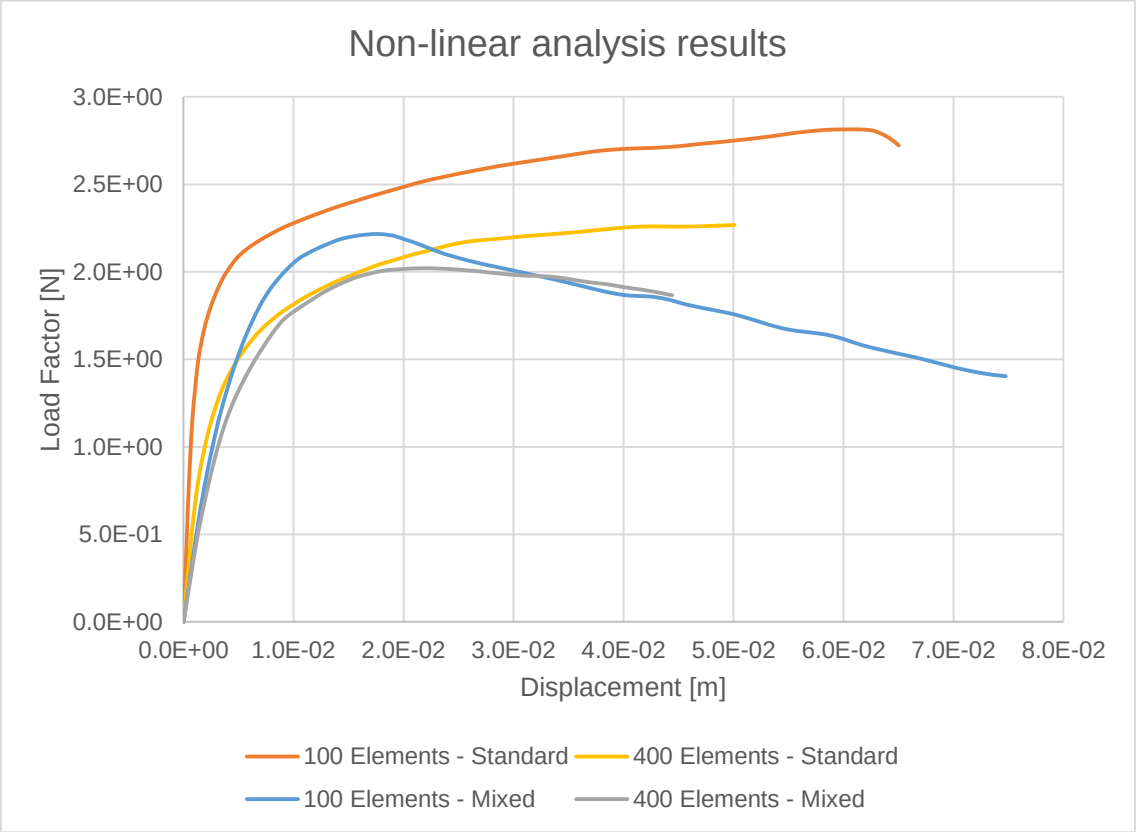

Figure 45. Non-linear analysis results comparison. 27 Gauss points

7.3.3 Non-linear results comparison

For the third example a comparison between the 27 Gauss points models for a 400 element mesh was studied, shown in **Figure 46**. Similar results for the early linear range is shown. Even though the standard element does not have a clear peak load and afterwards softening behaviour, we will assume it to happen at the same time that the mixed element model.

Two time steps are considered in the tensile damage comparison, the peak load and the last step, which is also determined by the mixed element due to the early fracture of the latter.

Furthermore, tensile damage at the loaded face and the opposite is compared, extension, intensity and location of the damage, as well as failure mechanism.

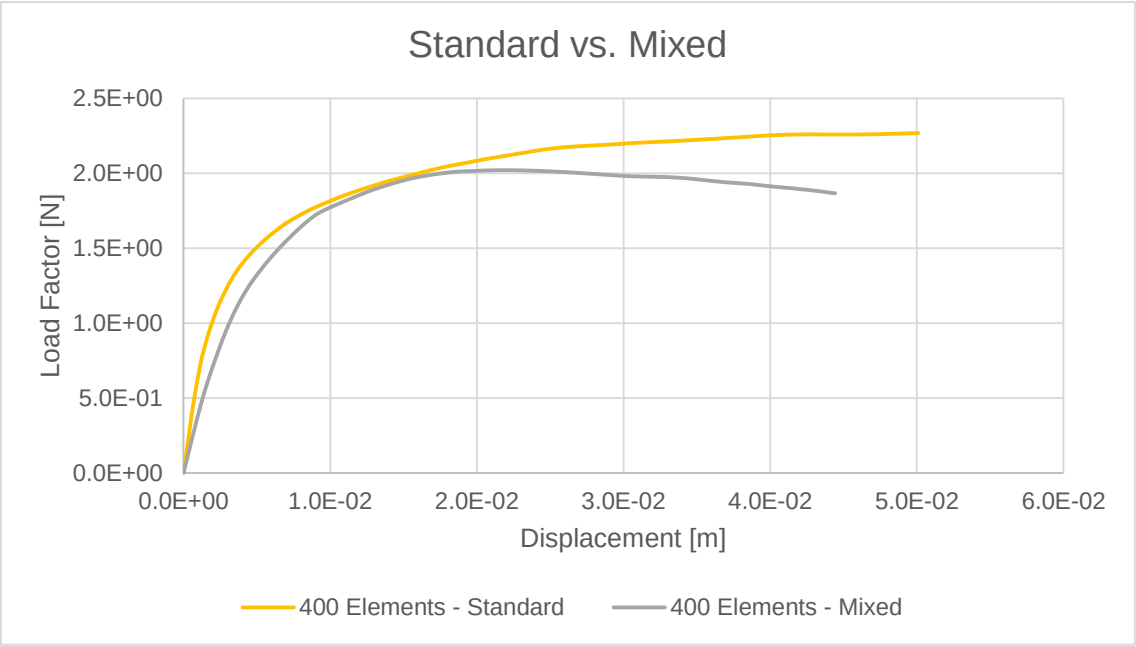

Figure 46. Non-linear analysis comparison. 400 Elements and 27 Gauss points

The tensile damage at the peak load for both sides of the wall, loaded face on top, are shown in **Figure 47**.

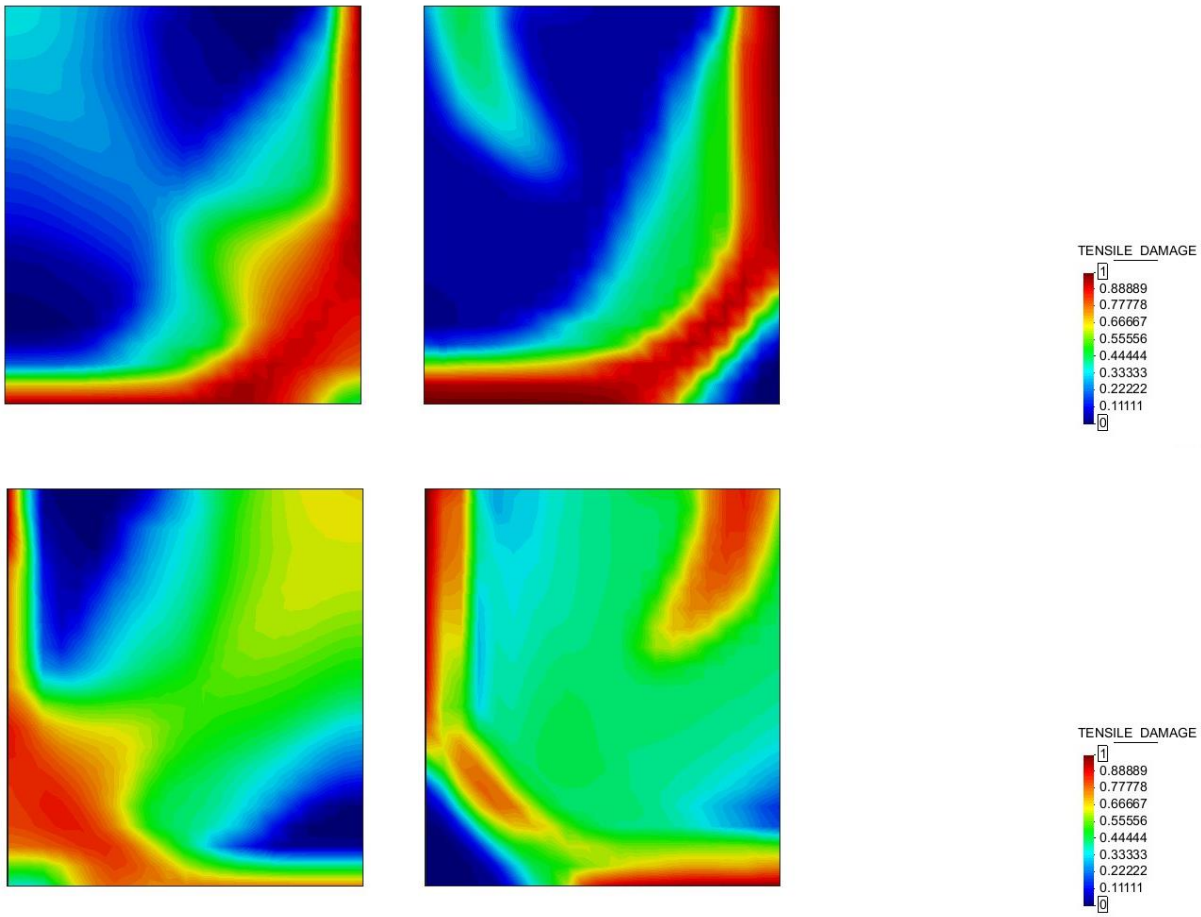

Figure 47. Tensile damage at the peak load. Standard (left). Mixed (right).

For the last time step the results are shown in **Figure 48**, being the loaded face the two figures on top.

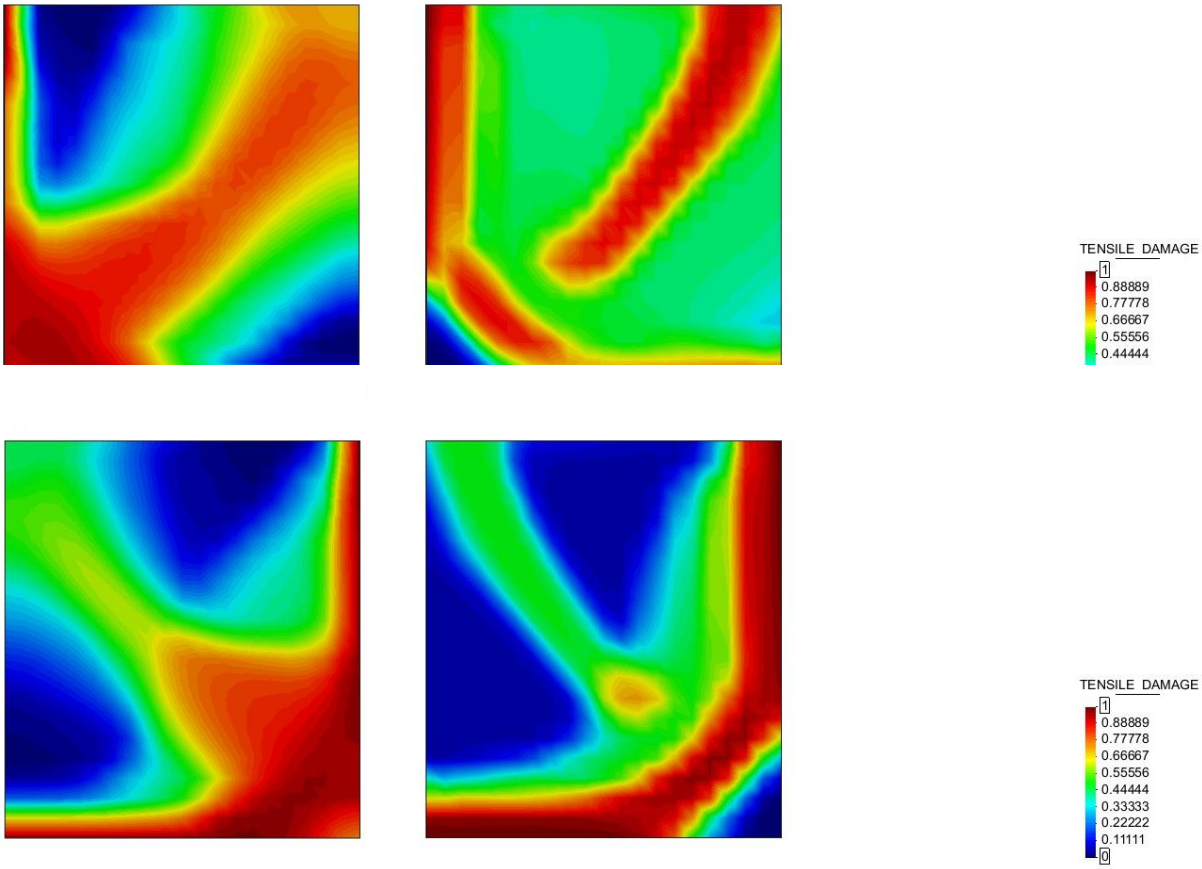

Figure 48. Tensile damage at the last step. Standard (left). Mixed (right)

On the loaded face of the wall the first tensile damage appear at the supports, eventually it advances to the corner. On the other side the damage appears at the wall's supports and free edge centre, eventually the damage is extended to the corner.

Both finite element results illustrate the same failure mode, however a slight difference appears at the corners of both sides, in which the standard element damage extension reaches the corner, while the mixed formulation show no damage whatsoever.

Figure 48 demonstrate again that even with high fracture energies the MFEM provides a marked mechanism, in which damage is not as extended but is focussed and intense.

Lourenço et al. [35] results are shown in **Figure 49**. In this case the failure mode is slightly different from this thesis example and the original analysis, this phenomena is due to the orthotropic behaviour of the author's model, in which the vertical direction is much weaker, on the contrary an isotropic Rankine material model is used for the non-elastic range modelling.

Lack of softening in results from irreducible formulation is illustrated by the great damage extension and lower intensities, **Figure 43**. On the other hand, one hundred element mesh and eight interpolation points, force-displacement curve show softening; besides, post processing illustrate a more pronounced failure mechanism is shown. Nonetheless, the interpolation is really coarse and the disparity in peak load do not provide an appropriate comparison curve.

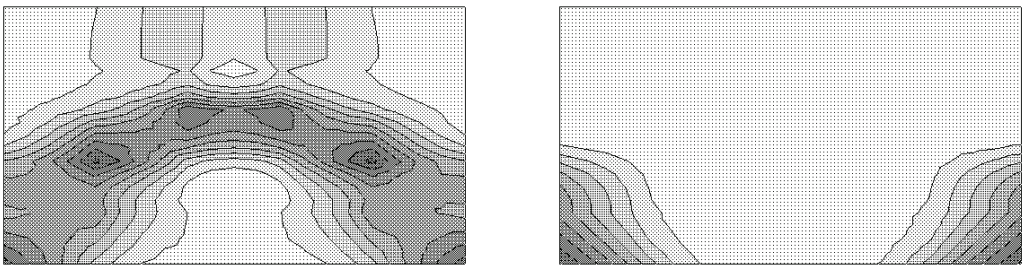

Figure 49. Plastic strain at ultimate load at the bottom face and the top face [35].

7.4 Finite element efficiency

7.4.1 Linear-elastic analysis

All six meshes sizes using MFEM and common FEM models are compared by means of model size, error and computational time.

Table 10. Example 3 linear-elastic analysis efficiency.

Element Type	**Number of elements**	**Number of nodes**	**Number of DOF**	**Displacement Error (%)**	**Stress Error (%)**	**Time (s)**
Mixed	100	242	726	0.7	7.6	0.641
	400	882	2646	2.3	0.9	2.422
	1600	3362	10086	1.3	0.0	21.31
	6400	13122	39366	0.4	0.2	331.72
	10000	20402	61206	0.2	0.1	776.42
	14400	29282	87846	0.0	0.0	1522.03
Standard	100	242	726	76.8	74.8	0.188
	400	882	2646	45.5	41.4	0.453
	1600	3362	10086	17.7	14.2	2.156
	6400	13122	39366	5.6	3.2	16.19
	10000	20402	61206	3.9	1.7	34.78
	14400	29282	87846	3.0	0.9	70.19

Stabilized mixed formulation 5% error is achieved in the 400 number of elements (20x20) model, consuming only 2.422 seconds. On the other hand, similar requirements is obtained in 34.78 seconds in irreducible models, nevertheless, more than 70.19 seconds is necessary to reduce the error to the same standards than the MFEM 400 element model.

7.4.2 Non-linear analysis

Once again MFEM inelastic analysis consume 34.2% more time than the irreducible method.

Table 11. Example 3 non-linear analysis efficiency.

Element Type	**Number of elements**	**Number of nodes**	**Number of DOF**	**Gauss Points**	**Time (s)**
Mixed	400	882	2646	27	26.109
Standard					19.453

7.5 Conclusions of the example

The conclusions for the wall supported on three sides' example are:

- Stabilized mixed formulation show an improved convergence and accuracy for deflection and stress/strain main fields.
- No clear slenderness dependence in displacement approximation is present in the stabilized mixed formulation convergence study, however a 1/18 minor length to thickness wall was studied.
- Stabilized mixed formulation elastic accuracy and computational cost remarkably overpasses standard element's.
- Both finite element methods provide satisfactory inelastic outcome for 8 and 16 Gauss points, being 8 sufficient.
- Irreducible form models show instabilities in non-elastic range using 64 and 125 interpolation points.
- Mesh refinement and interpolation points increase provide lower peak loads and reduced dissipated energies for both FEM.
- Lack of softening behaviour is observed in standard finite element models.
- Similar mechanisms and damage patterns are observed for both FEM.
- Stabilized mixed technique provide a more concentrated and intense damage, resulting in patent mechanism and a clear softening behaviour of the force-displacement curve.
- Irreducible formulation provides substantially faster inelastic analysis (25.5%), nevertheless, improved stress/strain approximation and interpolation is shown in the MFEM non-linear analysis solutions.

8. Example 4 – Wall supported on four sides

8.1 Description of the model

A simply supported wall on its four sides is chosen to be the fourth example, directly extracted from Lourenço et al. [34-35] as the panel WII. Additionally, the thickness of the wall has been increased from 0.15 to 0.40 metres, in order to study a possible slenderness convergence effect in the mixed element.

A whole wall model is used to ensure perfect symmetry in the linear analysis. Due to the x-axis and y-axis symmetry of the plate, only one quarter can be modelled in the non-linear analysis. However as to assure a perfect modelling of the horizontal crack in the middle of the wall and for saving computational time, just the right side of the wall was modelled for the inelastic analysis.

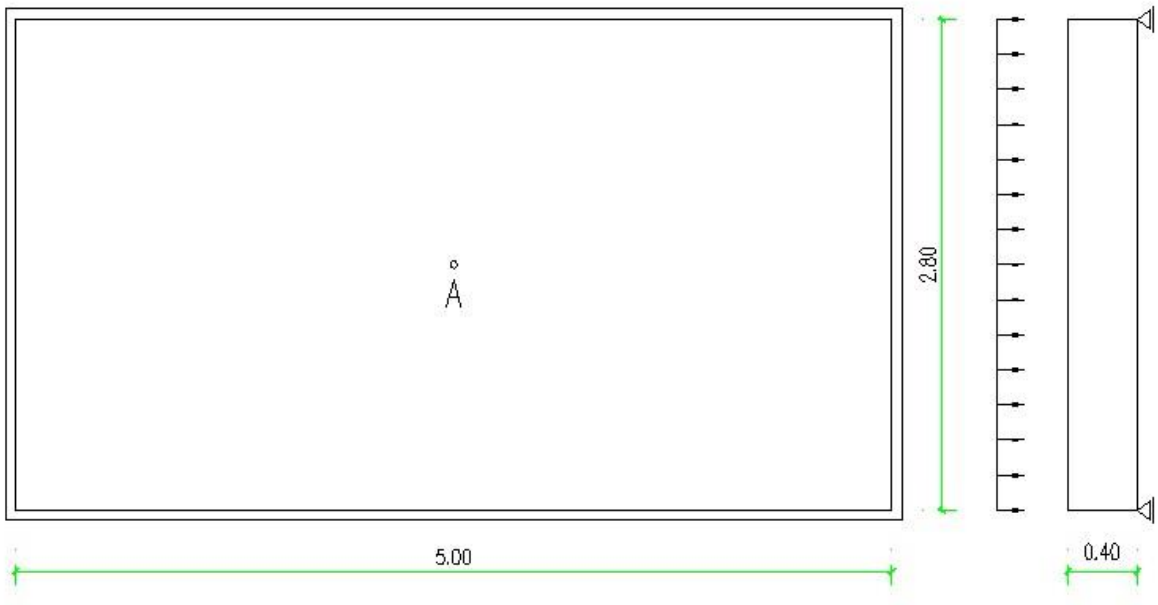

Figure 50.Wall supported on four sides' geometry

8.1.1 Mesh characteristics

The support conditions are similar to the previous example, except for the extra fixed support condition at the top edge of the wall. The half wall models have an additional in-plane horizontal translation boundary condition at the free edge.

Once more the meshing parameters are identical with the third example, in which only one element in the z-direction is considered and the same number of divisions in the x and y directions. Following this meshing process, 100, 400, 1600, 6400 and 10000 elements model are used in the analysis.

Moreover an overkill solution with four elements through the thickness is used for comparison in the linear range.

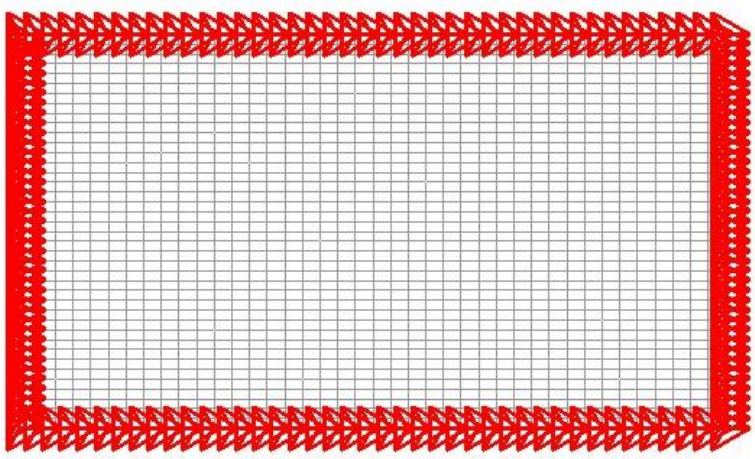

Figure 51. Wall supported on four sides' constraints and 1600 elements mesh

8.1.2 Material parameters

Same material parameters are used as in the third example.

Table 12. Example 4 material parameters

Young's modulus	5.00 GPa
Poisson's ratio	0.3
Tensile strength	2.5 MPa
Fracture energy	100 Nm/mm2

8.2 Linear analysis results

A 3000 N/M out-of-plane uniform load is applied on the wall. Out-of-plane displacement and the principal stress at the wall's centre are compared for all models (point A at **Figure 50**). Displacement and stress are plotted against the total number of elements.

Convergence of the out-of-plane deflection for mixed and standard element are shown in **Figure 52**. As it was expected, the increase in the wall thickness has a counter effect in the mixed element convergence rate. For instance, between the coarsest and the finest mesh the classical element differs a 17.4%, while the mixed element presents a 54.9% divergence.

Regarding the principal stress convergence, the mixed element under the same model meshes show a better behaviour, no matter the thickness of the element. In **Figure 53** it is displayed the convergence of principal stress with respect mesh refinement. Using the previous comparison between the coarsest and the finest mesh, in this case, the MFEM diverges only 5.2%, at the same time the irreducible formulation result differs a 20.3%.

Thus, it is shown that for 3D straight structures the mixed element has consistently superior results in stress/strain convergence and has a slenderness dependent displacement convergence, similar results with 2D straight and curved structures were observed in example 1 and 2.

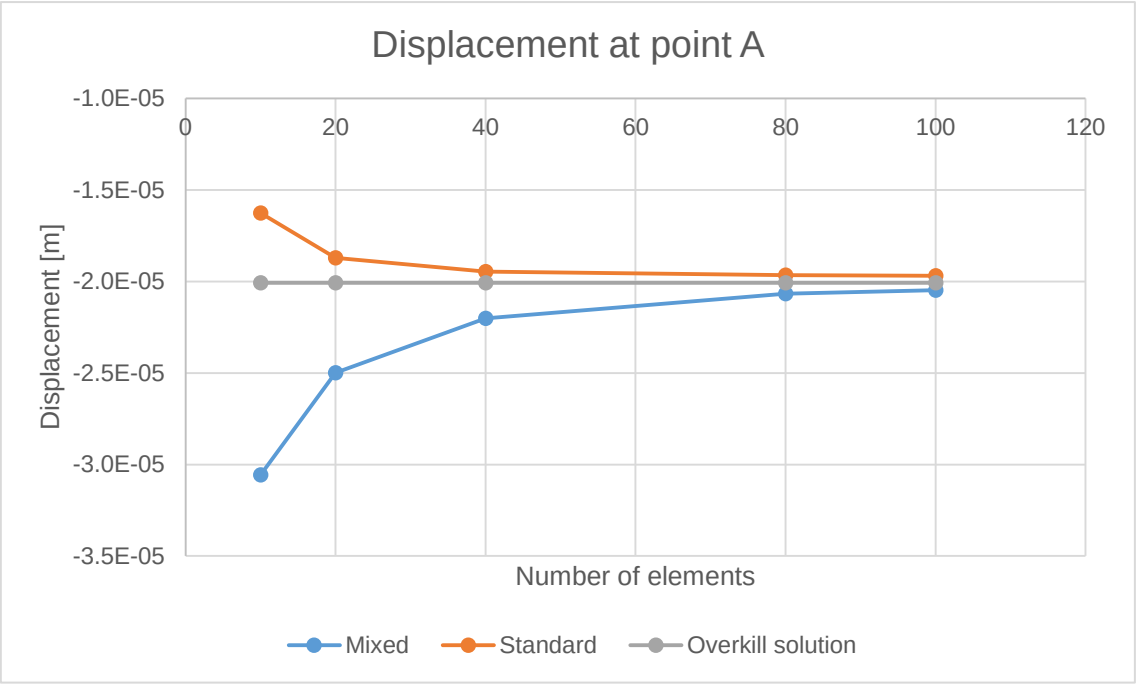

Figure 52. Convergence of the out-of-plane displacement with mesh refinement

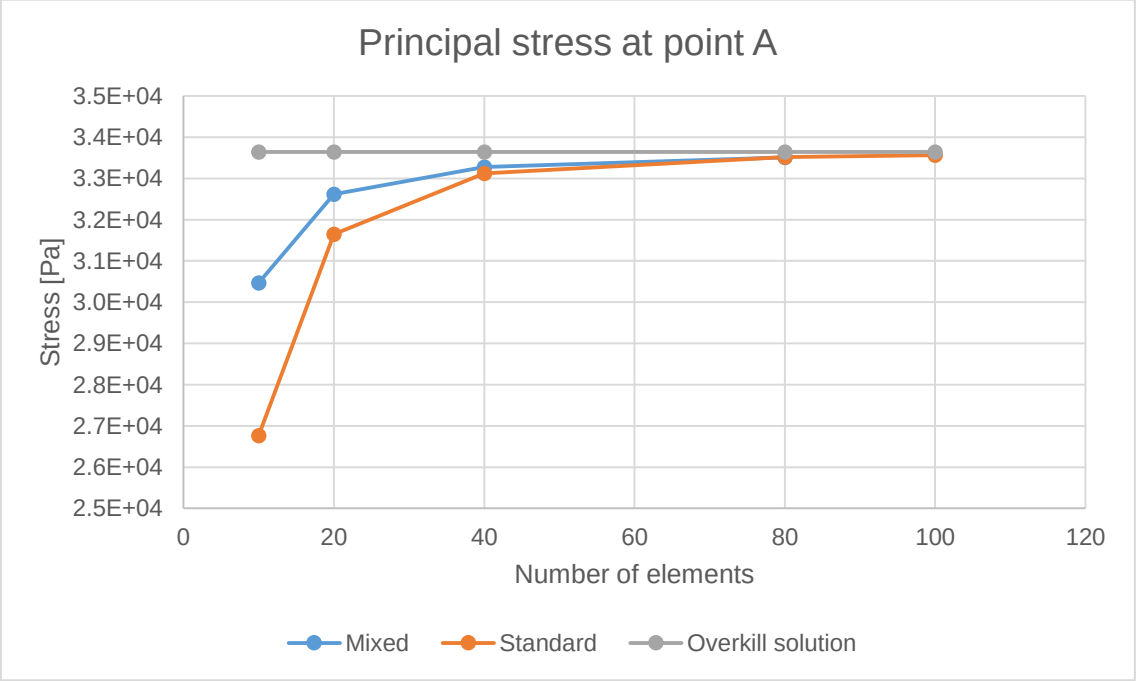

Figure 53. Convergence of the principal stress with mesh refinement

In order to prove the slenderness dependent of 3D straight structural elements, a further study on the original 15 centimetres wall supported on four sides by Lourenço et al. [34-35] is provided.

Figure 54 shows timprove results with respect **Figure 52,** in terms of displacement for the stabilized mixed formulation. Using the coarsest to finest mesh comparison, the classical element differs 61.5% while the mixed only 35.3%. Moreover, displacement convergence rate is clearly superior for MFEM.

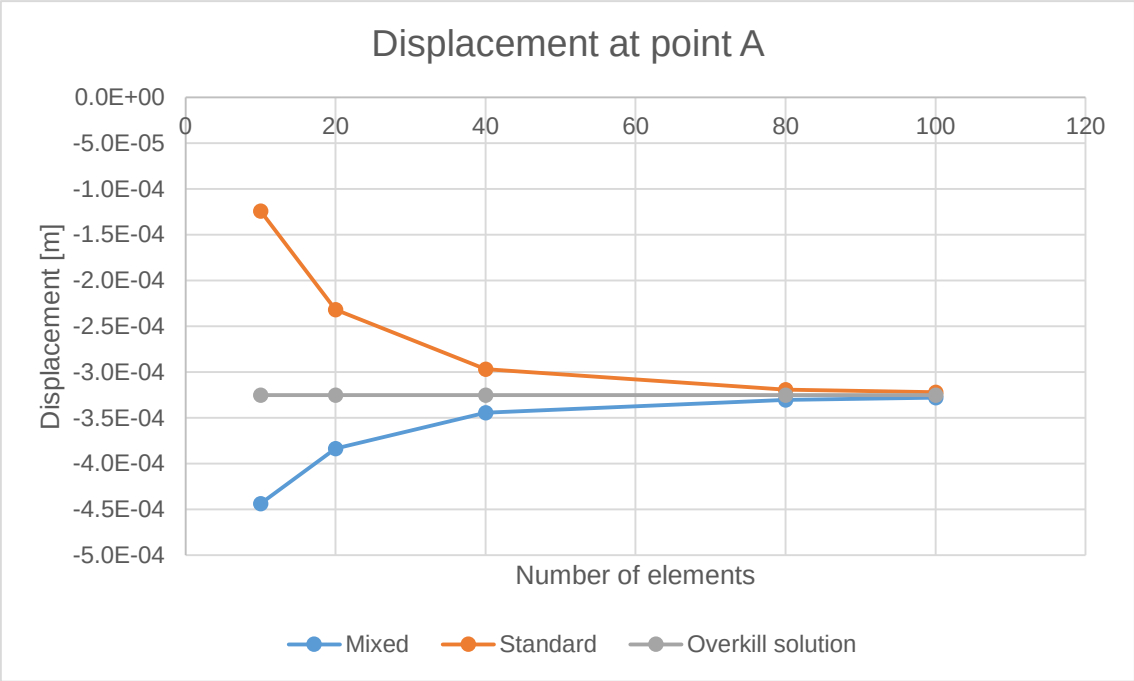

Figure 54. Convergence of the out-of-plane displacement with mesh refinement

As for the stress convergence, once more the mixed formulation undoubtedly display an improved accuracy for coarse meshes and an extraordinary convergence rate.

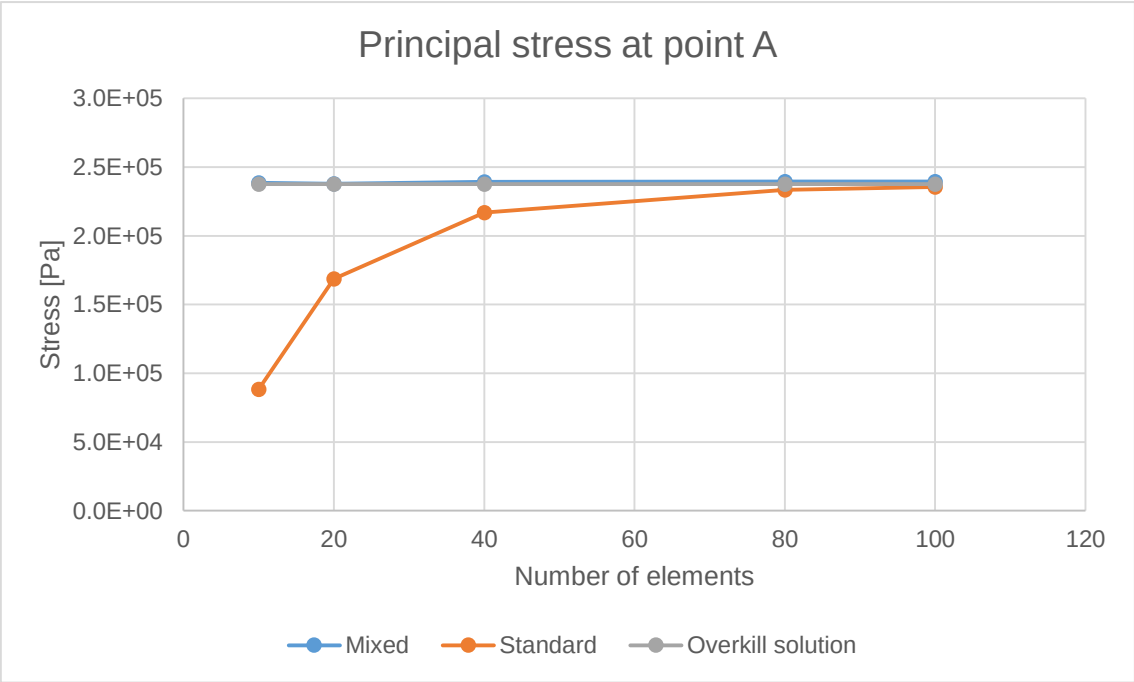

Figure 55. Convergence of the principal stress with mesh refinement

Figure 56 shows the out-of-plane displacement and the principal stress, at both sides of the wall (loaded face on top), for the finest mixed 10000 element mesh (100x100).

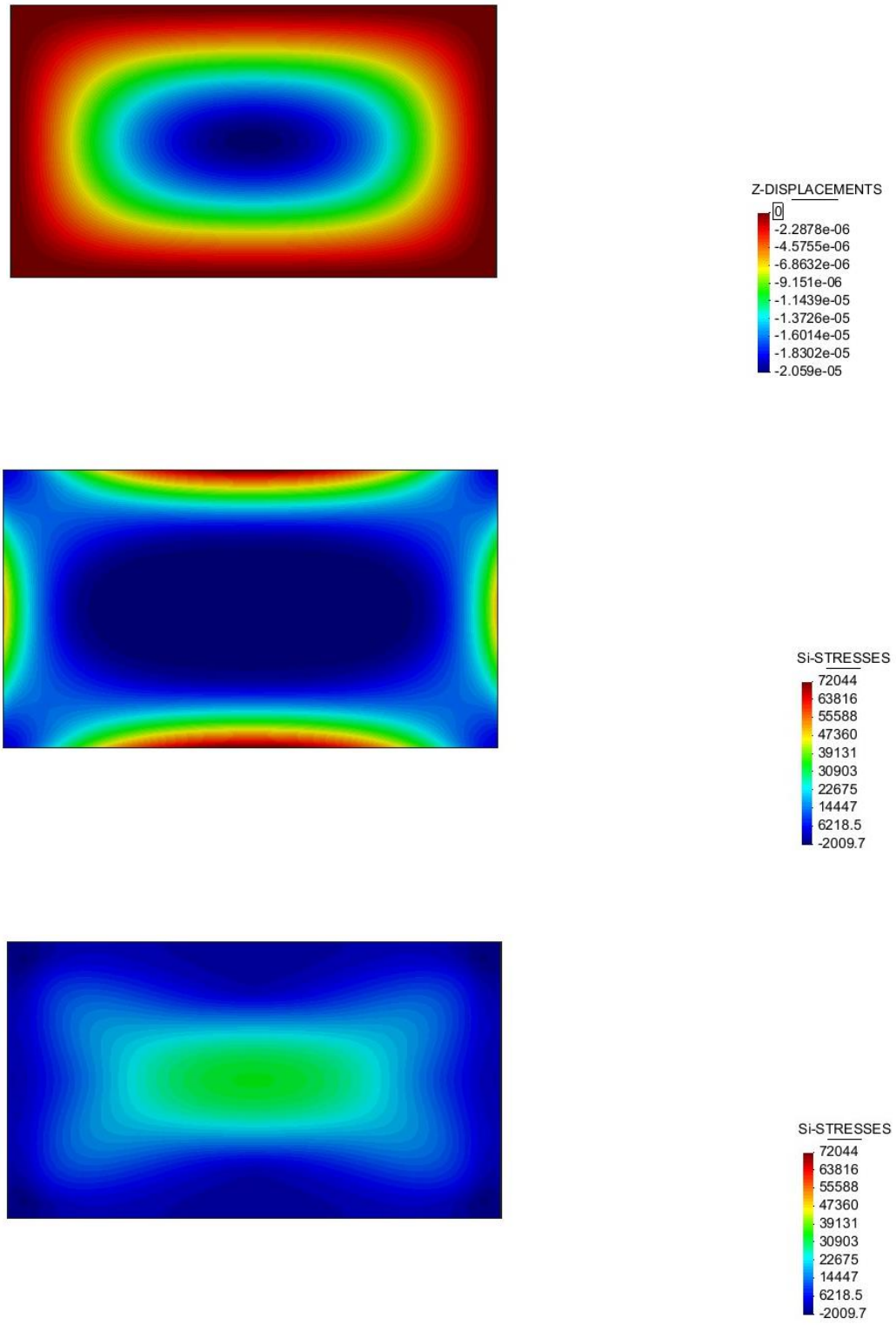

Figure 56. Wall supported on three sides displacement, loaded face stress and opposite face stress results

8.3 Non-linear analysis results

Two meshes were used in the non-linear analysis, 100 and 400 elements. All force-displacement curves graph the behaviour of centre of the plate.

8.3.1 Mesh sensitivity

The initial analysis using 8 Gauss are shown in **Figure 57** and **Figure 58**, for standard and mixed models respectively. The irreducible formulation results show no softening and appreciable peak-load cannot be observed. On the contrary, MFEM show excellent consistency, a slight reduction in peak-load and dissipated energy is observed as the mesh is refined; maximum load at 100 element mesh is 2.50E+01 and for the 400 element mesh 2.31E+01.

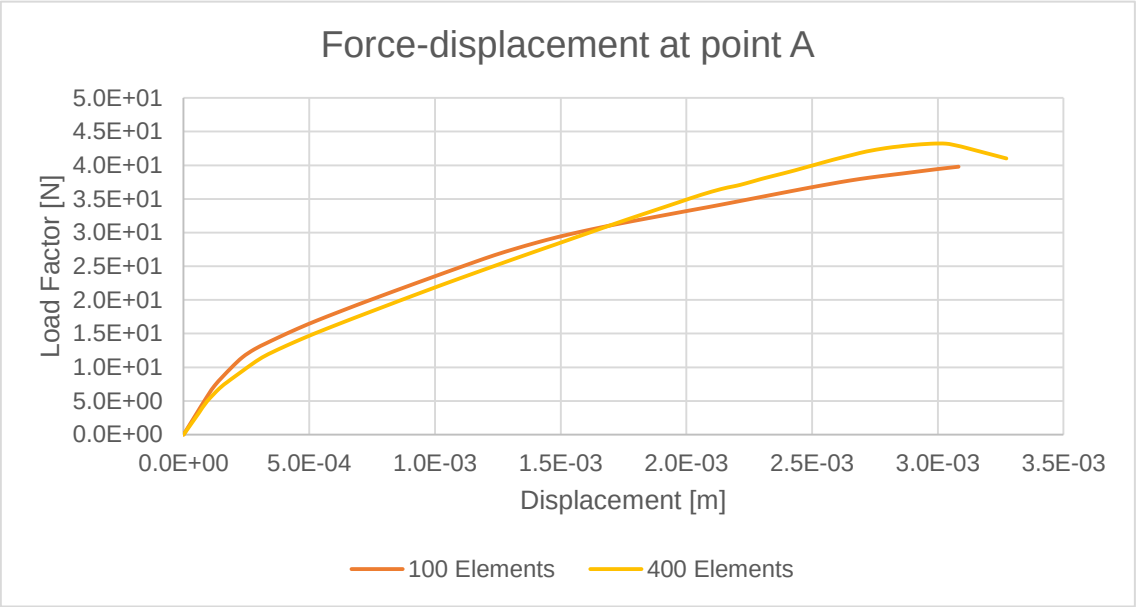

Figure 57. Standard finite element non-linear mesh sensitivity analysis results

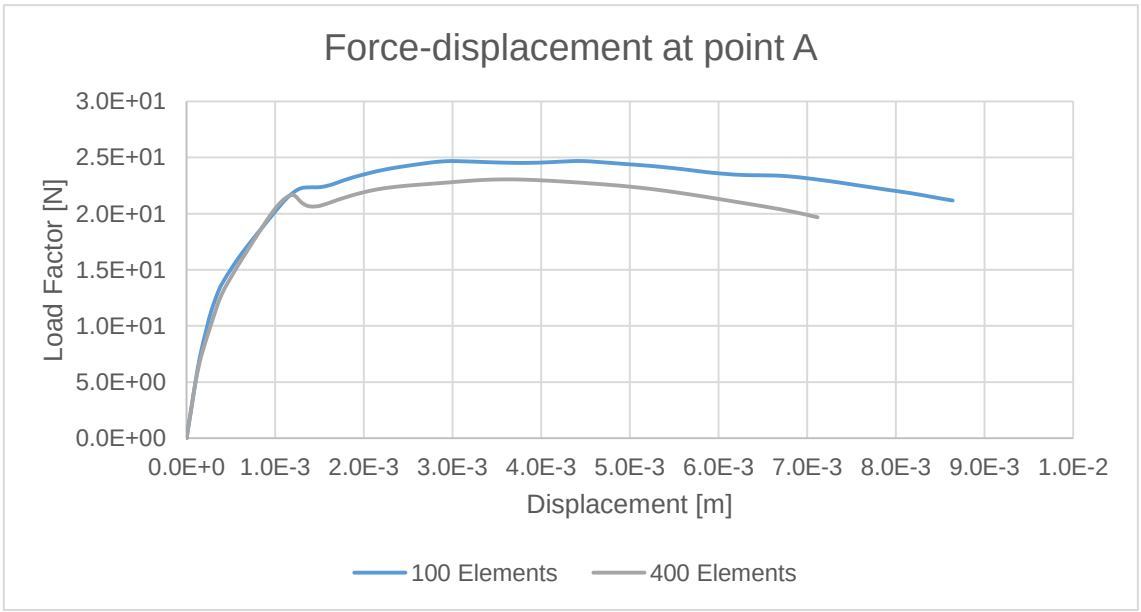

Figure 58. Mixed finite element non-linear mesh sensitivity analysis results

8.3.2 Integration through thickness

A study of the integration points through thickness was performed, in which 27 and 64 Gauss points are considered.

The standard element results for 27 Gauss points display an improved behaviour with respect 8 Gauss point results, excellent consistency is shown. The maximum peak load is slightly reduced from 3.31E+01 to only 3.25E+01 as well as the dissipated energy over the mesh refinement.

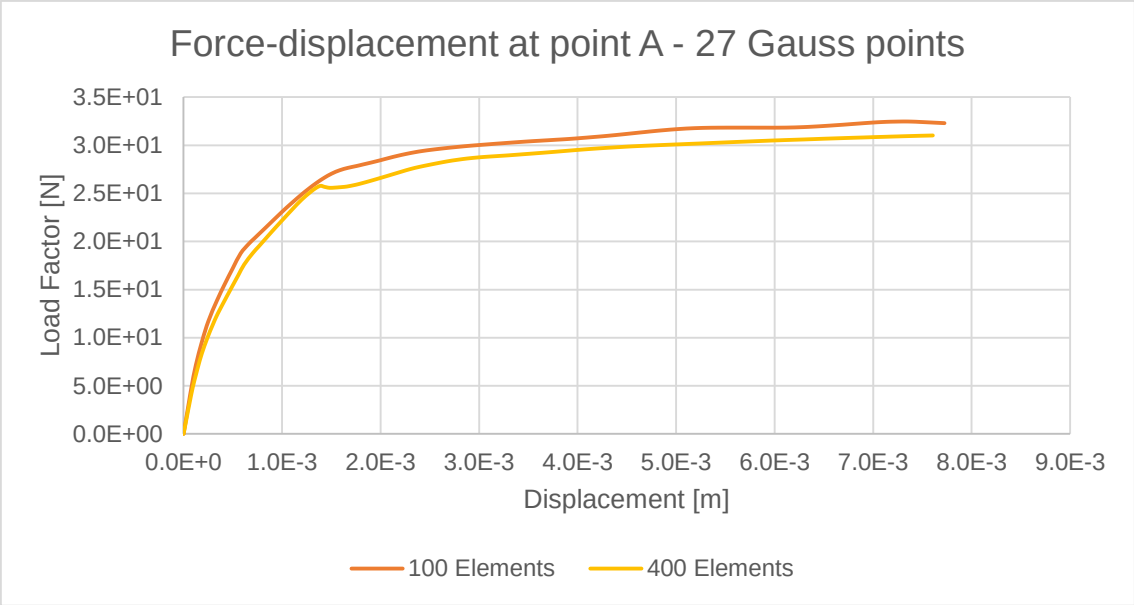

Figure 59. Standard finite element non-linear 27 Gauss points' analysis results

The mixed element for 27 Gauss points are steady in comparison with **Figure 58** peak load, 2.50E+01 and 2.21E+01 for 100 and 400 element models, and dissipated energy. Integration points' increase provide smoother curves and equivalent results in terms of mesh refinement.

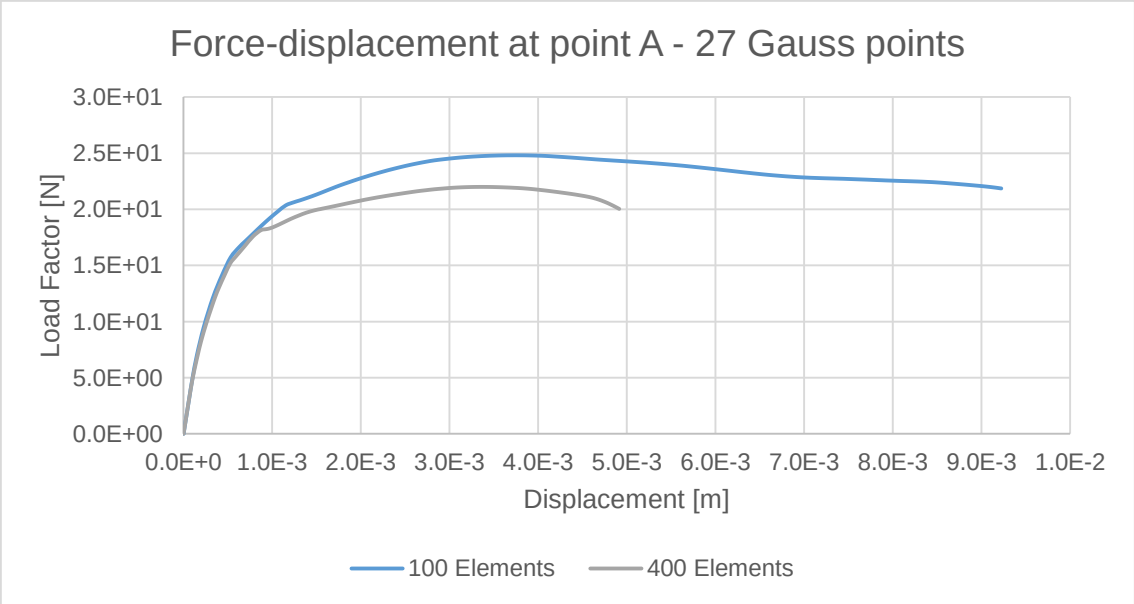

Figure 60. Mixed finite element non-linear 27 Gauss points' analysis results

As the Gauss points are increased to 64, the results in the standard element show no significant change; the peak load remains near 3.00E+01, consistently higher than the mixed element, no softening behaviour appears and the force-displacement can be assimilated to an almost perfect elasto-plastic model.

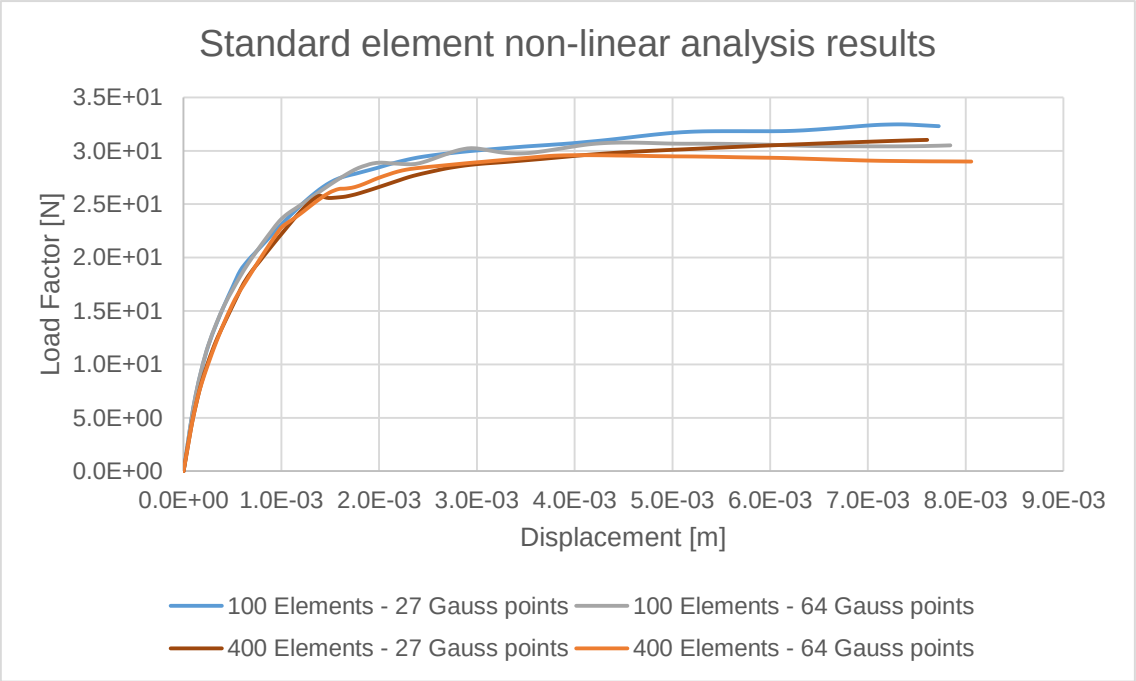

Figure 61. Standard finite element non-linear 27 and 64 Gauss points' analysis results

With regard the MFEM, the increase in the Gauss points provides a lower peak load and decreases the dissipated energy, furthermore also an even more pronounced softening behaviour appears.

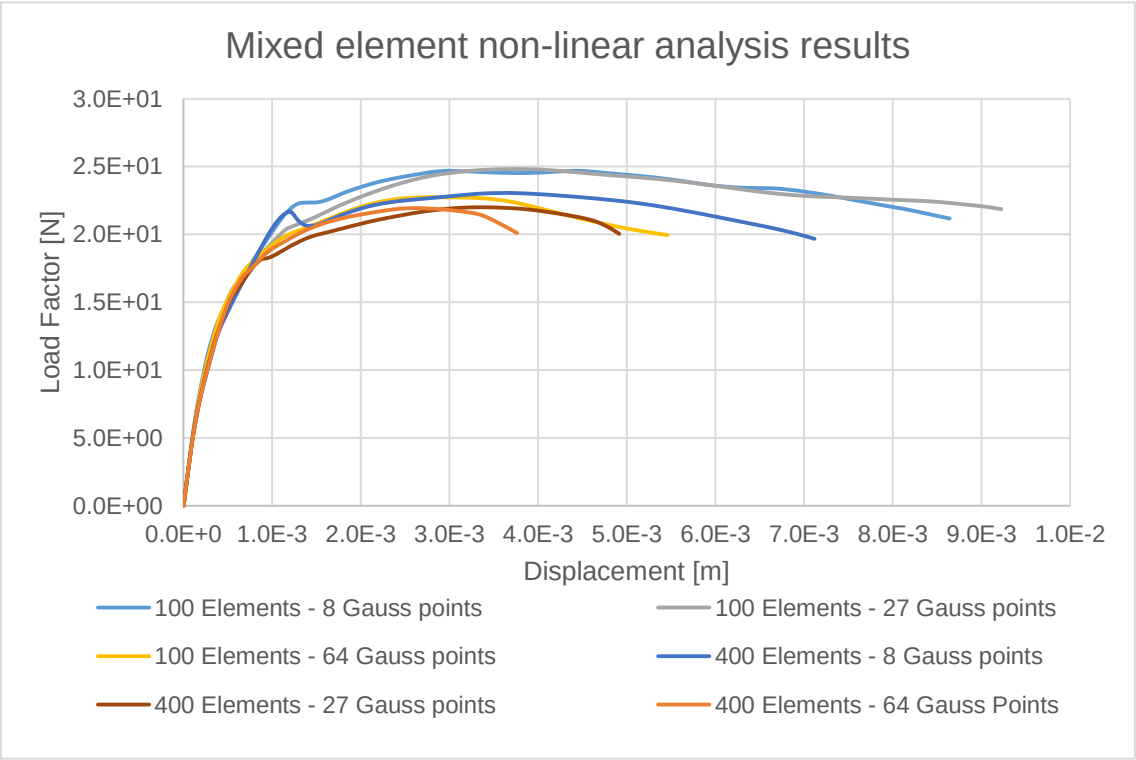

Figure 62. Mixed finite element non-linear 8, 27 and 64 Gauss point's analysis results

8.3.3 Non-linear results comparison

Finally, the two models chosen for the wall supported on four sides' comparison are the 27 Gauss points for the irreducible formulation and the 8 for the stabilized mixed one, both using the 100 elements models.

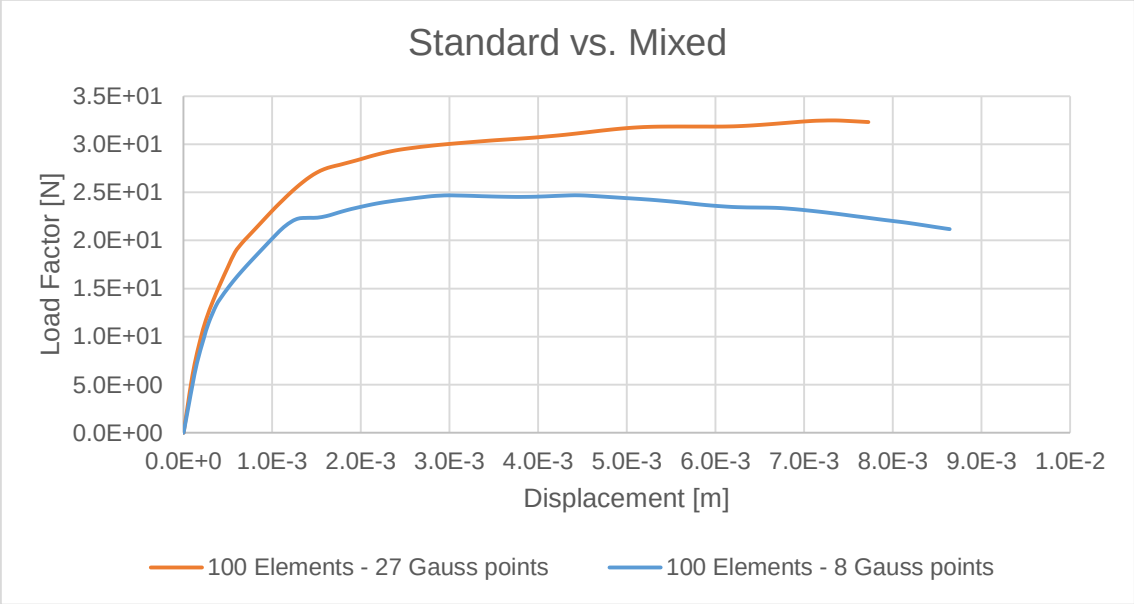

Figure 63. Non-linear analysis comparison. 100 Elements and 27 Gauss points (standard) or 8 (mixed)

Although comparable results in terms of elastic behaviour can be seen, the inelastic analysis strikingly varies; standard element peak load is not identifiable while the softening does not occur.

The tensile damage at the peak load for both sides of the wall, loaded face on top, are shown in **Figure 64**.

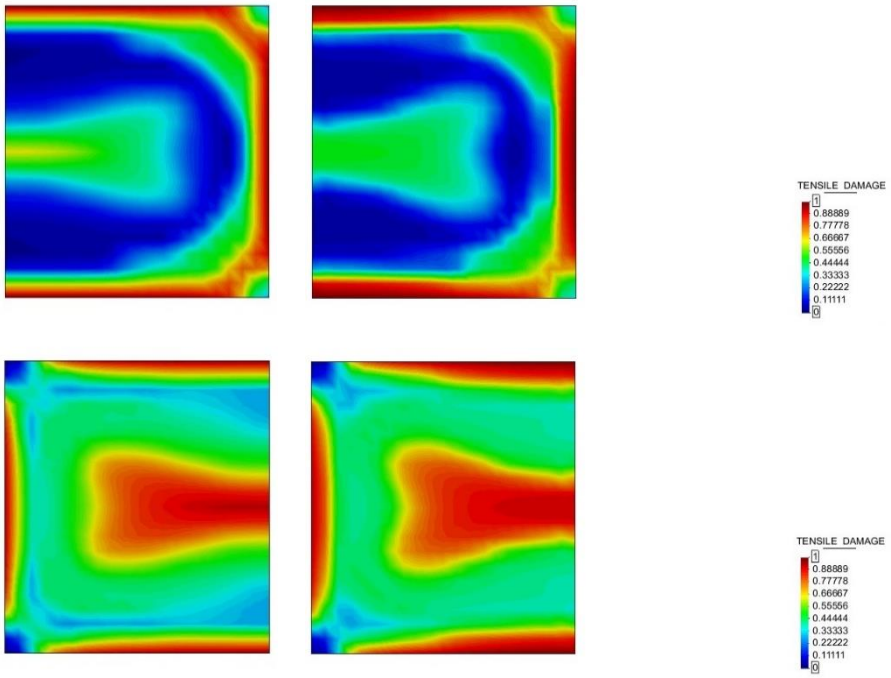

Figure 64. Tensile damage at peak load. Standard (left); Mixed (right)

For the last time step the results are shown in **Figure 65**.

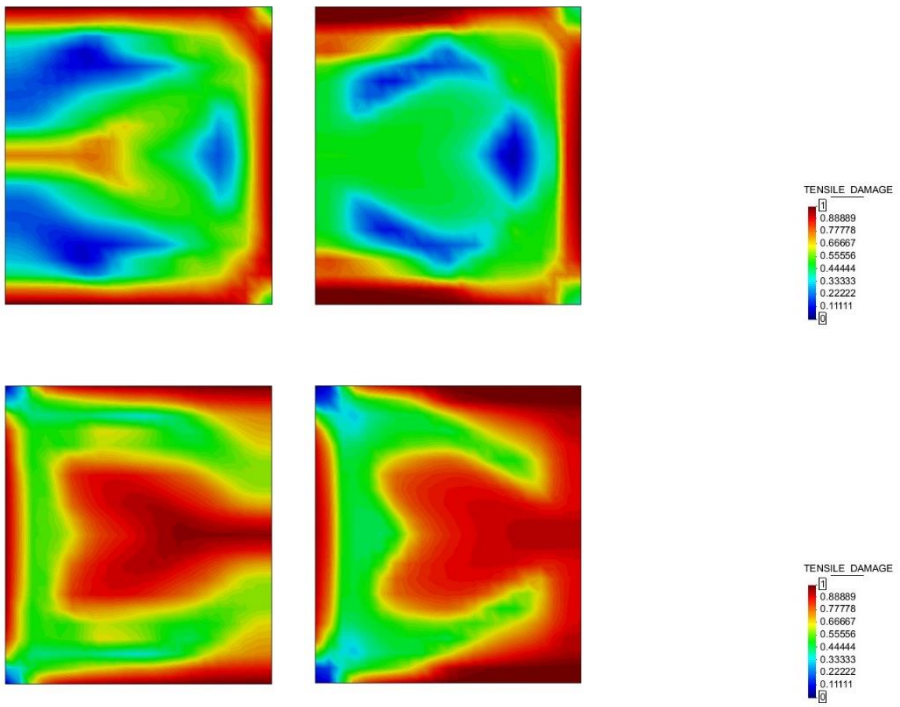

Figure 65. Tensile damage at last step. Standard (left); Mixed (right)

Both models show akin failure modes. At the peak load, the loaded face of the wall suffer the greatest tensile damage at the supports and the wall's centre, on the other side the cracks appear at the maximum momentum area, again the plate's middle point.

Once more, the tensile damage intensity is larger in the stabilized mixed formulation models, as a result a distinctive softening appear at the force-displacement curves. On the contrary, damage pattern in irreducible formulation models show lower intensities and extensions, resulting the almost perfect elasto-plastic force-displacement curves provided.

Lourenço's results are shown in **Figure 66**. For the loaded side of the wall the plastic strain concentrates at the supports and the corners. On the non-loaded face of the wall, the damage is concentrated at the centre of the wall and evolves to the edges. Once more, a slightly different failure mode is present due to orthotropic material model used by Lourenço.

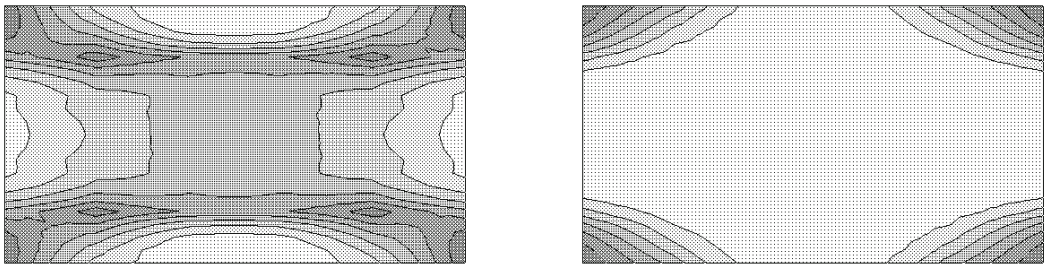

Figure 66. Plastic strain at ultimate load at the bottom face and the top face. [35]

8.4 Finite element efficiency

8.4.1 Linear-elastic analysis

A comparison in terms of model size, displacement/stress error and elapsed time is provided for all five models, using stabilized mixed and irreducible formulations, at **Table 13**.

Table 13. Example 4 linear-elastic analysis efficiency for wall thickness 0.4m.

Element Type	**Number of elements**	**Number of nodes**	**Number of DOF**	**Displacement Error (%)**	**Stress Error (%)**	**Time (s)**
Mixed	100	242	726	52.2	5.3	0.469
	400	882	2646	24.5	0.4	2.391
	1600	3362	10086	9.6	0.2	16.08
	6400	13122	39366	3.0	0.1	263.84
	10000	20402	61206	1.9	0.0	673.78
Standard	100	242	726	19.1	20.5	0.188
	400	882	2646	6.8	5.9	0.406
	1600	3362	10086	3.1	1.5	2.203
	6400	13122	39366	2.1	0.4	12.03
	10000	20402	61206	2.0	0.2	20.73

Displacement efficiency is favourable for irreducible formulation, requiring 2.203 to approximate with only a 3.1% error, on the same basis, MFEM requires 263.84 seconds for a similar error results (3.0%).

Regarding stress/strain approximation, both FEM achieve satisfactory error, 0.4% and 1.5% for mixed and standard elements respectively, within a similar elapsed time, 2.391s for mixed model and 2.203s for the standard one.

Repeating the comparison for the 0.15m thickness wall, the results are shown in **Table 15**.

Table 14. Example 4 linear-elastic analysis efficiency for wall thickness 0.15m.

Element Type	**Number of elements**	**Number of nodes**	**Number of DOF**	**Displacement Error (%)**	**Stress Error (%)**	**Time (s)**
Mixed	100	242	726	36.5	0.3	0.469
	400	882	2646	18.0	0.1	2.438
	1600	3362	10086	6.0	0.6	21.19
	6400	13122	39366	1.7	0.7	253.50
	10000	20402	61206	0.9	0.7	637.31
Standard	100	242	726	61.8	62.9	0.219
	400	882	2646	28.7	29.1	0.438
	1600	3362	10086	8.7	8.8	2.250
	6400	13122	39366	1.8	1.8	16.17
	10000	20402	61206	0.9	0.9	20.42

In this case, efficiency analysis show identic conclusions in the displacement error to time consumption ratio. Nevertheless, stabilized mixed 100 element model stress error is 0.3% consuming only 0.469 seconds, at the same time, irreducible formulation 10000 element model obtain similar error (0.9%) elapsing 20.42 seconds, almost forty-four-fold.

8.4.2 Non-linear analysis

Even though MFEM model uses only eight interpolation points and standard element model uses twenty-seven, in the inelastic range, stabilized mixed formulation model requires 23.8% more time than the irreducible formulation.

Table 15. Example 4 non-linear analysis efficiency.

Element Type	**Number of elements**	**Number of nodes**	**Number of DOF**	**Gauss Points**	**Time (s)**
Mixed	400	882	2646	8	4.312
Standard				27	3.484

8.5 Conclusions of the example

The conclusions for the wall supported on four sides' example are:

- Displacement convergence in mixed finite element models is slenderness dependent; providing improved solutions with respect irreducible method for slenderness ratios lower than 1/10-1/15.
- Stress/strain main field convergence rate and accuracy is remarkably improved.
- Linear elastic computational analysis show superior efficiency in the irreducible formulation models displacement approximation. On the contrary, stress/strain efficiency is clearly favourable to stabilized mixed formulation.
- A minimum of 27 Gauss points is required for non-linear analysis standard element models, under the same circumstances, mixed element models only require 8 Gauss points.
- Mesh refinement and interpolation points increase provide lower peak loads and reduced dissipated energy for both FEM.
- Irreducible technique using 27 and 64 interpolation points results show excellent consistency.
- Stabilized mixed technique's results are consistent for all interpolation points cases considered, 8, 27 and 64.
- Akin damage patterns and failure mechanisms are observed in both FEM, at peak load and last step.
- Improved stress approximation provides superior tensile damage interpolation and a patent facility for MFEM to generate softening.
- Irreducible formulation models display a greater damage extension without fully achieving a softening behaviour on the force-displacement curve.
- Computational efficiency analysis for non-linear range comparison show that irreducible formulation requires 19.2% time less than stabilized mixed model.

9. Example 5 – Ribbed barrel vault

9.1 Description of the model

The fifth example models a three dimensional curved structure, a cylindrical barrel vault with three ribs. Tested by Di Marco et al. [37] and numerically modelled by Creazza et al. [38].

Figure 67. Ribbed barrel vault laboratory test [37].

Figure 68 schematises the ribbed barrel vault's geometry. It has a cylindrical shape with 1 metre inner radius and 1.13 outer radius, additionally two ribs placed on the outer part and a third in the centre with an additional 0.13 metres thickness. Purposely an asymmetry in the loading and barrel geometry was imposed so to promote an indistinct failure mode. The loading directly applied along a line on the top right barrel/ribs connexion.

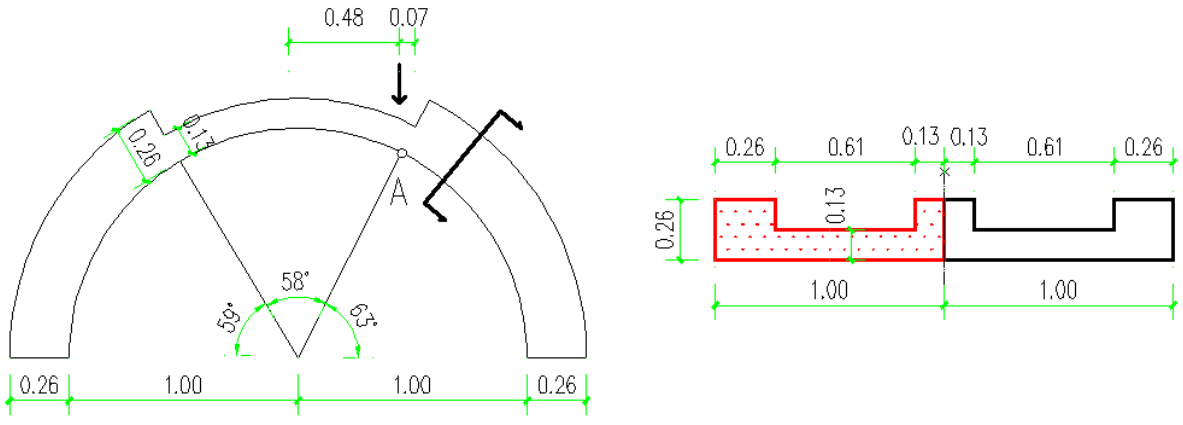

Figure 68. Ribbed barrel vault geometry

Due to the symmetry to the longitudinal axis, along the loading axis, only half of the barrel is modelled in the analysis, shown in red in **Figure 68**.

9.1.1 Mesh characteristics

Boundary conditions at the supports in the original paper are not specified, not in Di Marco et al [37] laboratory test or in Creazza [38] numerical model test. In this model the supports are fixed. Moreover, an additional out-of-plane fixed translation due to the modelling of only half ribbed barrel vault is imposed.

In this case, the example's geometry does not allow only one element through thickness. As a result, a minimum of two elements is required, one element through thickness in the barrel vault and two in the ribs to ensure continuity in the mesh. It is shown in **Figure 69**.

Only one mesh is used in the analysis, akin for mixed and standard element models.

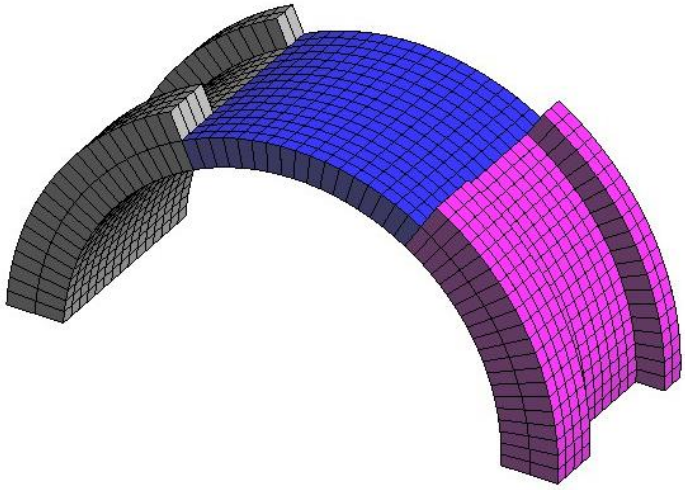

Figure 69. Ribbed barrel vault mesh characteristics

9.1.2 Material parameters

The numerical reference defines all material parameters for an isotropic non-linear analysis. However the fracture energy originally (2.6 Nm/m^2) used results in non-stable inelastic analysis, as a result a 100Nm/mm^2 fracture energy is used.

Table 16. Example 5 material parameters

Young's modulus	1.70 GPa
Poisson's ratio	0.25
Tensile strength	0.08 MPa
Fracture energy	100 Nm/mm2

9.2 Non-linear analysis results

9.2.1 Integration through thickness

In this particular example just one mesh is used for the analysis, furthermore a study for 8, 27 and 64 Gauss points was conducted.

Figure 70 shows the result comparison for irreducible and stabilized mixed formulations using the basic evaluation of 8 Gauss points. The graph displays an excellent similitude in terms of elastic range; similar response in inelastic range can be observe with a slight discrepancy in peak load, 2.04 for the mixed element versus 2.31 for the classical element, a 11.8% difference.

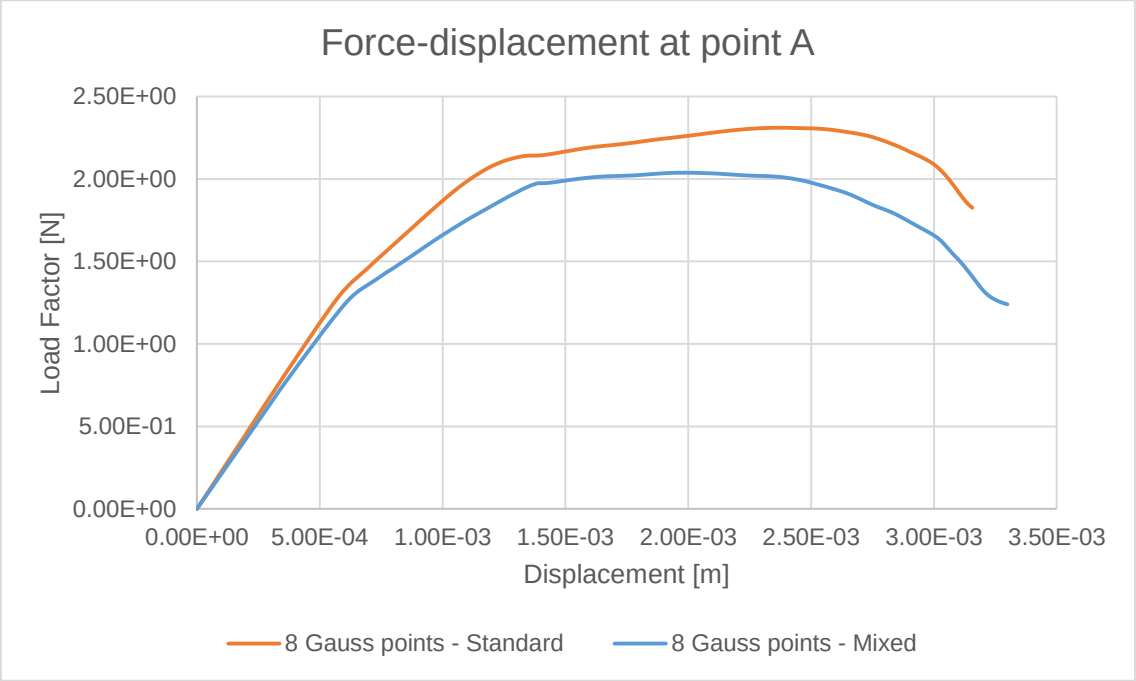

Figure 70. Non-linear analysis comparison. 8 Gauss points

As the Gauss points are increased to 27 both force-displacement curves increase in both peak load and dissipated energy. Similar comparison results for **Figure 71** are extracted, nevertheless the difference between maximum loads is reduced to 8.7%.

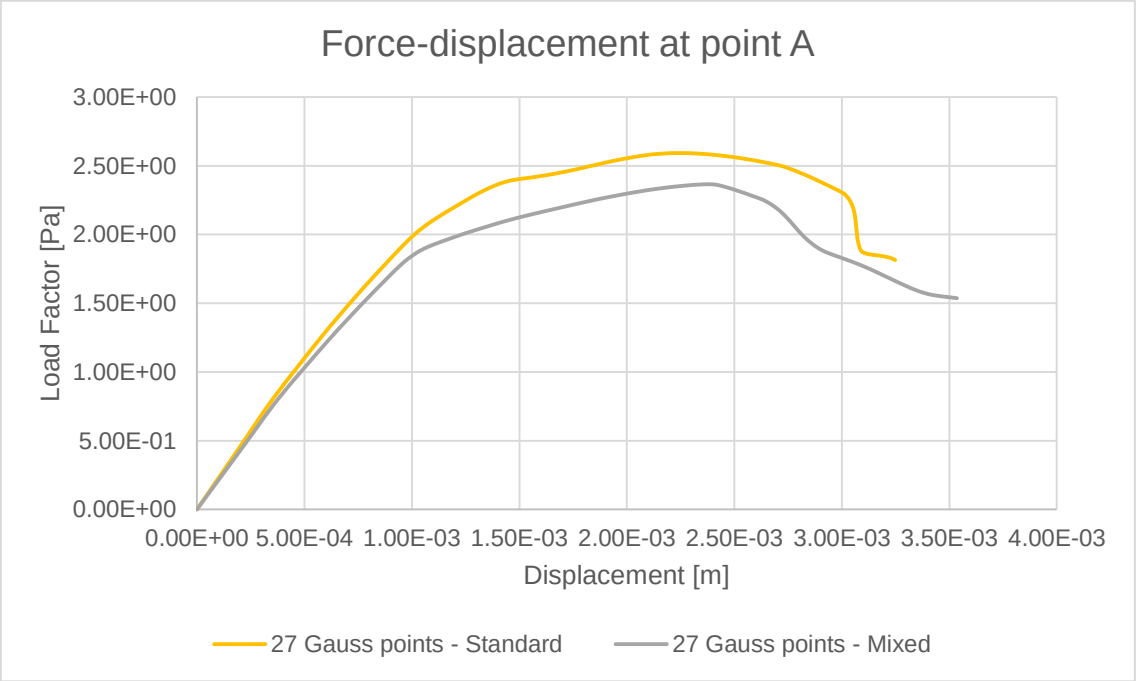

Figure 71. Non-linear analysis comparison. 27 Gauss points

A further increment in the integration points through thickness to 64 Gauss points results show excellent consistency for mixed and classical finite elements outputs, results are respectively shown in **Figure 72** and **Figure 73**.

In both cases 27 and 64 Gauss points show almost identical results, nonetheless standard element systematically provides more rigid solutions, greater peak loads, lower softening and earlier failure with respect stabilized mixed models.

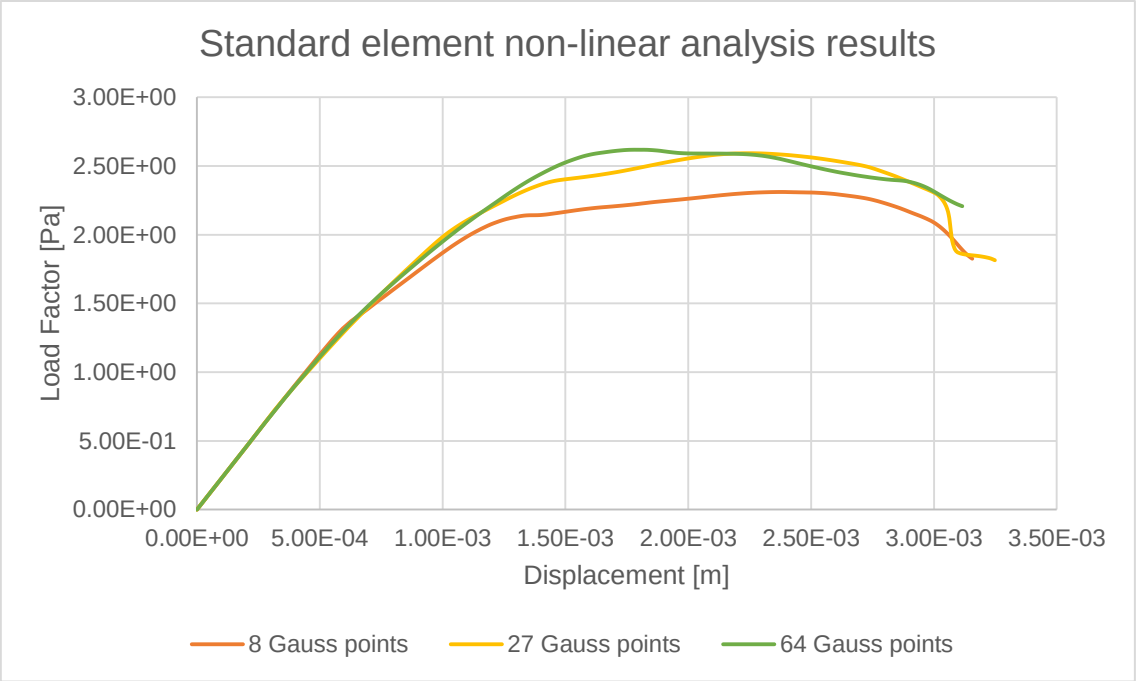

Figure 72. Standard finite element non-linear analysis results

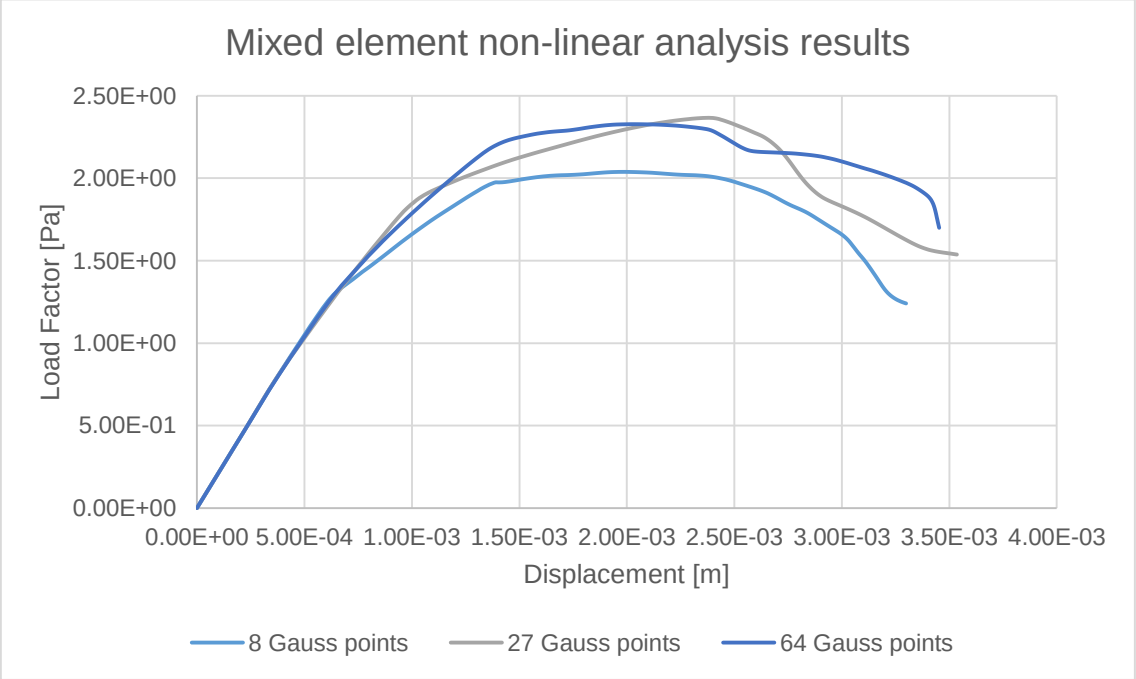

Figure 73. Mixed finite element non-linear analysis results

9.2.2 Non-linear results comparison

The final comparison accomplished using the 8 interpolation points' standard element model against the 27 Gauss points mixed element model. **Figure 74** display the inelastic force-displacement curves for both models.

Excellent resemblance in the elastic and inelastic range up to the ultimate load, afterwards the standard element model fails earlier and without an accentuated softening.

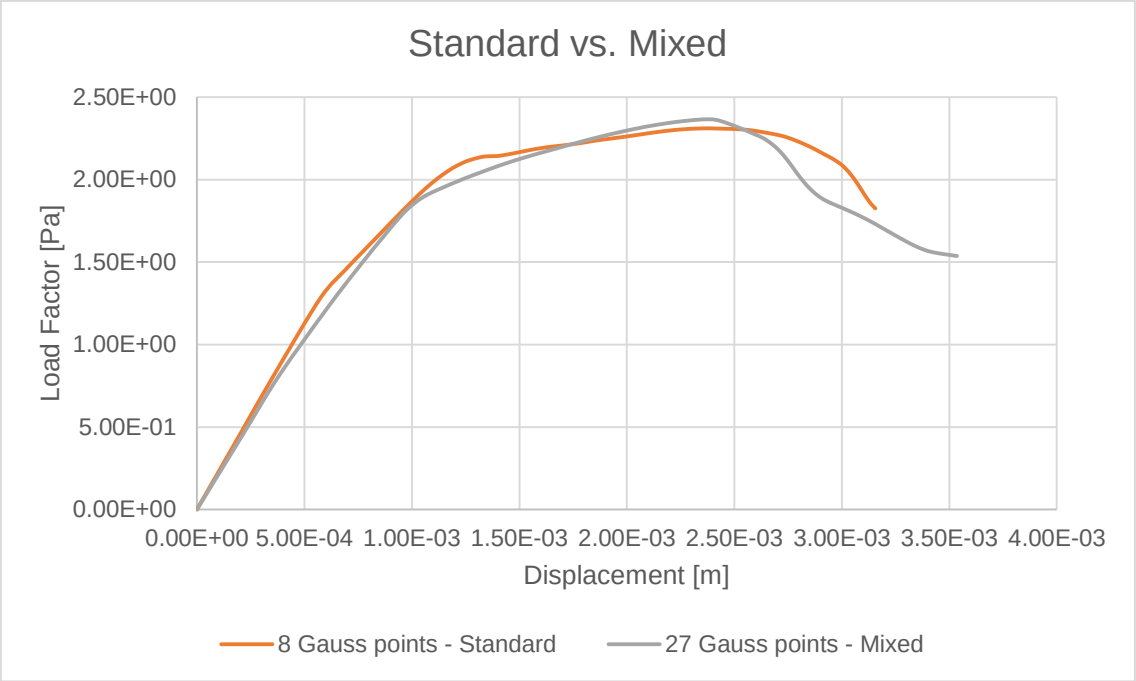

Figure 74. Non-linear analysis comparison. 8 Gauss points (Standard) and 27 Gauss points (Mixed)

The fifth example failure mode is provided by four clearly situated longitudinal plastic hinges and generated by the asymmetry in load and geometry.

The first longitudinal plastic hinge logically appears under the region bearing the load, transmitted to the vault via a beam placed at the beginning of the ribs. Afterwards, the second plastic hinge is generated at the left support. Thenceforward, the tensile damage is fully extended at end of the other ribs and at 45° with respect the horizontal axis, producing the third and fourth plastic hinges respectively.

Plastic hinge evolution using stabilized mixed formulation model is shown in **Figure 75**.

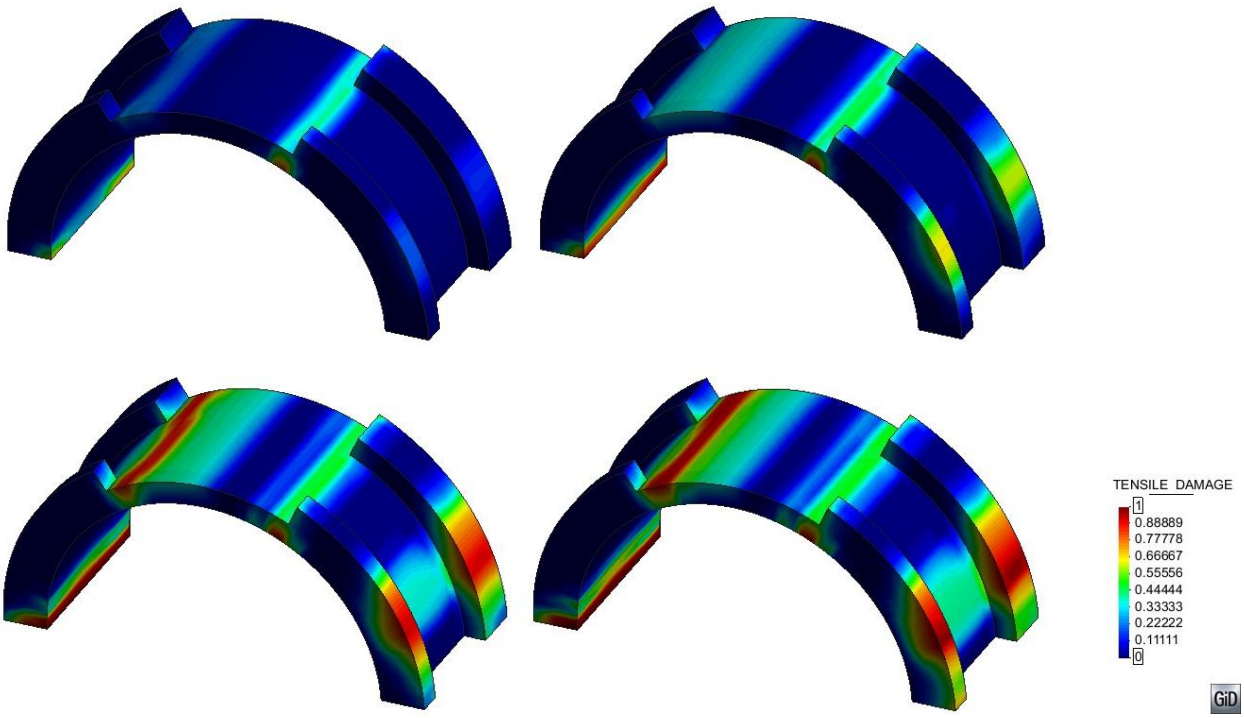

Figure 75. Mixed finite element failure mechanism evolution

For irreducible formulation model the results are plotted in **Figure 76**.

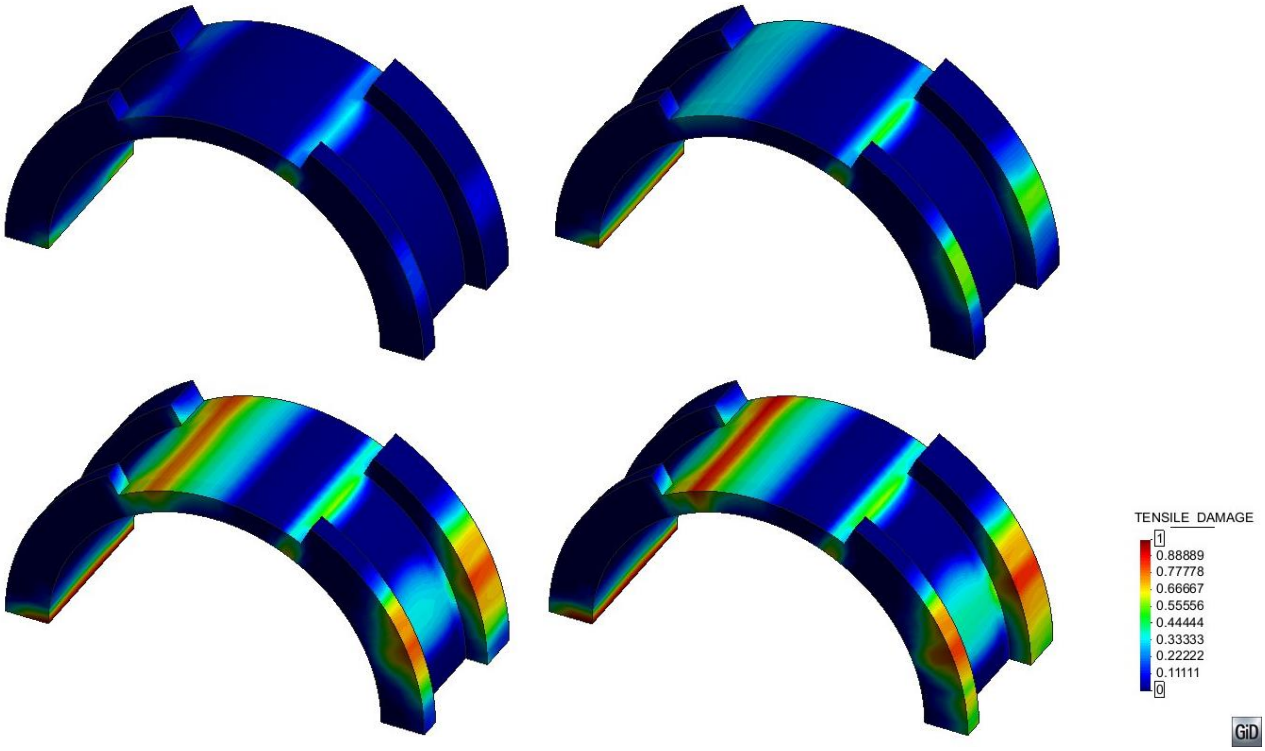

Figure 76. Standard finite element failure mechanism evolution

Analogous failure modes for mixed and standard element are shown in **Figure 75** and **Figure 76**. It can be observed that cracks and plastic hinges are at the same exact position and in the same order for both models, which completely coincide with the two references results formerly mentioned.

Besides, in **Figure 77** deformed shaped and tensile damage are displayed for the last time step, from which alike deformed shape is observed. However, following the same results trend and conclusions that in the previous examples, mixed element model tensile damage is greater in extend and intensity, resulting in the failure mechanism and force-displacement curves observed in **Figure 74**.

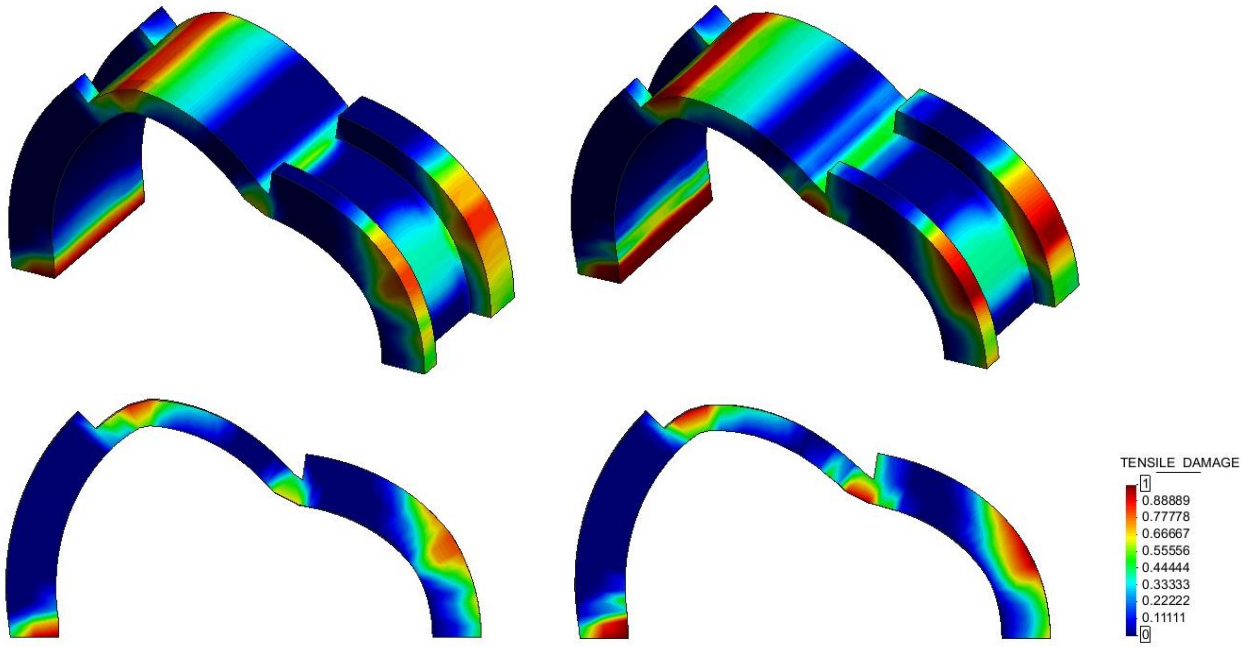

Figure 77. Deformed shape. Standard (left); Mixed (right)

9.3 Finite element efficiency

In this example only a non-linear finite element efficiency comparison is computed in terms of model size, interpolation points and computing elapsed tie.

Table 17. Example 5 non-linear analysis efficiency.

Element Type	**Number of elements**	**Number of nodes**	**Number of DOF**	**Gauss Points**	**Time (s)**
Mixed	1116	2232	6696	27	145.75
Standard				8	31.84

Once more, example's five results determine the additional computational time required by stabilized mixed method to achieve an akin non-linear load-displacement and failure mechanisms results.

9.4 Conclusions of the example

The conclusions for the ribbed barrel vault example are:

- Both FEM illustrate excellent consistency in the non-linear range for 8, 27 and 64 interpolation points.
- Excellent resemblance in linear-elastic range and ultimate load is observed
- Increase in interpolation points through thickness provide greater peak loads and dissipated energy for both FEM.
- Similar failure mechanisms are obtained, perfectly matching those shown in the laboratory test and numerical modelling references [37-38].
- MFEM models display a more extended and intense tensile damage in the plastic hinge. Therefore, patent mechanism and softening behaviour is observed.
- Irreducible formulation efficiency results show an enhanced comportment with respect the stabilized mixed formulation, reducing 78.2% the mixed model computational elapsed time.

10. Example 6 – Masonry four-wall box-structure

10.1 Description of the model

The sixth and last example, is a four-wall box-structure masonry construction dynamically tested in Lisbon under the European Project ECOLEADER-LIS (Enhancing Seismic Resistance and Durability of Natural Stone Masonry). Afterwards published at Ramos et al. [35] and numerically analysed by Endo et al. [39].

The masonry model was built with limestone units and lime mortar joints with polymeric grid reinforcement placed on the horizontal joints.

Figure 78. Four-wall box-structure [35].

The walls are 3.6 metres tall and 0.24 metres thick. Several openings are used to resemble the laboratory tested model with a real building; a 2x1m door at the south façade, two 1x1m windows at the east façade and a 1x1m window at the west façade. Additionally no slab is place on top as to achieve a weaker structural behaviour. **Figure 79** show a scheme of the model geometry.

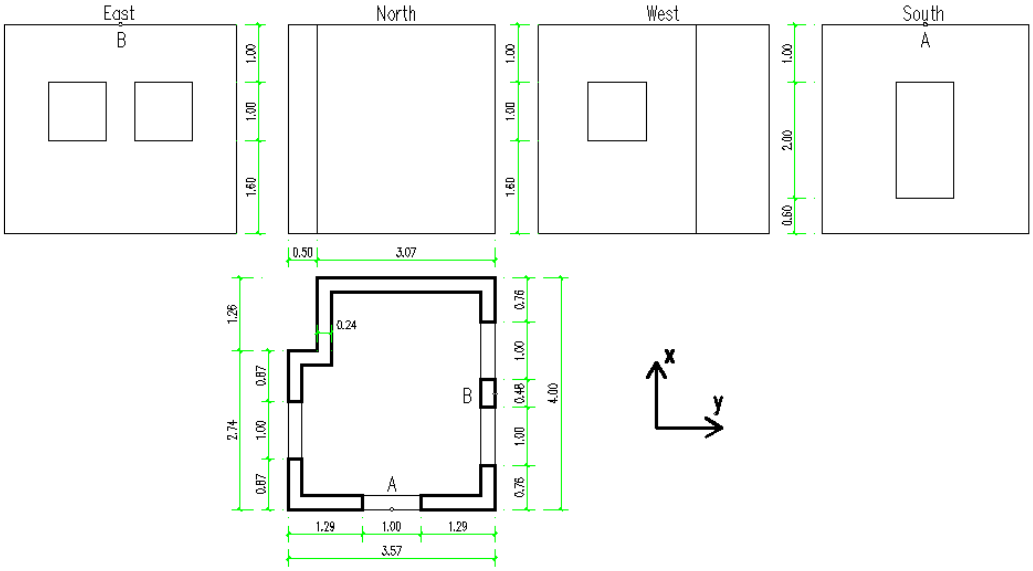

Figure 79. Four-wall box-structure geometry.

10.1.1 Mesh characteristics

As in example five, the boundary conditions are not specified in the original paper, however, following the common shaking table test procedures all the nodal translation and rotations are fixed at the base of the building.

Imposing only an element through the thickness in all models, this work contemplates the use of a single mesh of 24 centimetres hexahedra and a further study increasing the integrating points through thickness is also carried out.

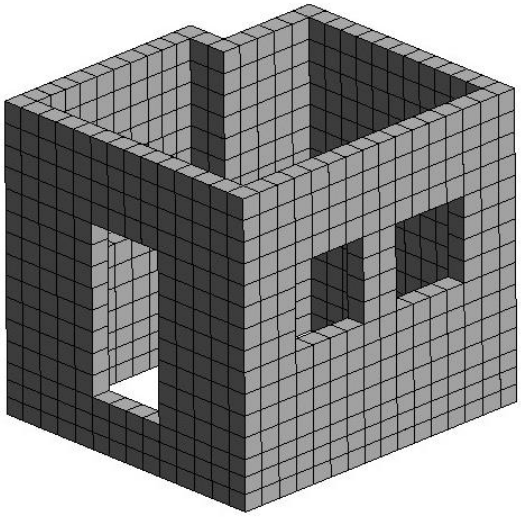

Figure 80. Four-wall box-structure mesh characteristics.

10.1.2 Material parameters

The material parameters are extracted from Ramos et al. [35], some of which are not sufficiently defined, in that case they were extracted from Endo et al. [39]. The material parameters are summarised at **Table 18**.

Table 18. Example 6 material parameters

Young's modulus	5.00 GPa
Poisson's ratio	0.20
Tensile strength	0.20 MPa
Fracture energy	50 Nm/mm2

10.1.3 Loading procedure

The original load is applied by means of a seismic excitation performed on the shaking table under a unidirectional horizontal random input motions. Ramos et al.[35] does not specify the input acceleration, therefore the numerical model test applies four different load scenarios, which are a mass proportional x and y, both positive and negative, push over test. Self-weight of the building is also considered.

10.2 Non-linear analysis results

Two identical meshes are used in the non-linear analysis comparison for both FEM. Under x-direction push over test, positive and negative excitation, the south façade top middle point displacement is measured (point A at **Figure 79**). On the same conditions but under y-direction excitation the east façade top middle point displacement is quantified (point B at **Figure 79**)

10.2.1 Integration through thickness

An initial comparison using 8 Gauss points is shown in **Figure 81**. Both x and y push over load scenarios provide similar results, in which mixed element peak load is slightly minor than the standard element. Excellent similitude in the elastic and early plastic range is observed.

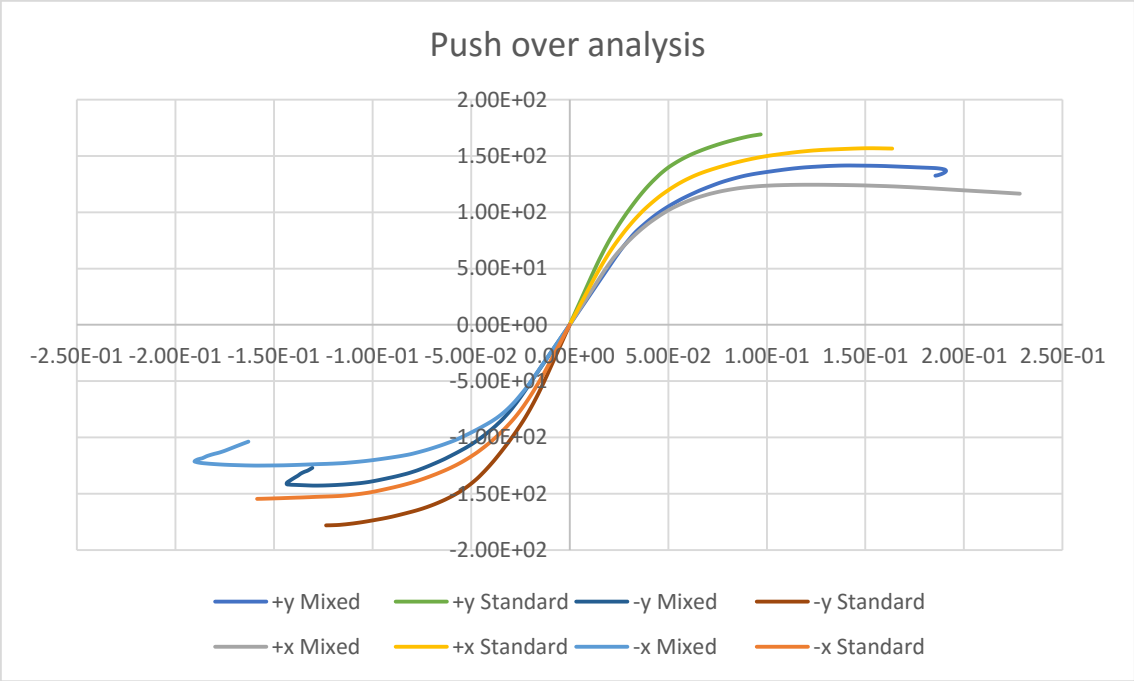

Figure 81. Non-linear analysis results. 8 Gauss points.

An evaluation for 27 Gauss points was conducted. The results from both finite elements are again reduced in terms of peak load and dissipated energy. As a conclusion the more we refine the mesh or the more we increase the integration point through thickness the more similar are the standard and mixed element force-displacement graphs. Additionally, the results standard element tend to match the mixed element.

10.2.2 Non-linear results comparison

Continuing with the last line of reasoning, if we compare the push over test outcome from the classical element using 27 Gauss points and the mixed element using only the basic 8 Gauss points, it is observed almost a perfect match both in elastic and non-elastic behaviour. Once more the only difference is the greater stiffness provided by the irreducible formulation. In **Figure 82** and **Figure 83** it is shown the x-direction and y-direction results.

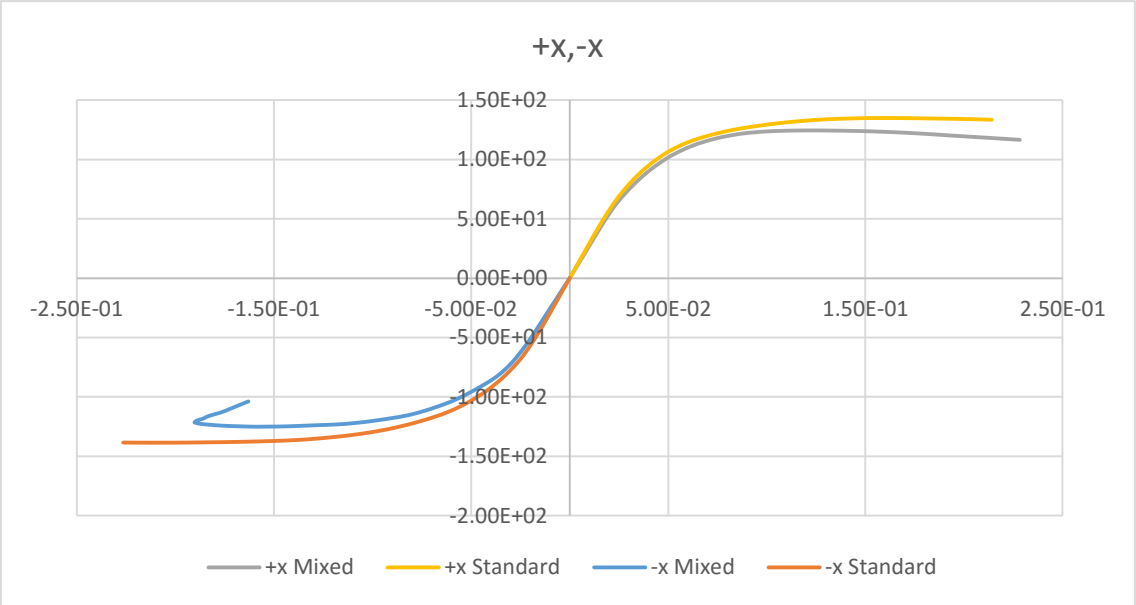

Figure 82. Non-linear analysis comparison. 27 Gauss points (Standard) and 8 Gauss points (Mixed).

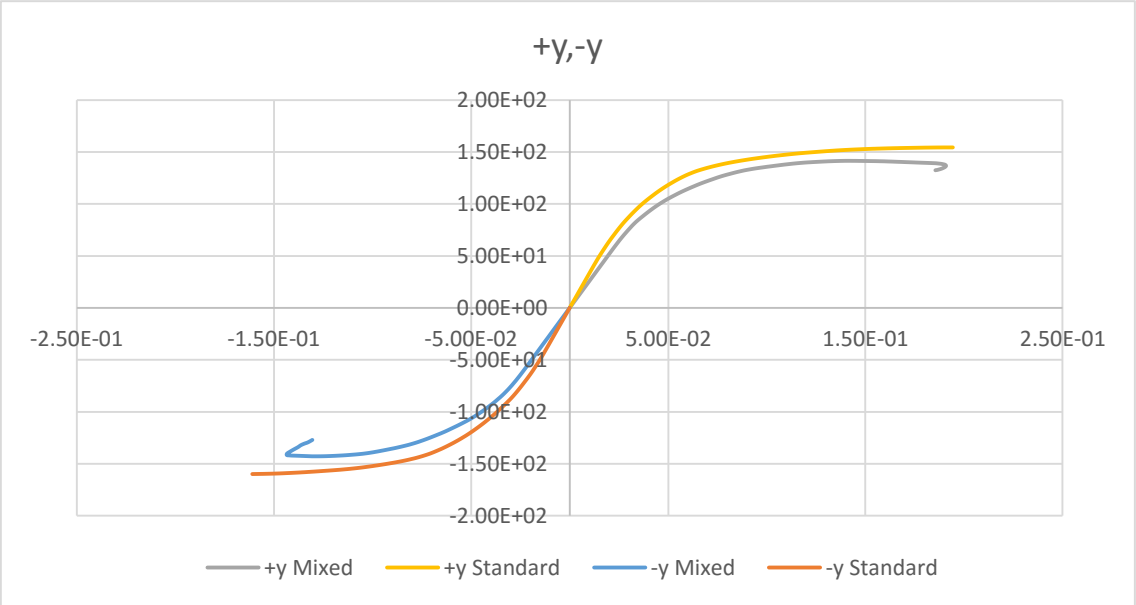

Figure 83. Non-linear analysis comparison. 27 Gauss points (Standard) and 8 Gauss points (Mixed).

The following figures contrast the tensile damage for the ultimate load using both FEM formulation, for the x-direction and y-direction, positive and negative, excitations.

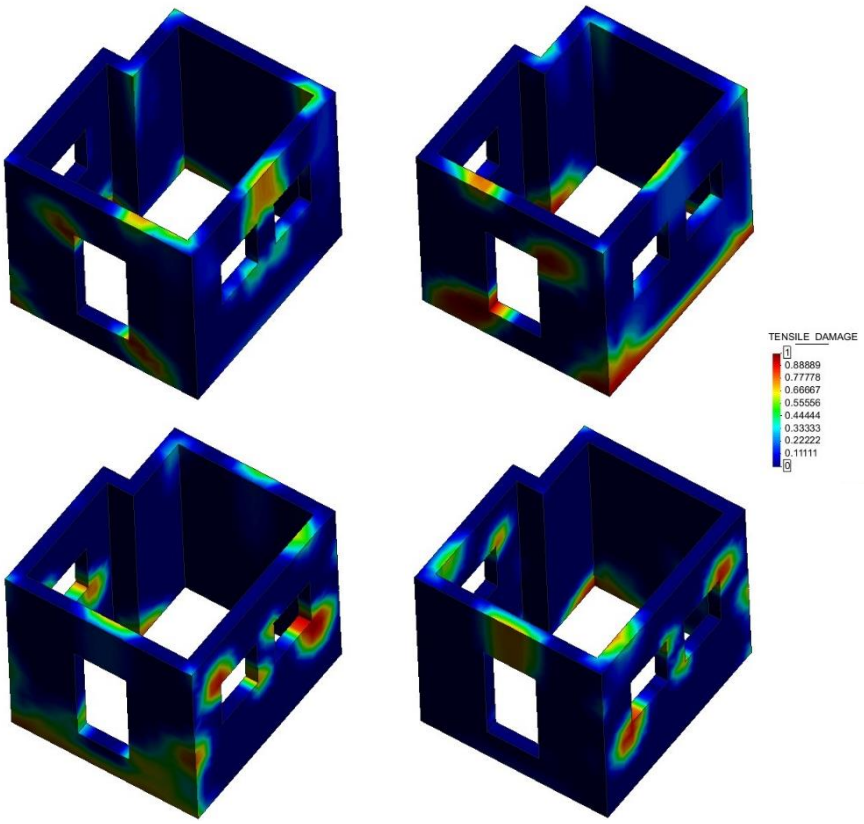

Figure 84. Mixed finite element tensile damage pattern for peak load situation.

(+x-x on the top and +y,-y on the bottom)

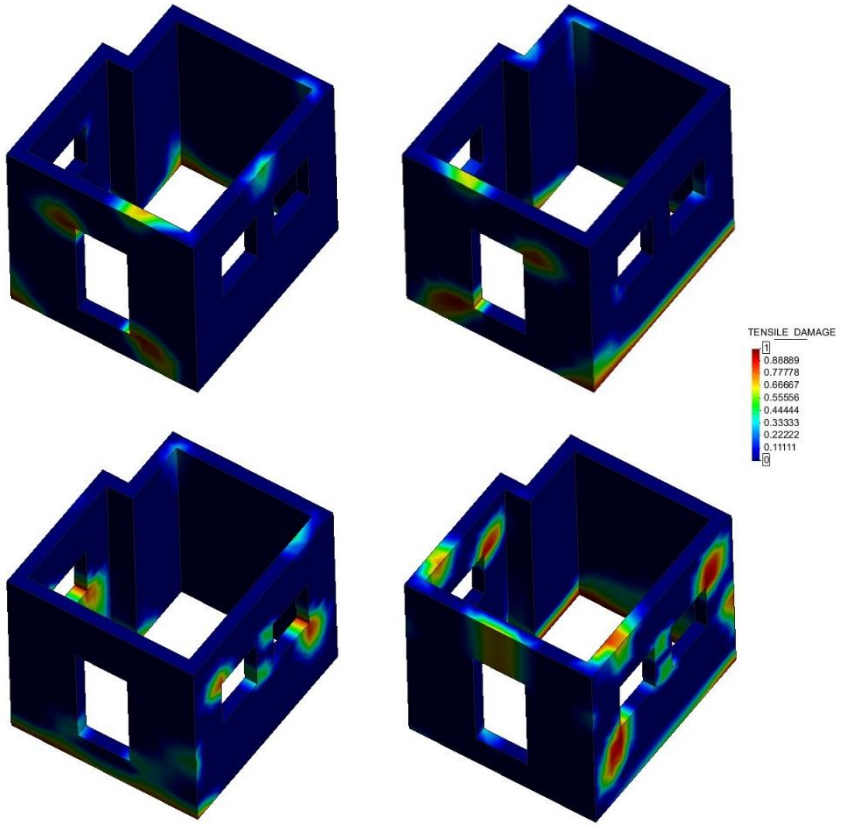

Figure 85. Standard finite element tensile damage pattern for peak load situation.

Figure 84 and **Figure 85** display similar failure modes and crack patterns for both finite element formulations. The results match with the typical cracks present in masonry structures under earthquake excitations, where in the faces perpendicular to the lateral load appear diagonal cracks at both end of openings.

Particularly, after observing the damage pattern results, a further comparison between Ramos et al. [35] investigation cracks **Figure 88** and x-direction, negative and positive, push-over test model results is provided. Limited exactitude is achieved with respect experimental results: crack on the top-right corner of the south face are not present, diagonal cracks on the north and west faces are not observed in the models; on the other hand a severe tensile damage is observed in all faces bases not present at the experimental results.

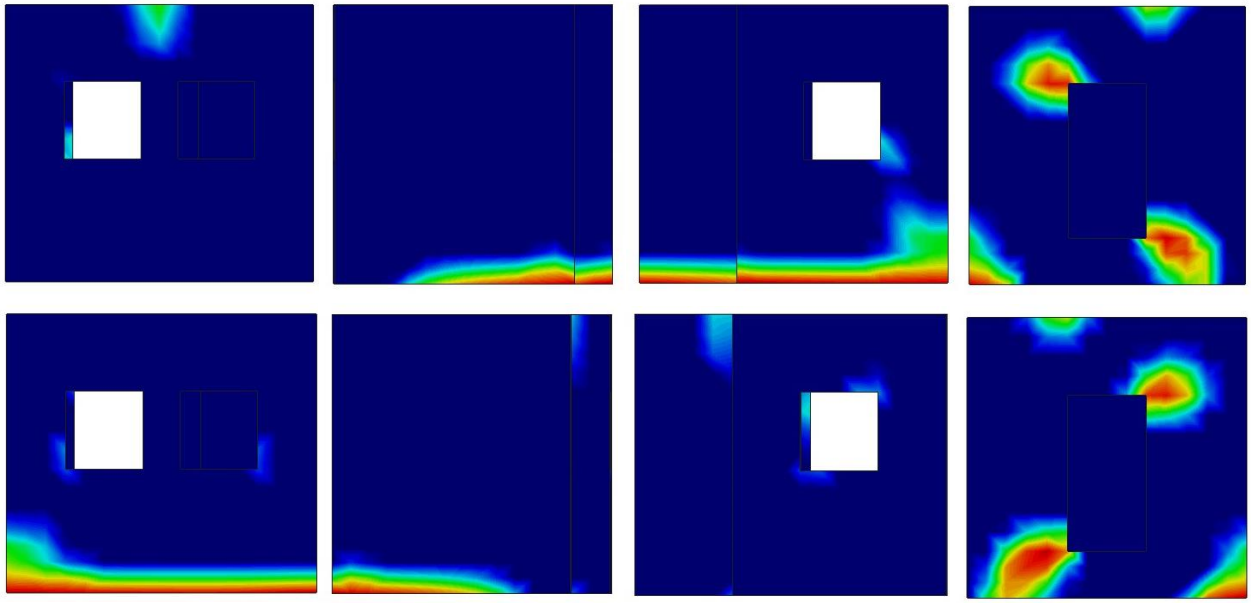

Figure 86. Standard finite element damage pattern results at peak load. (East, North, West and South)

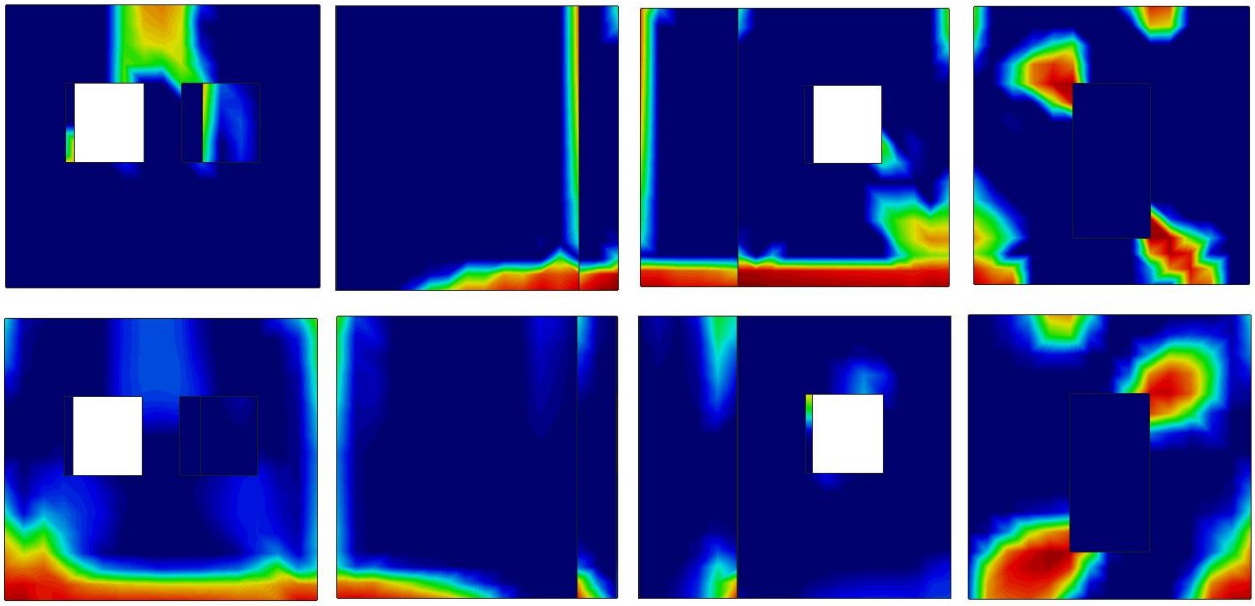

Figure 87. Mixed finite element damage pattern results at peak load. (East, North, West and South)

Figure 88. Damage pattern observed at Ramos [33].

Concluding, both finite element models results provide a partially accurate resemblance with the experimental solution. However, damage intensity and extension is greater in the mixed formulation models. As for the divergence with respect Ramos' results, the original reference aimed to compare the shell element modelled four-wall box-structure natural vibrations and modes of vibrations with the tested ones. Consequently, some of the damage are caused by random direction excitation and explain the partial match.

10.3 Finite element efficiency

A computational cost comparison between the mixed 8 interpolation points' model and the irreducible 25 Gauss points is provided in **Table 19**.

Table 19. Example 6 non-linear analysis efficiency.

Element Type		**Number of elements**	**Number of nodes**	**Number of DOF**	**Gauss Points**	**Time (s)**
Mixed	+x	1116	2232	6696	8	8.203
	-x					11.156
	+y					11.109
	-y					10.062
Standard	+x				27	5.109
	-x					5.391
	+y					5.062
	-y					4.922

Even though the stabilized mixed formulation model achieve accurate results using only 8 Gauss points, the double main field severely affect the elapsed time, almost two-fold.

10.4 Conclusions of the example

The conclusions for the masonry four-wall box-structure example are:

- Both formulation show excellent consistency in the non-linear range.
- Excellent similitude is observed for the force-displacement curve under x-direction and y-direction, negative and positive, push-over excitation.
- Increase the interpolation points through the thickness provide lower peak loads and reduce the dissipated energy. Moreover standard element force-displacement curve tend to match mixed element ones.
- Irreducible formulation requires a minimum of 27 Gauss points to achieve good results in stress/strain interpolation.
- Stabilized mixed formulation display solidity for 8, 27 and 64 interpolation points' non-linear analysis results.
- Both FEM show akin failure mode and damage pattern. On the contrary MFEM results provide more intensified and extended damage.
- Partial resemblance with the experimental results is obtained.

11. Results overview

11.1 Linear-elastic results analysis

Linear analysis results are noticeably favourable to stabilized mixed element models. In all six examples, faster convergence rate and improved accuracy in stress/strain approximation is observed. On the contrary, for 2D and 3D examples one, two and four, displacement convergence study results in a slenderness dependence; for minor length to thickness ratios lower than 1/15, MFEM results are clearly superior in displacement approximation, on the contrary irreducible formulation models show enhanced behaviour.

11.2 Non-linear results analysis

11.2.1 Mesh sensitivity

Both finite element method models non-linear analysis result show mesh size dependent factors, such as peak load, dissipated energy, stability and softening. The former two decrease as the mesh is refined for all examples but the fifth, opposite behaviour is observed. Stability linked to mesh size has variable remarks, both excessive fine and/or coarse meshes provide unstable solutions and convergence is not achieved. Finally, the post-peak softening clearly manifests as the mesh size is reduced.

Regarding crack patterns, no noticeable mesh size dependence is observed; coarse and fine meshes provide akin crack distributions and failure modes. However, damage intensity and distribution is not akin for all mesh sizes, the more the mesh is refined the better the stress approximation and the more concentrated and focussed the damage is.

11.2.2 Integration through thickness

Integration through thickness points have no effect in failure mode and crack distribution for both finite element formulations. On the other hand, increasing the integration points has similar effect to mesh refinement for the load-displacement curves, in other words, lesser peak loads and dissipated energies, more stable solutions with a clear softening post-peak behaviour are observed.

11.2.3 Damage

Stabilized mixed formulation models non-linear analysis results offer akin damage patterns with respect irreducible method's results. In all six examples, damage extension and intensity is favourable to the MFEM, which is provided by the same enhanced stress approximation shown in the linear-elastic range. As a results, mixed element models generate early mechanisms resulting in softening behaviour in the force-displacement curves.

11.3 Finite element efficiency

Linear-elastic accuracy to computational time required analysis are in favour of the stabilized mixed method models in examples one to three, fourth example is adverse to MFEM. Mesh refinement has similar increase in computational time for both formulations. On the contrary, incrementing the integration points through thickness to detriment of irreducible formulations.

In general terms, mixed formulations non-linear analysis elapsed time is greater than the standard element models; this difference is increased as the model size increases.

12. Conclusions

Stabilized mixed and irreducible formulation are suitable to represent out-of-plane bending behaviour of 2D and 3D, straight and curved structural elements, in elastic-linear and non-elastic range.

The linear-elastic conclusions are summarised:

- Both FEM converge to the same solution.
- Mixed element models consistently provide accurate and fast approximation of the stress/strain main field.
- Displacement nodal variable estimation is slenderness dependent for the mixed formulation; for minor length to thickness ratios lower than 1/15, MFEM provides improved approximations, on the other hand standard element models perform better.
- Efficiency is favourable to mixed formulation, which provides more accurate and earlier convergence using lesser computational time.

The non-elastic conclusions are:

- Same failure mechanism and similar force-displacement curves are observed in all cases. Moreover, akin results with the experimental test is shown.
- Irreducible formulation models require a larger number of integration points through thickness than MFEM do; 2D examples 1 and 2, require at least 16 Gauss points, while 3D examples, 3, 4, 5 and 6, require 27 Gauss points.
- Mixed formulation successfully capture non-linear range characteristics: failure mode, force-displacement curves, among others, using the minimum number of interpolation points for all six examples.
- Mesh refinement and integration point through thickness increase, results in bring closer outputs between the irreducible form force-displacement curves and the mixed ones. Concluding the enhanced approaches in non-linear range provided by the MFEM using rough meshes and lower integration points though thickness.
- Enhanced stress calculation provided by the stabilized mixed formulation results in damage patterns with greater intensity and extension than irreducible form ones.
- Efficiency is favourable to irreducible formulation, however stress/strain results are able to straightforwardly capture cracks appearance and extension.

13. References

[1] M. Cervera, M. Chiumenti, R. Codina, Mixed stabilized finite element methods in nonlinear solid mechanics. Part I: formulation, Comput. Methods Appl. Mech. Engrg. 199 (2010) 2559–2570.

[2] M. Cervera, M. Chiumenti, R. Codina, Mixed stabilized finite element methods in nonlinear solid mechanics. Part II: strain localization, Comput. Methods Appl. Mech. Engrg. 199 (2010) 2571–2589.

[3] M. Cervera, M. Chiumenti, R. Codina. A mixed three-field FE formulation for stress accurate analysis including the incompressible limit. Computer Methods in Applied Mechanics and Engineering 283 (2015): 1095-1116.

[4] Z. Salát. Numerical Modelling of Out-of-Plane Behavior of Masonry Structural Members.

[5] B.X. Fraeijs de Veubeke, Displacement and equilibrium models in the finite element method, in: O.C. Zienkiewicz, G. Hollister (Eds.), Stress Analysis, Wiley, 1965.

[6] Leonard R. Herrmann , Finite-Element Bending Analysis for Plates, Journal of the Engineering Mechanics Division, Vol. 93, Issue 5, (1967) 13-26.

[7] K. Hellan, Analysis of elastic plates in flexure by a simplified finite element method, Acta polytech. scand. Civil Engng. Ser., 46 (1967).

[8] D.S. Malkus, T.J.R. Hughes, Mixed finite element methods—reduced and selective integration techniques: a unification of concepts, Comput. Methods Appl. Mech. Engrg. 15 (1978) 63–81.

[9] D.N. Arnold, F. Brezzi, M. Fortin, A stable finite element for the Stokes equations, Calcolo 21 (1984) 337–344.

[10] Limin, Tang, Chen Wanji, and Liu Yingxi. "Formulation of quasi-conforming element and Hu-Washizu principle." Computers & Structures 19.1-2 (1984): 247-250.

[11] J.C. Simo, R.L. Taylor, K.S. Pister, Variational and projection methods for the volume constraint in finite deformation elasto-plasticity, Comput. Methods Appl. Mech. Engrg. 51 (1985) 177–208.

[12] J.C. Simo, M.S. Rifai, A class of mixed assumed strain methods and the method of incompatible modes, Int. J. Numer. Meth. Engrg. 29 (1990) 1595–1638.

[13] C.R. Dohrmann, M.W. Heinstein, J. Jung, S.W. Key, W.R. Witkowsky, Node-based uniform strain elements for three-node triangular and four-node tetrahedral meshes, Int. J. Numer. Meth. Eng. 47 (2000) 1549–1568.

[14] J. Bonet, A.J. Burton, A simple average nodal pressure tetrahedral element for incompressible and nearly incompressible dynamic explicit applications, Commun. Numer. Methods Eng. 14 (5) (1998) 437–449.

[15] E.A. de Souza Neto, F.M.A. Pires, D.R.J. Owen, F-bar-based linear triangles and tetrahedra for finite strain analysis of nearly incompressible solids. Part I: formulation and benchmarking, Internat. J. Numer. Methods Engrg. 62 (2005) 353–383.

[16] T.J.R. Hughes, G.R. Feijo´o, L. Mazzei, J.B. Quincy, The variational multiscale method-a paradigm for computational mechanics, echanics, Comput. Methods Appl. Mech. Engrg. 166 (1998) 3–28.

[17] R. Codina, Stabilization of incompressibility and convection through orthogonal sub-scales in finite element methods, Comput. Methods Appl. Mech. Engrg. 190 (2000) 1579–1599.

[18] M. Chiumenti, Q. Valverde, C. Agelet de Saracibar, M. Cervera, A stabilized formulation for incompressible elasticity using linear displacement and pressure interpolations, Comput. Methods Appl. Mech. Engrg. 191 (2002) 5253–5264.

[19] M. Cervera, M. Chiumenti, Q. Valverde, C. Agelet de Saracibar, Mixed linear/linear simplicial elements for incompressible elasticity and plasticity, Comput. Methods Appl. Mech. Engrg. 192 (2003) 5249–5263.
[20] M. Chiumenti, Q. Valverde, C. Agelet de Saracibar, M. Cervera, A stabilized formulation for incompressible plasticity using linear triangles and tetrahedra, Int. J. Plast. 20 (2004) 1487–1504.
[21] C. Agelet de Saracibar, M. Chiumenti, Q. Valverde, M. Cervera, On the orthogonal subgrid scale pressure stabilization of small and finite deformation J2 plasticity, Comput. Methods Appl. Mech. Engrg. 195 (2006) 1224–1251.
[22] M. Cervera, M. Chiumenti, C. Agelet de Saracibar, Softening, localization and stabilization: capture of discontinuous solutions in J2 plasticity, Int. J. Numer. Anal. Methods Geomech. 28 (2004) 373–393.
[23] M. Cervera, M. Chiumenti, C. Agelet de Saracibar, Shear band localization via local J2 continuum damage mechanics, Comput. Methods Appl. Mech. Engrg. 193 (2004) 849–880.
[24] M. Cervera, M. Chiumenti, Size effect and localization in J2 plasticity, Int. J. Solids Struct. 46 (2009) 3301–3312.
[25] M. Cervera, M. Chiumenti, and R. Codina. Mesh objective modelling of cracks using continuous linear strain and displacement interpolations. International Journal for Numerical Methods in Engineering 87, no. 10 (2011): 962-987.
[26] M. Cervera, M. Chiumenti, L. Benedetti, R. Codina. Mixed stabilized finite element methods in nonlinear solid mechanics. Part III: Compressible and incompressible plasticity. Computer Methods in Applied Mechanics and Engineering, 285 (2015) 752-775.
[27] D. Boffi, F. Brezzi, and M. Fortin, Mixed finite element methods and applications, vol. 44 of Springer Series in Computational Mathematics, Springer, Heidelberg, 2013.
[28] O. Guasch, M. Arnela, R. Codina, H. Espinoza. A stabilized finite element method for the mixed wave equation in an ALE framework with application to diphthong production. Acta Acustica united with Acustica 102, no. 1 (2016): 94-106.
[29] T. Wu, A. P-L. Hung, P. Hunter, and K. Mithraratne. On modelling large deformations of heterogeneous biological tissues using a mixed finite element formulation. Computer methods in biomechanics and biomedical engineering 18, no. 5 (2015): 477-484.
[30] P. Roca, M. Cervera, and G. Gariup. Structural analysis of masonry historical constructions. Classical and advanced approaches. Archives of Computational Methods in Engineering 17, no. 3 (2010): 299-325.
[31] M. Cervera, C. AgeletdeSaracibar, M. Chiumenti, COMET: COupled MEchanical and Thermal analysis, 2002 Data Input Manual, Version 5.0, Technical report IT-308. Available from http://www.cimne.upc.es
[32] GiD: The Personal Pre and Post Processor, 2009 http://www.gidhome.com.
[33] Bazant, P. Zdenek, and J. Planas. Fracture and size effect in concrete and other quasi-brittle materials. Vol. 16. CRC press (1997).
[34] Gazzola, E. A., R. G. Drysdale, and A. S. Essawy. Bending of concrete masonry walls at different angles to the bed joints. In Proceedings of 3th North American Masonry conference Arlington, Paper, vol. 27. 1985.
[35] Lourenço, Paulo B. Anisotropic softening model for masonry plates and shells. Journal of Structural Engineering 126, no. 9 (2000): 1008-1016.
[36] Gazzola, A. Edward, and Robert G. Drysdale. A component failure criterion for blockwork in flexure. In Advances in Analysis of Structural Masonry, pp. 134-154. ASCE, 1986.
[37] Di Marco, Roberto, Paolo Faccio, Paolo Foraboschi, and Enzo Siviero. Volte in muratura rinforzate con FRP. Costruire in laterizio 69 (1999): 66-71.

[38] Creazza, Giuseppe, Renato Matteazzi, Anna Saetta, and Renato Vitaliani. Analyses of masonry vaults: a macro approach based on three-dimensional damage model. Journal of structural engineering 128, no. 5 (2002): 646-654.
[39] Endo, Yohei, Pere Roca i Fabregat, and Luca Pelà. Modelling and Structural Analysis of historical masonry systems including vaulted structure. PhD diss., Ph. D. Thesis, Department of Construction Engineering, Technical University of Catalonia, 2015.